



Bachelor in Aerospace Engineering
2016/2017

Bachelor Thesis

Development of a rotor blade aeromechanic model for simulating helicopter performances

Ignacio Castillo Sauca

Tutor

Pablo Fajardo Peña
Leganes, 10th July 2017



This work is subject to Creative Commons License **Attribution-NonCommercial-NoDerivs**

Contents

1	Introduction	3
2	Rotor Forces	7
2.1	Methods	8
2.1.1	Momentum Theory	8
2.1.2	Blade Element Theory	12
2.2	Induced velocity	17
2.3	Aerodynamic forces	23
3	Helicopter Forces	28
3.1	Blade movements	28
3.2	Forces on the hinge	34
3.3	Main body forces and moments	38
3.3.1	Tail rotor and tailplane	39
3.3.2	Total forces	43
3.3.3	Total moments	47
4	Flight Trim	51
4.1	Analytical flapping	51
4.2	Forces at the tip path plane	55
4.3	Longitudinal trim	59
4.4	Lateral trim	63
5	Results and Movement Integration	65
5.1	Helicopter and environment data	65
5.2	Trim conditions	66
5.3	Rotor results	67
5.4	Helicopter motion	72
6	Conclusions and impact	78
6.1	Future works	78
6.2	Possible applications	79
6.3	Project Budget	80
7	Appendix	81

List of Figures

1	Pressure gradient in forward flight showing the dissymmetry of lift [1]	4
2	Momentum theory for vertical flight [2]	8
3	Stream tube flight [3]	10
4	Momentum theory for forward flight [4]	11
5	Blade section in vertical flight [10]	12
6	Orientation of the no feathering plane in forward flight [9]	15
7	Angle between vortex and free flow [11]	21
8	Comparison between methods [15],[16]	23
9	Flapping and lagging angles of a blade	29
10	Helicopter with tailplane [30]	40
11	Exaggerated angles around the rotor and tailplane	41
12	Relation of induced velocities and tailplane heights ($\xi = 1.07$) [33]	41
13	Relation of induced velocities and tailplane heights ($\xi = 2.07$) [34]	42
14	Tailplane with respect to TPP, rotor plane, and vortex ε_0	43
15	Forces on the rotor and main body [35]	44
16	Forces on the rotor and main body [41]	46
17	Force components in no feathering plane and TPP	56
18	Velocity components in no feathering plane and TPP	57
19	Longitudinal forces for trim [50]	60
20	Induced velocity	68
21	Side view of v_i	68
22	Front view of v_i	68
23	Thrust levels	70
24	Bladde flapping	71
25	Side flapping view	71
26	Front flapping view	71
27	Horizontal velocity disturbance	72
28	Vertical velocity disturbance	72
29	Pitch angle evolution	73
30	Horizontal velocity disturbance without tailplane	74
31	Vertical velocity disturbance without tailplane	74
32	Pitch angle evolution without tailplane	75
33	Yaw evolution	75
34	Roll evolution	76
35	Roll with and without controller [64]	77

1 Introduction

Helicopters and other rotary-wing aircrafts work in a rather different way compared to fixed-wing aircraft. The main difference between these two types of aircraft lies on how the aerodynamic forces are generated, besides the kind of lifting surfaces and control devices needed for that. While with fixed-wing aircraft, as the name says, such surfaces are still and the very movement of the vehicle induces the forces, helicopters make use of one or more rotors with blades for that. These blades rotate around their axis, and create a force almost perpendicular to the rotor disc, which -in the case of helicopters- shall act as thrust for propelling the vehicle as well as lift to counteract the weight.

Besides their rotation, the blades are held loosely at the rotor, so that due to the aerodynamic forces they are able to move in what are known as lagging, flapping and feathering motions. This will also have further effects both on the forces distribution and the rotor disc orientation, and can be taken advantage of by means of adequate control systems.

Forces on the blades

The rotation of the blades affects mainly the distribution of the aerodynamic forces along the rotor disc, especially when the velocity of the helicopter increases. This can be briefly seen in two ways:

On the one hand, the very fact that they are rotating creates a variation of speed depending on the blade section. While the blade tip can be considered to be traveling with a speed magnitude of ΩR -being Ω the rotor's angular velocity and R the disc radius, the hinge that connects the blade with the rotor shaft will have a much lower speed in order to create lift. This is not a great problem alone, since due to symmetry the forces are the same along the azimuth angle, and the lift distribution can be modified if, choosing the right blade, the incidence angle is the proper one at each section.

The bigger issues arise when the helicopter is flying with some velocity component besides the vertical one. For instance, if it is flying at a certain forward speed, at one side of the disc there will be an "advancing" blade and at the other side a "retreating" one, taken from the relative wind velocity against the blade. Such effect will have two consequences. The first one is the appearance of stronger forces on one side of the rotor disc -the advancing side, since the dynamic pressure will be higher there and so will be the lift generated. On the other side, however, the forces will be weaker due to the "slower" velocity of the blade. This "slower flow" may lead to the second consequence, which consists of the stall at some parts of the blade where either the incidence is too high or the velocity at that point too low -i.e., stall at high velocities. This effect covers a small portion of the disc area, which increases with the forward speed of the helicopter, and its effect can be appreciated in figure 1

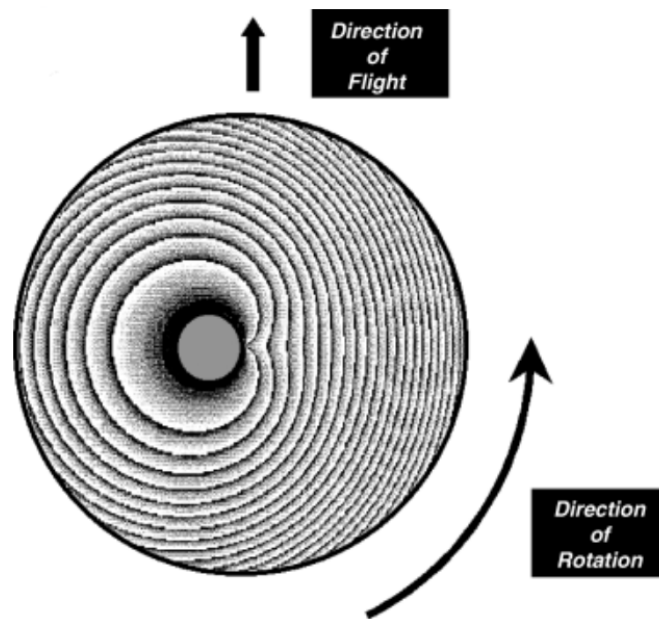


Figure 1: Pressure gradient in forward flight showing the dissymmetry of lift [1]

The aerodynamic forces previously described -with their respective asymmetry- provoke flapping movements on the blades, depending on their position. If this is observed from the point of view of the blade tip, there appears another disc -the tip path plane or TPP, which may change its incidence with respect to the free flow due to the blade's movements. Since such movements are provoked by the aerodynamic forces, then such forces can modify the disc's incidence. Thereby, those forces might again get affected by the new disc orientation, starting all over again and giving as a result an equivalent rotor force whose magnitude and direction might change depending on the helicopter's speed, the blade position at that moment or any control input that might be imposed.

Considering all this, it becomes clearer how the aerodynamic forces of a helicopter can vary differently than those from a fixed-wing aircraft. This may highly affect the stability of the helicopter during flight, since a slight movement of the vehicle could change the rotor's incidence and hence the aerodynamic forces, thus making the vehicle's motion change again and repeat the same process until a big loss of stability is reached.

Control system

In order to correctly control the forces acting on the rotor, there is a swash plate located at the shaft which connects to each blade and modifies their incidence. This way, besides having by default certain geometric pitch, some increment can be added or subtracted to the angle of attack. Making a good use of this, one can get stronger or weaker aerodynamic forces at the blade, and obtain a resultant force

with the desired magnitude and direction, thus enabling the control of the aircraft.

The swash plate works changing the blade's pitch in two different ways: One of them varies what is called the collective pitch, which increases at once the incidence of all the blades, and hence modifies above all the magnitude of the resultant force. This is usually useful for climbing and descending, and is achieved by rising vertically the swash plate around the shaft so that all angles of attack increase equally.

For orienting the resultant forces another movement of the swash plate can be used. Such movement is called cyclic pitch, and it varies the blades' angle of attack depending on their current azimuth angle. This can be performed by slightly tilting the swash plate in a certain direction, so that every blade has its incidence decreasing or increasing as they move towards or from the desired location. Furthermore, this movement is useful not only to orient correctly the forces, but also to counteract such effects as the blade stall when there are areas with too low speed -or too much blade incidence for it.

Aims of the thesis

The purpose of this project is to numerically develop a code that computes the different forces on the rotor of a helicopter at each time -in order to be able to integrate its movement, and also takes into account some main body forces such as the drag and weight. Besides, a series of trim conditions shall be established in the code, from the helicopter's data and the trimmed equations of motion. With all that, the helicopter shall be put under a flight case with such conditions, and its movement will be integrated by means of the procedure explained during the project.

Due to the scope of the methods used in this project, the main case that will be observed shall be steady forward flight. Such methods are also able to perform some analysis in vertical flight, which is most of the time less complex than forward flight. Hence, in some situations vertical flight formulas and examples will also be included in order to better introduce certain concepts.

In order to calculate the forces distribution, two theories will be used: the Momentum Theory and the Blade Element Theory -also known together as Blade Element Momentum Theory (BEMT). These offer a fair and useful approach without the need of vortex models that might increase substantially the times and complexity of the computation. The moments and motion of the blades can then be obtained with the calculated forces. Finally, with the blades' dynamics fully described, the resultant rotor forces and moments will be translated to the whole helicopter in order to evaluate its final behavior. The vehicle shall be then put in trim conditions and its movement will be integrated along its different degrees of freedom, to observe whether it is stable or not and take any conclusion from that.

Besides the tasks previously described, in the last section some further com-

ments will be made. These will analyze the regulatory framework as well as the socio-economic environment, trying to introduce possible applications that this project might be compatible with, as well as any improvement or requisite that could help the project to become more complete and cover more -and more complex- cases in helicopter flight. Afterwards, a brief summary of the budget needed for this project will also be made.

2 Rotor Forces

Before rushing and starting to compute variables, there is a previous approach that can be useful to simplify some components in some of the proposed methods, as it will be seen later.

As mentioned before, the pitch angle θ is composed by both the geometric pitch, which is given along with the inherent properties and dimensions of each blade, and the “feathering” pitch, which can be changed by means of the collective or cyclic control of the swash plate. Let’s call these three angles θ_{base} , θ_0 and θ_c respectively, such that:

$$\theta = \theta_{\text{base}} + \theta_{\text{feathering}} = \theta_{\text{base}} + \theta_0 + \theta_c \quad (1)$$

It was also noted before that the cyclic pitch depended on the azimuth angle $\psi = \Omega t$ (being t the time passed in order to compute such angle), so its form may be expressed as follows:

$$\theta_{\text{feathering}} = \theta_0 + \theta_c = \theta_0 - A_1 \cos\psi - B_1 \sin\psi \quad (2)$$

Now this can be joined with equation (1) and the result’s right hand side will have two parts; one of them constant along the azimuth angle ($\theta_{\text{base}} + \theta_0$) and the other changing with it.

Since this feathering may depend on the azimuth angle, in some methods, such as the Blade Element Theory, there will appear complicated operations when there are integrals or time-dependent variables, so it would be a good idea to avoid such operations. In order to do so, a plane can be established that suppresses these variable pitch components. As it can be seen from equation (2), the angle of the blade changes in such a way that if there is a reference frame with the vertical axis tilted at certain degree, the terms $A_1 \cos\psi$ and $B_1 \sin\psi$ disappear. In fact, longitudinally the plane is tilted forward with an angle B and laterally with an angle A . These directions are referred to a body reference frame where the longitudinal axis points forward, the lateral axis points to the starboard direction and the vertical one points downwards.

When this is done, the result is a plane where the only pitch angle is considered to be $\theta = \theta_{\text{base}} + \theta_0$, which will be constant along azimuth angle. Keep in mind, though, that the geometric pitch may vary along the radius of the blade, but at least it will not be time-dependent.

This is called the “no feathering Plane” -due to the fact that it suppresses the feathering motion, and is one of the three planes used in this project. The other two are the Rotor Disc plane and the tip path plane, which, as also said before, is a plane containing the movements of the blade tips. This last plane will be useful for some approximations both in the calculation of the induced velocity, and when

setting the trim conditions.

2.1 Methods

In order to compute the forces acting on the blades, several approaches may be taken. Some simplifications and assumptions can be made in a couple of them, so that it is not necessary to develop complex aerodynamic models such as rotor wakes models.

The two methods that have been implemented here are the Momentum Theory and the Blade Element Theory.

2.1.1 Momentum Theory

This first method takes directly the equations of Navier Stokes into a control volume starting where the air flow is supposed to be still unperturbed, and ends far downstream. It passes also just by the sides of the rotor disk, assuming that the air does not move in and out the imaginary walls created by such volume. Figure 2 shows this applied to vertical flight:

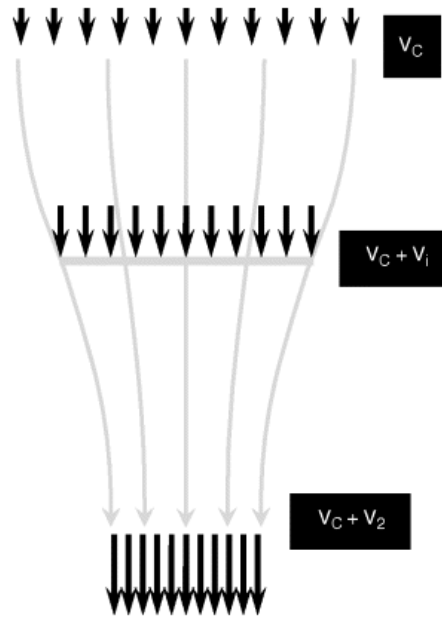


Figure 2: Momentum theory for vertical flight [2]

Now as it can be seen, there are three important sections in the picture. The highest belongs to the unperturbed velocity v_z , with a magnitude here of $v_z = v_c$. This is the velocity that the rotor itself would have if observed from an outside, fixed reference frame. The other two velocities appear with the values $v_c + v_i$ and $v_c + v_2$, since the rotor induces a certain velocity to the flow. It can also be seen that the streamlines are not straight vertical along the stream tube, which will make the velocity of the flow inside to change. That explains the component v_2

that is added to the original one at the end of the tube. The term v_i follows the same reasoning, but has a much more important value. It is placed at the section where the rotor disc is situated, and it indicates the induced velocity due to the movement of the rotor blades, which helps create the necessary thrust.

These expressions can be solved out using the two first equations of Navier Stokes and Bernoulli's equation, after which the thrust will be obtained. Starting with the first of those three -the mass conservation equation, once the integrals have been solved the output is the following:

$$\rho S_c v_c = \rho S_2 (v_c + v_2); \quad S_c v_c = S_2 (v_c + v_2) = S_{\text{rotor}} (v_c + v_i) \quad (3)$$

Where ρ indicates the air density -which is considered constant in this project- and S_i each area (the third one would represent the rotor area)

Also, Bernoulli can be applied to the three sections displayed at the stream tube. Taking into account that both at its top and bottom the static pressure is the atmospheric one p_c , one can have:

$$\text{Top-Disc: } p_c + \frac{1}{2} \rho v_c^2 = p_{\text{upper}} + \frac{1}{2} \rho (v_c + v_i)^2 \quad (4)$$

$$\text{Bottom-Disc: } p_c + \frac{1}{2} \rho (v_c + v_2)^2 = p_{\text{lower}} + \frac{1}{2} \rho (v_c + v_i)^2 \quad (5)$$

After this it can be seen that by subtracting equation (4) to (5), and realizing that the pressure jump times the area is the force generated, the actual thrust comes out with the following form:

$$T = S \Delta p = S_{\text{rotor}} (p_{\text{lower}} - p_{\text{upper}}) = \frac{1}{2} \rho S_{\text{rotor}} (v_2^2 + 2v_c v_2) \quad (6)$$

This expression for the thrust is written now as a function of the unknown v_2 , but as it was said earlier, the important variable here is the induced velocity, v_i . In order to rewrite the equation, the momentum equation from Navier Stokes should be adopted, which after playing with equation (3) gives out the following form:

$$\begin{aligned} T &= \rho S_2 (v_c + v_2)^2 - \rho S_c v_c^2 = \rho [S_2 (v_c + v_2)^2 - S_c v_c^2]; \\ T &= \rho S_{\text{rotor}} (v_c + v_i) (v_c + v_2 - v_c); \\ T &= \rho S_{\text{rotor}} (v_c + v_i) v_2 \end{aligned} \quad (7)$$

Equations (3) and (7) can be combined in order to solve for the term v_2 . After that, both the final velocity increase v_2 and the complete thrust expression, indicated in equation (9), are shown. Then, rewriting S_{rotor} as just S and the vertical velocity v_c as v_z , the results from the momentum equation and Bernoulli's equation can be joined to solve for the unknown velocity, v_2 :

$$\begin{aligned}
\frac{1}{2}\rho S(v_2^2 + 2v_z v_2) &= \rho S(v_z + v_i)v_2; \\
v_i v_2 &= \frac{1}{2}v_2^2; \\
v_2 &= 2v_i
\end{aligned} \tag{8}$$

Then the vertical force can be computed as:

$$T = 2\rho S(v_z + v_i)v_i \tag{9}$$

This reasoning leads to the formula for the thrust in forward flight, which will follow most of the rest of calculations -since at the end of the project, the helicopter's movement will be integrated in forward flight.

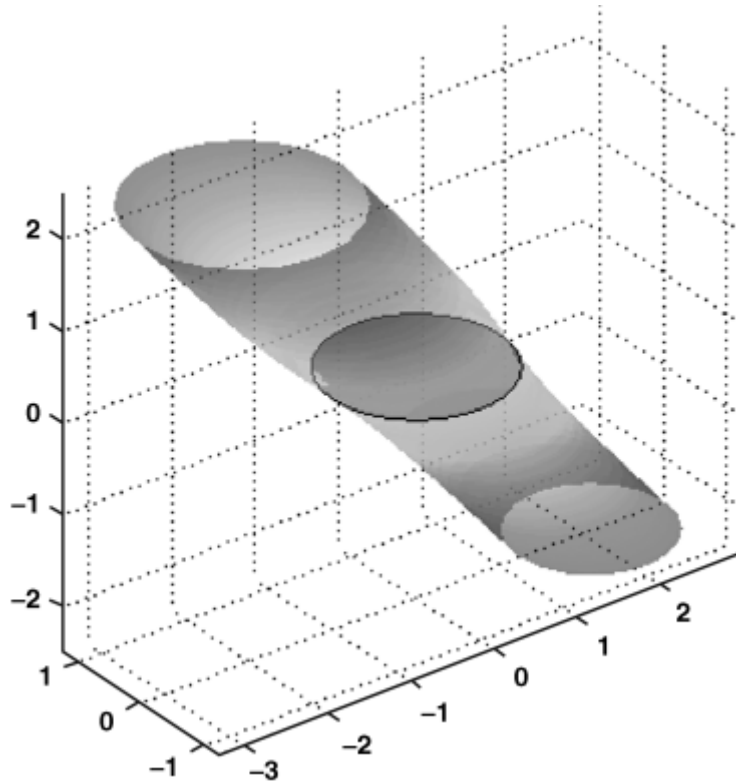


Figure 3: Stream tube flight [3]

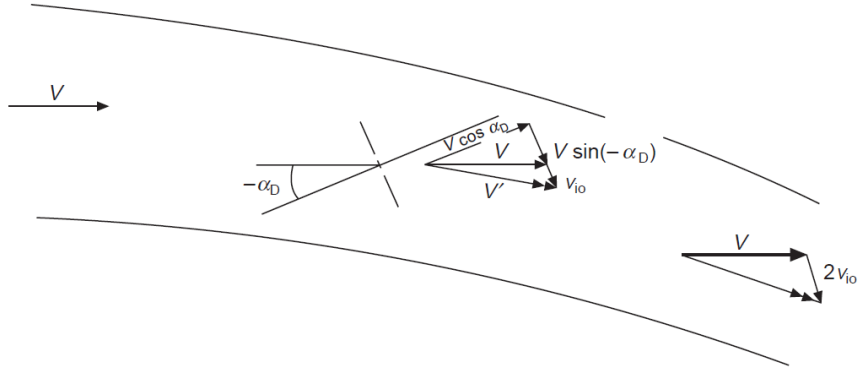


Figure 4: Momentum theory for forward flight [4]

Figure 3 shows a representation of the stream tube for the case of forward flight, again with the top and bottom layers as well as the rotor section between them.

Now that the velocity has a component in the horizontal direction v_x , the previous equations are slightly more complex. In fact, when the forward velocity is relatively slow, the flow around the rotor disc becomes turbulent and the approach used here is no longer valid. Instead of the Moment or Blade Element theories, some other methods should be applied, which are outside the scope of this project. Hence, the aim here focuses on the high speed case, where better approximations can be made.

In order to obtain an acceptable result, Glauert^{[5],[6]} assumed the rotor disc to be -for that case- an elliptically loaded wing, in such a way that its form would be circular just like the rotor disc itself. Then, according to figure 4, the disc is supposed to have an incidence angle with the coming flow of α_D , such that:

$$V' \approx V = \sqrt{V^2 \cos^2 \alpha_D + (V \sin \alpha_D - v_{i0})^2} \quad (10)$$

Where v_{i0} is considered to be the mean induced velocity on the rotor disc, as was v_i before. This will be explained and expanded in the following section with the help of the Blade Element Theory. Finally, by assuming that the disc only induces velocity in the z axis, the equation for forward flight is the following one:

$$T = 2\rho S V v_{i0} = 2\rho S v_{i0} \sqrt{V^2 \cos^2 \alpha_D + (V \sin \alpha_D - v_{i0})^2} \quad (11)$$

These equations of thrust are the basis of what will be later used in order to compute a more accurate value for variables such as the induced velocity, the thrust itself and other outputs like the horizontal force and the torques.

2.1.2 Blade Element Theory

It has just been seen that for vertical and forward flight the total thrust can be computed from only a few variables. However, using the Momentum Theory does not give out an actual distribution of the forces, but rather their total value for each case.

In reality, however, the rotor does not consist of a “solid” disc through which air passes, but instead it is composed of a series of rotating blades, which are the ones in charge of producing the aerodynamic forces. Moreover, the linear velocity of these blades is not the same at each section or azimuth position, due both to their rotation and the horizontal velocity of the helicopter. This fact affects also the induced velocity. As it was said earlier, the induced velocity in the Momentum Theory is considered to be the average one in each z -section. However, in this case it will depend on its position (radially $-r$ and azimuth $-\psi$), so the problem will not be as straight-forward as before.

A good assumption is to consider the blade of the rotor as a very long wing. While the coming velocity distribution will not be constant, the wing can be considered as a distribution of airfoils out of which the forces at that point can be computed, independently of the rest. Considering then vertical flight, for example, figure 5 shows the velocity components and the orientation of the aerodynamic forces.

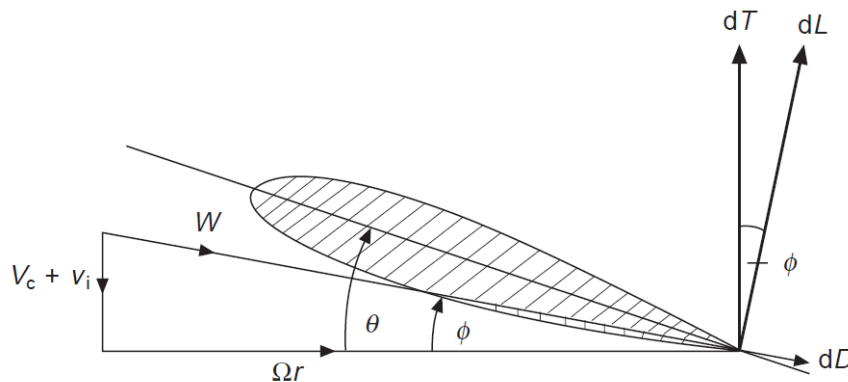


Figure 5: Blade section in vertical flight [10]

As it can be seen for vertical flight, the horizontal velocity is $U_T = \Omega r$, which implies the increase of such speed as this radius becomes larger. The components $U_P = v_c + v_i$ -which represent the vertical velocity at this point as it was seen in Momentum Theory, together with the horizontal one, form the total velocity for this airfoil W , as well as the the angle over the horizontal plane ϕ . Besides this angle, there is also the pitch angle θ , which as was noted before is given by both the geometric pitch -which depends on the blade itself- and the feathering pitch, controlled externally in order to change the magnitude and direction of forces.

With these 2 angles the angle of attack of the blade -at this radial and azimuth position- can be computed:

$$\alpha = \theta - \phi \quad (12)$$

And as with any other airfoil, the lift force can be calculated from this using the lift equation:

$$dL = \frac{1}{2}\rho V^2 c C_L dr = \frac{1}{2}\rho W^2 c (C_{L_0} + C_{L_\alpha} \alpha) dr \quad (13)$$

In this theory C_L is taken with an angle reference such that there is only $C_{L_\alpha} \approx 5.7$. This shall be the lift coefficient used from now on to calculate such force, and will be denoted as a . Apart from it, the component c represents the chord of the blade -which might or might not be constant, ρ the air density, and dr the differential thickness on the blade -while its referred variable r would be the actual position at the blade.

A useful transformation here is to develop a non dimensional variable $x = \frac{r}{R}$, which allows to write the equation as a function of the total disc radius R . This leads to its differential form to be $dx = \frac{dr}{R}$, and hence $dr = Rdx$. Besides, the total velocity W can be approximated to the horizontal velocity U_T since the angle formed by the vertical and horizontal components is usually small ($\phi \approx \frac{U_P}{U_T}$). The same reasoning can be applied to the angle of attack, and afterwards the lift may be displayed in the following way:

$$\alpha = \theta - \phi \approx \theta - \frac{U_P}{U_T} = \theta - \frac{v_c + v_i}{\Omega r} \quad (14)$$

$$dL = \frac{1}{2}\rho a c U_T^2 \left(\theta - \frac{U_P}{U_T} \right) dr = \frac{1}{2}\rho a c \Omega^2 R^3 \left(\theta x^2 - x \frac{v_c + v_i}{\Omega R} \right) dx \quad (15)$$

This equation is almost complete. One last change that can be done is to make dimensionless the velocity components v_c and v_i . Such is achieved by dividing them by the denominator ΩR , which gives out both dimensionless variables as functions of the radial position, λ_c and λ_i .

Finally, these changes can be applied to equation (15) to obtain the lift formula for vertical flight:

$$dL = \frac{1}{2}\rho a c \Omega^2 R^3 [\theta x^2 - (\lambda_c + \lambda_i)x] dx \quad (16)$$

On the other hand the drag of this airfoil may be computed with the corresponding equation in a similar way:

$$\begin{aligned}
dD &= \frac{1}{2}\rho V^2 c \delta dr = \frac{1}{2}\rho(\Omega r)^2 c \delta dr \\
&= \frac{1}{2}\rho c \Omega^2 R^3 \delta x^2 dx
\end{aligned} \tag{17}$$

Where δ acts as a drag coefficient.

Now equations (16) and (17) can be integrated along the blade to give the total forces at that blade. For the case of the thrust in vertical flight, the angle ϕ can be assumed to be small, so from figure 5 the differential of thrust can be approximated as $dT \approx dL$. Hence, integrating the lift and multiplying it by the total number of blades b will finally give the total thrust of the rotor.

The main components of these two equations are the same in forward flight; however, the velocities change, due to different factors. The first and most obvious is the large x-component of the velocity now, which eliminates the symmetry of the forces around the azimuth angle. Furthermore, now that such forces are not symmetrical and neither is the coming flow -with respect to the normal direction to the rotor disc, the motion of the blades that was introduced previously -like flapping and lagging- appears in a more asymmetric way.

Back in vertical flight, such flapping and lagging movements could be assumed to have a much less noticeable effect, and even be neglected due to the small values of the flapping and lagging angles. This way the velocity components could be reduced to the ones already seen, v_c and v_i .

However, now in forward flight this motion is such that the tip path plane tilts from the rotor axis, leaving an extra blade movement that depends on the azimuth angle, and thus adding some velocity components besides the ones previously described.

In order to compute the velocity of the blade now in forward flight^[8], let us consider the no feathering plane mentioned before, which is flying towards the free-stream with an incidence of α_{nf} :

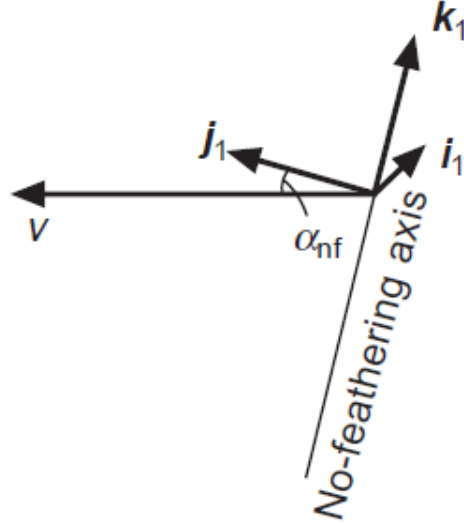


Figure 6: Orientation of the no feathering plane in forward flight [9]

Figure 6 shows that the no feathering plane moves with the velocity

$$\vec{V} = V \cos \alpha_{nf} \cdot \vec{j}_1 - V \sin \alpha_{nf} \cdot \vec{k}_1 \quad (18)$$

Parting from here, this velocity can be added to the one the blades have, Ωr . Expressed in the reference frame of the blade, the components are x in the radial and y in the azimuth direction. It must be noted that the azimuth angle ψ starts in 0 at the rear of the rotor -and has a value of 180° at the most forward side:

$$\vec{V}_{\text{blade,nf}} = \begin{cases} -V \cos \alpha_{nf} \cos \psi & \vec{e}_x \\ (\Omega r + V \cos \alpha_{nf} \sin \psi) & \vec{e}_y \\ -V \sin \alpha_{nf} & \vec{e}_z \end{cases} \quad (19)$$

Lastly, the blades advance also against the induced velocity component of the air; and the flapping motion must be taken too into account. Before that, however, and since flapping just came into scene, it is a good idea to rotate the velocity components so that they are expressed the blade frame, which will be slightly titled due to this motion. Suppose the change of frame from “horizontal” blade to flapping blade:

$$A_{fb} = \begin{bmatrix} \cos \beta & 0 & -\sin \beta \\ 0 & 1 & 0 \\ \sin \beta & 0 & \cos \beta \end{bmatrix}$$

Where the flapping angle β would turn out to be positive when the blade is tilted down. Then the velocity from equation (19) would be written as follows:

$$\vec{V}'_{\text{blade}} = \begin{cases} V \sin \alpha_{nf} \sin \beta - V \cos \alpha_{nf} \cos \psi \cos \beta & \vec{i} \\ (\Omega r + V \cos \alpha_{nf} \sin \psi) & \vec{j} \\ -(V \cos \alpha_{nf} \cos \psi \sin \beta + V \sin \alpha_{nf} \cos \beta) & \vec{k} \end{cases} \quad (20)$$

Finally the two remaining terms can be added. Both act on the vertical axis, since the flapping contribution acts perpendicular to both the blade and \vec{j} directions, and the induced velocity can be considered to be downwards of the airfoil profile. Thus, the final velocity equation for the blade is:

$$\vec{V}_{\text{blade}} = \begin{cases} V \sin \alpha_{\text{nf}} \sin \beta - V \cos \alpha_{\text{nf}} \cos \psi \cos \beta & \vec{i} \\ (\Omega r + V \cos \alpha_{\text{nf}} \sin \psi) & \vec{j} \\ -(V \cos \alpha_{\text{nf}} \cos \psi \sin \beta + V \sin \alpha_{\text{nf}} \cos \beta) - r\dot{\beta} + v_i & \vec{k} \end{cases} \quad (21)$$

If equation (21) has its sign changed, the result is the velocity of the air relative to the blade. Apart from that, the flapping terms can be linearized, since this angle is small.

Out of this velocity, the first term -the \vec{i} one- can be considered to be negligible. The third one, instead, will be the vertical velocity U_P for the calculation of forces. As for the tangential velocity U_T , it will be the \vec{j} -component of equation (21), so that finally the velocities used to find the forces are:

$$U_T = \Omega r + V \cos \alpha_{\text{nf}} \sin \psi \quad (22)$$

$$U_P = V \cos \alpha_{\text{nf}} \cos \psi \sin \beta + V \sin \alpha_{\text{nf}} \cos \beta - r\dot{\beta} - v_i \quad (23)$$

Again, as with vertical flight some components can be made non dimensional by dividing over ΩR . Here the operations are a bit different, and now a new set of variables is defined:

$$\mu = \frac{V \cos \alpha_{\text{nf}}}{\Omega R} \quad (24)$$

$$\lambda' = \frac{V \sin \alpha_{\text{nf}} \cos \beta - v_i}{\Omega R} \quad (25)$$

Equation (24) defines what is called the advance ratio. As it can be seen by looking at its components, the advance ratio establishes a relation between the rotor's angular velocity and the actual velocity of the vehicle. This is important because when applied to equation (23), a clearer vision of how the helicopter's speed affects the blade's relative velocity and incidence appears:

$$U_T = \Omega R(x + \mu \sin \psi) \quad (26)$$

The other term, λ , defined in equation (25) is the equivalent in forward flight to the previous sum of λ_c and λ_i . The main difference is that this time the sign of this component is negative, since U_P this time is taken from the wind velocity relative to the blade. With this and the advance ratio into account the vertical velocity can be displayed as follows:

$$U_P = \Omega R(\lambda' + \mu\beta\cos\psi + x\frac{\dot{\beta}}{\Omega}) \quad (27)$$

With these last two formulas, equation (15) can be rearranged slightly differently. Notice again that for vertical flight, the term U_P was the velocity of the rotor itself, whereas in this case it is the velocity *of the wind* relative to the rotor blade. Thus, the part corresponding to the angle ϕ must change its sign here, giving the following final equation:

$$\begin{aligned} dL &= \frac{1}{2}\rho ac U_T^2 \left(\theta + \frac{U_P}{U_T} \right) dr = \frac{1}{2}\rho ac (\theta U_T^2 + U_P U_T) dr \\ &= \frac{1}{2}\rho ac \Omega^2 R^3 \left[\theta (x + \mu \sin\psi)^2 + \left(\lambda' + \mu\beta\cos\psi + x\frac{\dot{\beta}}{\Omega} \right) (x + \mu \sin\psi) \right] dx \end{aligned} \quad (28)$$

Similarly to the vertical flight case, the thrust can be approximated as $dT \approx dL$. However, unlike before, this formula should not be integrated along the span x and then multiplied by the blades, since that could be done only in the vertical flight case. In this case, though, the forces depend on the azimuth angle ψ as it is showed in equation (28). Hence, two options could be taken.

The first option is to integrate this last equation along a whole revolution, and afterwards divide the result by 2π . What this accomplishes is to obtain the average value of the forces along the span of the blade. Then, integrating the result along such span and multiplying it by the number of blades should give the resultant *average* force on the rotor for each revolution.

The other option is to just leave equation (28) as it is, and do the same procedure with each blade -at its respective position. This way the “real” forces and moments can be computed at each step of time, and can be useful if a more “precise” approach is desired. This is the option that will be used for most of the following steps; however, the first one will also be useful to compute certain variables as the trim conditions, since the desired value shall not change with time and it is not the scope to find out force distributions in trim.

2.2 Induced velocity

As it was shown over last section, the induced velocity v_i is a highly important component for the equations of the forces. However, it is an unknown in each of the formulas for the thrust.

There are ways to compute it using the Momentum Theory alone. First, if the weight of the vehicle is known -which usually is, the equation for hover can be applied; this is, equation (11) with the condition that the velocity is 0 (the helicopter is “hovering” in the air). From that, the hovering induced velocity can

be found, and afterwards equation (11) can be made non-dimensional using this parameter. The result, having divided the thrust by the reference weight and the velocities on the other side of the equation by the hovering induced velocity, is the following:

$$\bar{v}_i \sqrt{\bar{V}_x^2 + (\bar{V}_z - \bar{v}_i)^2} = \bar{T} \quad (29)$$

This equation can be solved for \bar{v}_i , and if the result is multiplied by the hovering induced velocity, the real mean induced velocity is obtained. As for \bar{T} , assuming the helicopter is in equilibrium and the thrust is equal to the weight, this term will be ± 1 depending on whether the vertical velocity is positive or negative.

For axial descending flights, however, this procedure is no valid as before. Due to the appearance of vortices at low velocities within the vertical flight range $(-2v_{i,\text{hover}}, 0)$, the flow is not so well defined, and equation (29) cannot be applied. In order to get a fair approximation in this range, polynomials for the induced velocity have been empirically developed (whose coefficients vary depending on the source):

$$\bar{v}_i = 1 + k_1 \bar{V}_z + k_2 \bar{V}_z^2 + k_3 \bar{V}_z^3 \dots \quad (30)$$

There are two main drawbacks using this method directly. The first one is that the thrust may not be known, so solving for the term v_i if the helicopter is not in equilibrium or $\bar{T} = T/W \neq \pm 1$ might not be as straightforward as it appears. On the other hand, the value of v_i obtained using this method is assumed to be an average of the induced velocity distribution over the rotor. Thus, in order to use more precise methods like the Blade Element Theory it is not enough to just apply the v_i from equation (11).

While the Momentum theory alone might not be that useful alone to find an accurate distribution of velocities and forces, it can be very helpful when applied together with the Blade Element Theory. As it was seen before, equation (28) gives a more precise value of such elements, both depending on the radial and azimuth location. Again, the unknowns are the force and the induced velocity, but with the aid of the Momentum Theory there are now enough equations to find them. Together, this set of methods is also called “Blade Element Momentum Theory”, or BEMT.

The first and most simple case to solve for these variables is the vertical flight. That is so due to the symmetry that appears during this type of flight. Since there is only vertical inflow, the rotor is assumed to move normally to it, so the induced velocity distribution shall be the same without dependence of the azimuth angle, and only varies radially.

Hence, equation (16) can be assumed to be also its own average along a circumference contained in the rotor disc, for each section of one blade span. Then, it

may be multiplied by the total number of blades b to obtain the complete average over the circumference, and not just the value relative to one blade. With that in mind, the Momentum Theory can be modified to match the one just mentioned. Taking into account that this theory obtains the required values as a mean of their distribution over a certain area, such area can be set to be the circumference with thickness dr located at the same radius as the one chosen for Blade Element Theory.

Now that both equations refer to the same area, they can be joined together, thus eliminating the term dL and with v_i as the only unknown:

$$4\rho\pi R^2 x v_i (v_z + v_i) dx = \frac{1}{2} \rho abc \Omega^2 R^3 [\theta x^2 - (\lambda_c + \lambda_i) x] dx \quad (31)$$

This formula can be simplified by eliminating redundant elements such as the differentials. Then, changing the velocity elements by their non-dimensional form -so as to operate all of them correctly, the equation ends up like this:

$$8\pi R x \lambda_i (\lambda_c + \lambda_i) = abc [\theta x^2 - (\lambda_c + \lambda_i) x] \quad (32)$$

Finally, the induced component λ_i can be solved for rearranging this equation:

$$\lambda_i^2 + \lambda_i \left(\lambda_c + \frac{abc}{8\pi R} \right) + \frac{abc}{8\pi R} (\lambda_c - \theta x) = 0 \quad (33)$$

Here a new concept can be introduced. The term $\frac{bc}{\pi R}$ inside equation (33) can be rewritten to give the expression $\frac{bRc}{\pi R^2}$, and shows the relation of the total area of the blades over the rotor disc area. This concept is given the name of solidity, and is displayed with the letter σ :

$$\lambda_i^2 + \lambda_i \left(\lambda_c + \frac{a\sigma}{8} \right) + \frac{a\sigma}{8} (\lambda_c - \theta x) = 0 \quad (34)$$

Solving equation (34) -with the positive value of the root- and multiplying by ΩR to dimensionalize the result gives finally the induced velocity distribution for vertical flight:

$$v_i = \Omega R \left[- \left(\frac{\lambda_c}{2} + \frac{a\sigma}{16} \right) + \sqrt{\left(\frac{\lambda_c}{2} + \frac{a\sigma}{16} \right)^2 + \frac{a\sigma}{8} (\theta x - \lambda_c)} \right] \quad (35)$$

An interesting thing here is the term θx that appears inside the root. The first component refers to the blade's pitch while the second one to the blade's section location. If the blade can be set to have a variable geometric pitch, the value of θ will change over the span of the blade. On the one hand, this must be taken into account in order both to compute the values of the distribution and to integrate over x . However, the geometry may be said to be $\theta x = \theta_{\text{tip}}$, where θ_{tip} is a pre-determined angle at the end of the blade, and the pitch evolves gradually to that value with the form of the formula given. Such is called an ideal blade, and if that

is the case, then the term θx in equation (35) can be rewritten as just θ_{tip} , which makes the induced velocity constant all over the rotor disc.

While this procedure served for the vertical flight case, when studying forward flight it is not so useful. To begin with, if the forward velocity is relatively low -the advance ratio μ from equation (24) being lower than 0.1, the flow around the rotor disc is turbulent, and simplifications or assumptions that agree with the ones made in this project are difficult to make. In order to get a good study here, other theories such as vortex shed theories should be applied. For that reason, the scope here is to evaluate the behavior in the “high speed” case, where the advance ratio is greater than 0.1.

For this case, the free stream and the rotor disc are almost parallel, as opposed to vertical flight, where the flow incised perpendicularly to the disc. For this reason, the assumption that the induced velocity is the same without dependence on the azimuth angle cannot be made anymore, and thus the integration of the Blade Element Theory’s formula along such angle is now less useful. It still has some utility, however, as will be seen later.

In order to get a distribution for forward flight, then, some different theories were proposed.

A simple model was introduced by Glauert^[10], where the induced velocity is treated as a distribution parting from the mean value, which is symmetric in the longitudinal axis:

$$v_i(x, \psi) = v_{i0}(1 + Kx\cos\psi) \quad (36)$$

The value K from equation (36) is usually a value around 1.2, which gives the resulting induced velocity distribution the shape of a plane tilted around the \vec{j} axes of the body, in such way that the most forward part of the disc has a negative value while the back area is positive. However, there are more ways to express K . Some of them include the study of a vortex wake produced by the blades of the rotor. Depending on the flight velocity, the volume containing such wake would have certain angle with the normal to the free velocity:

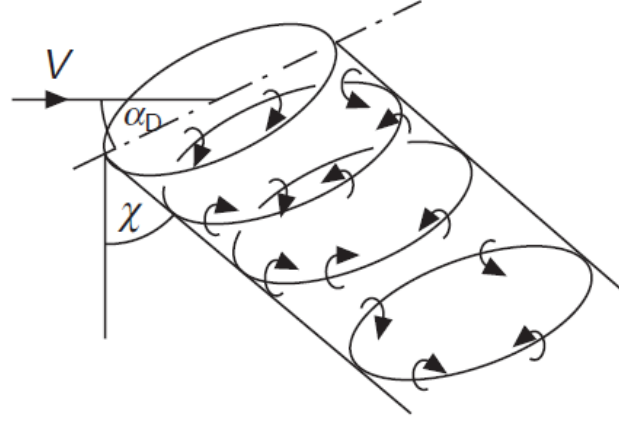


Figure 7: Angle between vortex and free flow [11]

The induced velocity could be applied using the Biot-Savart law to the wake. Since this procedure was very complicated and few exact expressions could be arranged with such method, only a series of elliptical integrals could be expressed on the disc axis. Thus, an approximation to this method resulted to be that K could be expressed as $\tan(\chi/2)$, although this failed to show the correct behavior at the leading edge (forward) of the disc.

Besides these two methods, there is another one which enables to obtain a much more accurate distribution of the induced velocity in forward flight, according to the comparisons with flight and wind tunnel experiments, as it will be seen in figure 8. Such is the method of Mangler and Squire^{[13],[14]}.

The procedure consisted on assuming a uniform velocity field where there were small perturbations in the region of the disc -the induced velocity. Then, potential flow conditions are satisfied and Laplace equation may be used to integrate the velocity.

After adequately integrating such method, the formula of the induced velocity ends up being a series of sum that depend in the incidence and azimuth angle, and the radial distance:

$$v_i = 4v_{i0} \left[\frac{1}{2}c_0 - \sum_{n=1}^{\infty} c_n(\eta, \alpha_D) \cos(n\psi) \right] \quad (37)$$

Where η has been obtained from x :

$$\eta^2 = 1 - x^2 \quad (38)$$

The components c_n vary in the following way: for odd values with $n > 4$, $c_n = 0$. Besides that, it has the following values:

$$n=0; \quad c_0 = 15\eta \frac{(1 - \eta^2)}{8} \quad (39)$$

$$n=1; \quad c_1 = -\frac{15\pi}{256}(5 - 9\eta^2)(1 - \eta^2)^{1/2} \left(\frac{1 - \sin\alpha_D}{1 + \sin\alpha_D} \right)^{1/2} \quad (40)$$

$$n=3; \quad c_3 = \frac{45\pi}{256}(1 - \eta^2)^{3/2} \left(\frac{1 - \sin\alpha_D}{1 + \sin\alpha_D} \right)^{3/2} \quad (41)$$

$$n \equiv \text{even}; \quad c_n = (-1)^{(n-2)/2} \frac{15}{8} \left[\frac{\eta + n}{n^2 - 1} \cdot \frac{9\eta^2 + n^2 - 6}{n^2 - 9} + \frac{3\eta}{n^2 - 9} \right] \times \left(\frac{1 - \eta}{1 + \eta} \right)^{n/2} \left(\frac{1 - \sin\alpha_D}{1 + \sin\alpha_D} \right)^{n/2} \quad (42)$$

As it can be seen then now, equation (37) does not only depend on the longitudinal position, as did Glauert's method, but it defines a value of the induced velocity for every point of the rotor disc. The only term remaining initially unknown is the mean induced velocity v_{i0} , but since, again, this is an average value, now it is possible to join the Momentum and Blade Element Methods -once this last one is integrated over the whole rotor- to solve for this component.

This method could be compared with experimental tests and the results were very accurate -more so as opposed with the previous methods, as it can be observed in figure 8:

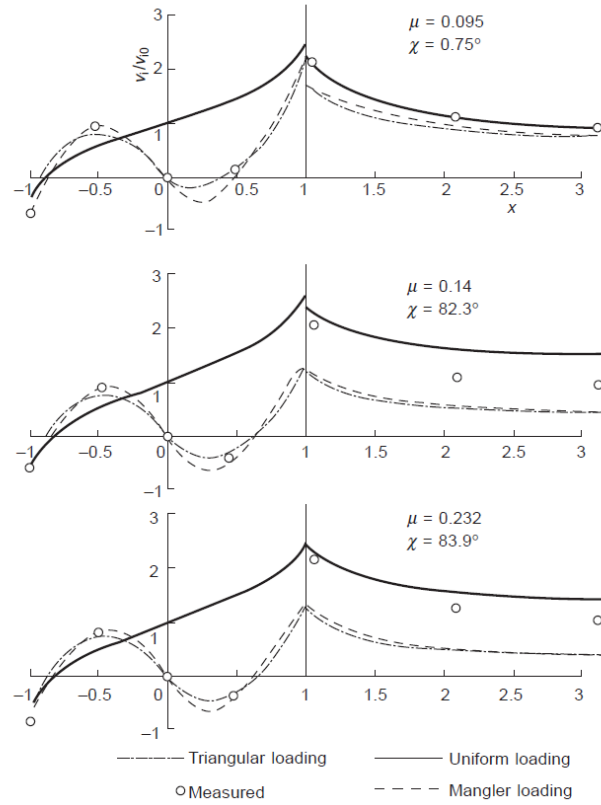


Figure 8: Comparison between methods [15],[16]

In the image above it can be seen that the method of Mangler and Squire highly resembles to the measured data. For that reason, this is the method used in this project for forward flight, in order to get more accuracy in the results.

In all these methods it has been seen that the induced velocity for forward flight can be expressed as a distribution based on a mean velocity. This mean velocity, however, is unknown for now, and will be obtained while computing the forces on the rotor.

2.3 Aerodynamic forces

Now that the induced velocity is known, the computation of the forces is one step closer. However, before rushing into the equations, let's observe a couple things:

The first one is to compare equations (16) and (28). As it was shown before, the first one belongs to vertical flight while the second one is used for forward flight. Nonetheless, this last equation can also be used for the former case, and it is even more complete since it takes into account blade movements like flapping. The only thing that should be changed for that is to eliminate the component μ , since the assumption here would be that the incidence of the flow is perpendicular to the rotor disc.

The other aspect to be taken into account is the flapping of the blade. This, at a first case, is an unknown, and there would be some ways to more or less resolve it. A first approximation could be to compute the forces assuming that there is no flapping and then try to find a value for this movement and its derivative -since it has been seen that both flapping and flapping velocity appear in the equation. With these values, calculating again the forces and keep on going until they more or less converge would be a method, but it is not the one used here. Since the flapping angle is usually small, there should not be much trouble assuming that this process will converge; however, it would take much time for just one try, and this will not be the case used here. The aim of this project is centered on the integration of the movement of both blades and helicopter, so the flapping position and velocity will be obtained from there at each step. The procedure will be later explained, so for now let's assume that the flapping and its derivative is already known at the moment of computing the forces.

Remembering equation (28), the formula was like this:

$$dL(x, \psi) = \frac{1}{2} \rho a c \Omega^2 R^3 \left[\theta(x + \mu \sin \psi)^2 + \left(\lambda' + \mu \beta \cos \psi + x \frac{\dot{\beta}}{\Omega} \right) (x + \mu \sin \psi) \right] dx \quad (43)$$

Now as it was said previously, there are some unknown components in this equation, such as the induced velocity contained inside λ' . For the vertical flight case, obtaining it is rather simple, since the only step is to apply equation (35) with the aid of the helicopter's data and vertical flight speed. The equation for lift distribution is complete after that, assuming that the term μ is 0 and the flapping motion is known.

The case of forward flight is more complex than this previous one, because although there is Mangler and Squire's method -or even Glauert- for finding the induced velocity, both need a previous average v_{i0} for its distribution. As it was shown in equation (11), this average can be assumed to depend on the thrust, T , and the incidence angle α_D . This angle, however, can be neglected since the forward flight for which this method is applied is usually very small.

Given this, a useful solution to this dilemma is to apply the Blade-Element Momentum Theory. This way the thrust to which the average induced velocity refers shall be the integrated distribution over the disc from equation (43).

In order to integrate lift equation, it may be rewritten with the induced velocity expressed in its Mangler and Squire form. Since this method uses the incidence angle with respect to the tip path plane instead of the no feathering one, here both will be supposed to be the same, since they are usually similar. Besides, although the flapping is supposedly known, let us assume here that it is a series of sines and cosines, in the following form:

$$\beta = a_0 - \sum_{n=1}^{\infty} (a_n \cos(n\psi) + b_n \sin(n\psi)) = a_0 - a_1 \cos\psi - b_1 \sin\psi - a_2 \cos 2\psi - b_2 \sin 2\psi + \dots \quad (44)$$

$$\frac{\dot{\beta}}{\Omega} = \frac{\partial \beta}{\partial \psi} = a_1 \sin\psi - b_1 \cos\psi + 2a_2 \sin 2\psi - 2b_2 \cos 2\psi \dots \quad (45)$$

The reason to do this despite knowing the flapping is due to the integration of the thrust. The flapping motion may be known at a certain moment, but that is just because of the numerical integration previously performed. Thus, the general flapping behavior over the disc is initially unknown, save from the fact that within steady flight conditions it acts as a series of sines and cosines, whose coefficients become much smaller as the order n increases^{[17],[18]}.

With this and the induced velocity in mind, and remembering the expressions of μ and λ' from equations (24) and (25), equation (43) can finally be operated with.

The first thing to do is to obtain the average thrust at the rotor by integrating this formula over a whole loop and dividing it by 2π . After that only remains to integrate the result along the blade span and multiply it times the total number of blades. This way the whole average thrust will be available to solve for the mean induced velocity, v_{i0} .

Having said this, the average thrust per unit span is:

$$dT(x) = \frac{1}{2\pi} \int_0^{2\pi} dL(x, \psi) d\psi \quad (46)$$

$$= \frac{1}{2} \rho a c \Omega^2 R^3 \left[\theta \left(x^2 + \frac{1}{2} \mu^2 \right) + \frac{V \sin \alpha_{nf}}{\Omega R} x - \frac{v_{i0}}{\Omega R} 2C_0 x + \frac{1}{2} \mu^2 b_2 \right] dx \quad (47)$$

Notice that by integrating equation (43) over the whole revolution, most of the terms for flapping disappear, as well as the sine and cosine terms belonging to Mangler and Squire's expression. In fact, the term b_2 may also be neglected for this case, since as it was said before, these components become much smaller as n increases. Also, the components $\frac{V}{\Omega R}$ and $\frac{v_{i0}}{\Omega R}$ may be expressed as \hat{V} and λ_i . The equation is then integrated along the span and multiplied times the number of blades, and retaining that $\lambda = \hat{V} \sin \alpha_{nf} - \lambda_i$, the following expression is obtained:

$$T = \frac{1}{4} \rho a b c \Omega^2 R^3 \left[\frac{2}{3} \theta_0 \left(1 + \frac{3}{2} \mu^2 \right) + 2 \int_e^1 \theta_{base} \left(x^2 + \frac{1}{2} \mu^2 \right) dx + \lambda \right] \quad (48)$$

Here the remaining integral belongs to the geometric pitch of the blade, which will depend on the helicopter's properties. As for the rest, the chord c is assumed here to be constant. The lower limit of integration e refers to the start of the blade,

which may be 0 or other value depending on whether the blade is connected to a separated hinge. While right now there is little difference in the result, since the distance e to the hinge is also very small, it will become relevant when computing the flapping and lagging motions at each time step.

Now that the full, average thrust per revolution is defined, it can be added to the formula for the mean induced velocity in forward flight, which leads to the following equation:

$$v_{i0} \approx \frac{T}{2\rho SV} = \frac{T}{2\rho\pi R^2 V} \quad (49)$$

$$= \frac{abc\Omega^2 R}{8\pi V} \left[\frac{2}{3}\theta_0 \left(1 + \frac{3}{2}\mu^2 \right) + 2 \int_e^1 \theta_{\text{base}} \left(x^2 + \frac{1}{2}\mu^2 \right) dx + \lambda \right]$$

With this all the components but the induced velocity are known, so the only remaining task is to solve for this term, giving out the expression for v_{i0} -remember that $\lambda = \hat{V} \sin\alpha_{\text{nf}} - \lambda_i = \frac{V \sin\alpha_{\text{nf}} - v_{i0}}{\Omega R}$:

$$v_{i0} = \frac{abc\Omega^2 R}{8\pi V + abc\Omega} \left[\frac{2}{3}\theta_0 \left(1 + \frac{3}{2}\mu^2 \right) + 2 \int_e^1 \theta_{\text{base}} \left(x^2 + \frac{1}{2}\mu^2 \right) dx + \frac{V}{\Omega R} \sin\alpha_{\text{nf}} \right] \quad (50)$$

At last, the term v_{i0} is known and equation (43) can finally be applied to obtain the thrust distribution. The only requisites are to set the angle ψ to whichever position the desired blade is in, and the aerodynamic forces over that blade will be easily computed. If this is to be performed for every blade, and taking into account that $\psi = \Omega t$, one can assume that $\psi_i = \Omega t + 2\pi \frac{i-1}{b}$, where i belongs to each blade. Here the lagging movement could also be taken into account, both for the very angle ψ and inside the rotation Ω , obtaining the following angles and rotations:

$$\psi_{\text{blade}} = \psi_{\text{rotation}} + \xi_{\text{lag}} \quad (51)$$

$$\Omega_{\text{blade}} = \Omega + \dot{\xi}_{\text{lag}} \quad (52)$$

However, its effect is most of the time negligible, so it is not worth increasing so much the complexity of the problem by adding these terms right now.

The remaining aerodynamic force component is the drag, which similarly to vertical flight, has the following form:

$$dD = \frac{1}{2} \rho U_T^2 c \delta dr = \frac{1}{2} \rho \Omega^2 R^3 (x + \mu \sin\psi) c \delta dx \quad (53)$$

Since the value of δ was taken from statistical data, in this project it was $\delta = 0.013$. This implies that in this case, the drag coefficient has been assumed to be only

C_{D0} , neglecting the effect of α .

Finally, the last step is to obtain these forces in such way that they are properly oriented with respect to the adequate reference frames, in order to make computations easier in the future. To begin with, both lift and drag can be displayed so as to obtain vertical (the thrust T) and horizontal forces on the rotor. Remember also that the blades are affected by the flapping movement, whose angle is positive when the blade is tilted downwards:

$$dT(x, \psi) = (dL \cos \phi + dD \sin \phi) \cos \beta \approx dL \quad (54)$$

Where the angle ϕ is the one formed by the horizontal and vertical velocities, U_T and U_P . Being usually a small angle, it can be approximated as $\phi \approx U_P/U_T$.

Note that this approximation has been the one used to compute the thrust in these previous steps. As for the horizontal forces on the no feathering plane, their respective expressions and approximations are as follows:

$$dH_{\text{radial}}(x, \psi) = (dL \cos \phi + dD \sin \phi) \sin \beta \approx \beta dL \quad (55)$$

$$dH_{\text{rear}}(x, \psi) = (dL \sin \phi - dD \cos \phi) \approx dL \phi - dD \quad (56)$$

These are the forces expressed in the radial, tangential and vertical directions of the no feathering plane. Another way to express them is in the x , y and z positions of such plane, playing this time with the angle ψ . Notice that here the vertical force, T , is the same since both vertical directions are also the same one, but the other two forces must be changed. Notice, too, that in this disposition the direction $-x$ points rear of the disc, in the wind's direction, and direction $-y$ follows a right-hand rule assuming that the vertical $-z$ points upwards:

$$dH_x = dH_{\text{radial}} \cos \psi - dH_{\text{rear}} \sin \psi \quad (57)$$

$$dH_y = dH_{\text{radial}} \sin \psi + dH_{\text{rear}} \cos \psi \quad (58)$$

Now that all these forces have been computed and displayed in different directions, they can be integrated and operated with in order to find the moments on the blade hinges, and from that calculate the blade movements -flapping and lagging.

3 Helicopter Forces

Right now the aerodynamic forces on each blade at any time have been computed; however, there are still some terms in such equations that need to be taken care of. Moreover, the actual forces acting on the rotor hinge, which will then translate to the rest of the helicopter's body, still need to be computed.

To begin with, the components referring to the flapping and its derivatives need to be calculated for each time step. This will be useful both for writing the correct inputs in the thrust equation and for obtaining the blade's acceleration, which will serve to find the forces acting on the hinge. The last step would be then finding the rest of the forces and moments acting on the whole helicopter in order to have a full rigid body diagram.

3.1 Blade movements

Let us recall the thrust and horizontal force distribution equations, assuming that both angles ϕ and β are generally small:

$$dT \approx dL \quad (59)$$

$$dH_x \approx dL(\beta \cos\psi - \phi \sin\psi) + dD \sin\psi \quad (60)$$

$$dH_y \approx dL(\beta \sin\psi + \phi \cos\psi) - dD \cos\psi \quad (61)$$

On the other hand, let us consider a generic blade rotating around the rotor shaft. This rotation, along with the blade's own weight and the aerodynamic forces on itself, will produce movements induced by the moment of the forces on the hinge and their centrifugal acceleration. Assuming that we are considering such blade on the no feathering plane, these movements will only be flapping and lagging, since this plane eliminates feathering and sets a constant pitch angle.

Hence, the effect of the blade's motion will position it at certain angles with respect to the no feathering plane. Given this, it may be advisable to reorient the forces and moments to match a reference frame in the same orientation as the blade at each time. The expression of these angles will depend on the design of the blade's hinge. The order of the flapping hinge versus the lagging hinge, as well as their distance to the shaft axis, will determine both the order of the reference frame transformations and the effect of the forces and moments, although the overall procedure to solve this problem will not change.

In this project specifically the lagging and flapping hinges are assumed to be at the same location -i.e., there will be only one distance e to the hinge for all the blade movements. As for the order of the angles, the lagging is supposed to be

taken first into account, and after it the flapping will come into scene. Thus, the final picture of how such angles would look similar to this:

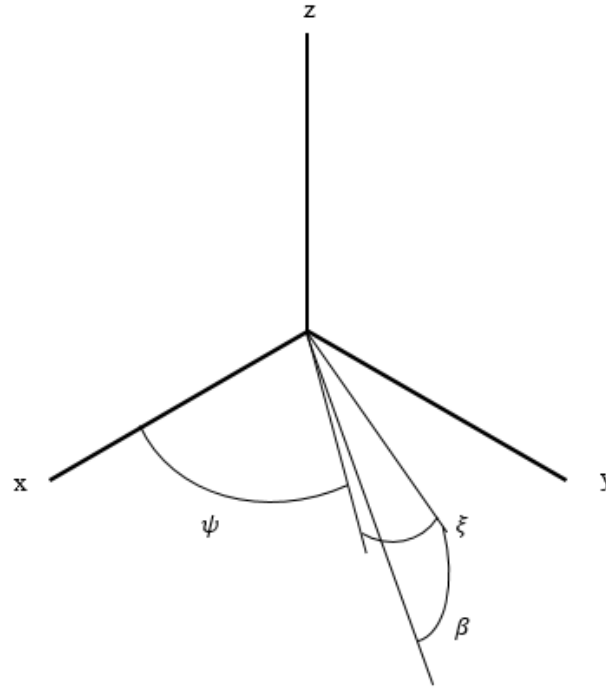


Figure 9: Flapping and lagging angles of a blade

In figure 9 the hinge distance e has been neglected, only for the purpose of showing how the blade lagging and flapping angles are disposed. Following the right hand rule, a positive lag here advances the blade and a positive flap angle tilts its further side from the axis downwards.

This, however, was only a choice of sign criteria. Other articles, books and pieces of work, for example, choose to set the flapping angle as positive when the blade is tilted upwards^[19], or even change the order and compute first the flapping and then the lagging^[20]. In this case the choice was made to comply with the right hand rule in the frame of the blade, whose directions point outward, forward and upward.

Now that the angles and their signs are defined, it is advisable to transform the forces' directions into the ones belonging to an already lagged and flapped blade. The same will be done to the accelerations and rotations needed to compute the blade movement. This way, everything will be represented in just one frame and will be easier to compute the rest of the solutions.

In order to do all this, the transformation matrices must be obtained. Such matrices will convert, respectively, the $-xyz$ frame to the ψ frame -the blade's orientation if it were only for the shaft rotation; from there to its lagged orientation $-\xi$ and from this one to the flapped $-\beta$. Hence, the transformation matrices finally

are:

$$A_{xyz}^{\psi} = \begin{bmatrix} \cos\psi & \sin\psi & 0 \\ -\sin\psi & \cos\psi & 0 \\ 0 & 0 & 1 \end{bmatrix} \quad (62)$$

$$A_{\psi}^{\xi} = \begin{bmatrix} \cos\xi & \sin\xi & 0 \\ -\sin\xi & \cos\xi & 0 \\ 0 & 0 & 1 \end{bmatrix} \quad (63)$$

$$A_{\xi}^{\beta} = \begin{bmatrix} \cos\beta & 0 & -\sin\beta \\ 0 & 1 & 0 \\ \sin\beta & 0 & \cos\beta \end{bmatrix} \quad (64)$$

Notice that there is no transformation for the feathering angles. This is so because all these steps are being taken still at the no feathering plane. This way two things happen: first, the equations are slightly eased because the feathering terms are not necessary; and second, the final solution for the blade movements will be *with respect to the no feathering plane*. This must be kept in mind in the future, since the computed flapping angle might need to be adapted to other frames.

With the transformation matrices already displayed, the forces found in equations (59), (60) and (61), which right now are expressed in the $-xyz$ reference frame, may be converted to the $-\beta$ one:

$$\vec{F}_{\beta} = A_{\xi}^{\beta} A_{\psi}^{\xi} A_{xyz}^{\psi} \cdot \vec{F}_{xyz} = A_{xyz}^{\beta} \cdot \vec{F}_{xyz} \quad (65)$$

$$d\vec{F}_{\beta} = \begin{bmatrix} dF_i^{\vec{r}} \\ dF_j^{\vec{r}} \\ dF_k^{\vec{r}} \end{bmatrix} = A_{xyz}^{\beta} \begin{bmatrix} dH_x \\ dH_y \\ dT \end{bmatrix} \quad (66)$$

Now all the aerodynamic forces are disposed in such way that their components are aligned with the $-\beta$ reference frame. With this the moments at the hinge can also be easily computed. For that, the distance between the hinge and the location of the forces is considered to be right in the span of the blade, so that the cross product is:

$$d\vec{M} = \begin{vmatrix} \vec{i} & \vec{j} & \vec{k} \\ r & 0 & 0 \\ dF_i^{\vec{r}} & dF_j^{\vec{r}} & dF_k^{\vec{r}} \end{vmatrix} = \begin{bmatrix} 0 \\ -rdF_j^{\vec{r}} \\ rdF_k^{\vec{r}} \end{bmatrix} \quad (67)$$

And so, the total moment in the hinge of the blade due to the aerodynamic moments is:

$$\vec{M}_{\text{hinge}} = \begin{bmatrix} L \\ M \\ N \end{bmatrix} = \int_e^1 d\vec{M} dx \quad (68)$$

The same procedure could be done with the gravity force on the blade; however,

its value is negligible compared to the aerodynamic forces (a blade's mass is usually around 70-80kg -meaning around 700-800N- while the forces may go up to the order of 10^4N).

Since now the moments have already been calculated, the Extended Euler's Equations of Motion can be written^[21]. Taking the assumption that the actual reference frame is on the principal axis -thanks to the previous transformations, such equations are as follows:

$$L = A\dot{\omega}_1 - (B - C)\omega_2\omega_3 + M_b(y_g a_z - z_g a_y) \quad (69)$$

$$M = B\dot{\omega}_2 - (C - A)\omega_3\omega_1 + M_b(z_g a_x - x_g a_z) \quad (70)$$

$$N = C\dot{\omega}_3 - (A - B)\omega_1\omega_2 + M_b(x_g a_y - y_g a_x) \quad (71)$$

In the equations above the component M_b is the mass of each blade. Also, the terms A , B and C represent the moments of inertia of the blade, related to its principal axes, x (blade's length), y (chord's thickness) and z (blade's thickness), and assumed at the middle chord:

$$A = \sum m(y^2 + z^2) \approx \sum my^2 = \frac{1}{12}M_b c^2 \quad (72)$$

$$B = \sum m(x^2 + z^2) \approx \sum mx^2 = \frac{1}{3}M_b(R - eR)^2 \quad (73)$$

$$C = \sum m(x^2 + y^2) \approx A + B \quad (74)$$

It can be seen here that the thickness of the blade can be considered negligible, compared both to its chord and length.

As for the other components of the Extended Euler's Equations, ω_i and $\dot{\omega}_i$ represent the angular velocity and acceleration of the blade, while a_i belongs to the linear acceleration at the blade's hinge. Finally, x_g , y_g and z_g are the distance from the hinge to the center of mass of the blade. In this case the blade is assumed to have an uniform mass, so such distance can be simplified to be $x_g = R\frac{1-e}{2}$ and $y_g = z_g = 0$.

Now most of the concepts for the Extended Euler's Equations have been defined, save for the rotations and accelerations of the blade. Moreover, they need to be transformed to the blade's reference frame.

Starting with the blade's rotation, $\vec{\omega}$, it can be separated in different components. On the one hand, and assuming constant collective pitch, there is the own shaft rotation, Ω , which moves the blade around the shaft. However, there are also $\dot{\beta}$ and $\dot{\xi}$, which are the rotations due to flapping and lagging respectively. Furthermore, each one of them is in its own reference frame, so there will be different transformations for all three. Besides of them, let us add a term $\dot{\theta}$, even

though here in the non feathering plane it is known to be 0. Said that so, the final blade rotation in the $-\beta$ reference frame is:

$$\vec{\omega} = \begin{bmatrix} \omega_1 \\ \omega_2 \\ \omega_3 \end{bmatrix} = A_{xyz}^\beta \begin{bmatrix} 0 \\ 0 \\ \Omega \end{bmatrix} + A_\xi^\beta A_\psi^\xi \begin{bmatrix} 0 \\ 0 \\ \dot{\xi} \end{bmatrix} + A_\xi^\beta \begin{bmatrix} 0 \\ \dot{\beta} \\ 0 \end{bmatrix} + \begin{bmatrix} \dot{\theta} \\ 0 \\ 0 \end{bmatrix} \quad (75)$$

With this rotation finally obtained, its derivative $\dot{\omega}$ can also be found. Remember for this that the transformation matrices also depend on variables like Ω , β and ξ , so their derivatives will still need to be computed:

$$\dot{A}_{xyz}^\psi = \begin{bmatrix} -\Omega \sin \psi & \Omega \cos \psi & 0 \\ -\Omega \cos \psi & -\Omega \sin \psi & 0 \\ 0 & 0 & 0 \end{bmatrix} \quad (76)$$

$$\dot{A}_\psi^\xi = \begin{bmatrix} -\dot{\xi} \sin \xi & \dot{\xi} \cos \xi & 0 \\ -\dot{\xi} \cos \xi & -\dot{\xi} \sin \xi & 0 \\ 0 & 0 & 0 \end{bmatrix} \quad (77)$$

$$\dot{A}_\xi^\beta = \begin{bmatrix} -\dot{\beta} \sin \beta & 0 & -\dot{\beta} \cos \beta \\ 0 & 0 & 0 \\ \dot{\beta} \cos \beta & 0 & -\dot{\beta} \sin \beta \end{bmatrix} \quad (78)$$

These three matrices can be applied together to find \dot{A}_{xyz}^β and \dot{A}_ψ^β :

$$\begin{aligned} \dot{A}_{xyz}^\beta &= \dot{A}_\xi^\beta A_\psi^\xi A_{xyz}^\psi + A_\xi^\beta \dot{A}_\psi^\xi A_{xyz}^\psi + A_\xi^\beta A_\psi^\xi \dot{A}_{xyz}^\psi \\ \dot{A}_\psi^\beta &= \dot{A}_\xi^\beta \cdot A_\psi^\xi + A_\xi^\beta \cdot \dot{A}_\psi^\xi \end{aligned} \quad (79)$$

The derivative of the rotation can be then written:

$$\begin{aligned} \dot{\vec{\omega}} &= \begin{bmatrix} \dot{\omega}_1 \\ \dot{\omega}_2 \\ \dot{\omega}_3 \end{bmatrix} \\ &= \dot{A}_{xyz}^\beta \begin{bmatrix} 0 \\ 0 \\ \Omega \end{bmatrix} + \dot{A}_\psi^\beta \begin{bmatrix} 0 \\ 0 \\ \dot{\xi} \end{bmatrix} + A_\xi^\beta A_\psi^\xi \begin{bmatrix} 0 \\ 0 \\ \ddot{\xi} \end{bmatrix} + \dot{A}_\xi^\beta \begin{bmatrix} 0 \\ \dot{\beta} \\ 0 \end{bmatrix} + A_\xi^\beta \begin{bmatrix} 0 \\ \ddot{\beta} \\ 0 \end{bmatrix} + \begin{bmatrix} \ddot{\theta} \\ 0 \\ 0 \end{bmatrix} \end{aligned} \quad (80)$$

The only remaining component now is the blade's hinge acceleration. For this, taking the term Ω from the shaft rotation, such acceleration is:

$$a_{\text{hinge}} = \begin{bmatrix} -eR\Omega^2 \cos \psi \\ -eR\Omega^2 \sin \psi \\ 0 \end{bmatrix} \quad (81)$$

Which is expressed in the $-xyz$ frame, so in order for it to match the $-\beta$ frame as the other components, it needs to be multiplied by the transformation matrices:

$$a_{\text{hinge},\beta} = \begin{bmatrix} a_x \\ a_y \\ a_z \end{bmatrix}_\beta = A_{xyz}^\beta \begin{bmatrix} -eR\Omega^2 \cos\psi \\ -eR\Omega^2 \sin\psi \\ 0 \end{bmatrix} \quad (82)$$

Now all the components of equations (69), (70) and (71) are ready, and they can be used to find the flapping and lagging movements. Notice that this system can be rearranged and expressed as a set of three second order differential equations. The procedure to solve the system analytically would be tough by hand, and the transformation matrices might even need to be linearized. However, with a matlab function such as Ode45 the formulas can be displayed solving for the second derivatives, and afterwards integrating them. First of all, let us remember equation (80). Fortunately, the elements belonging to the second derivatives are separated, so this formula can be rewritten as follows:

$$\ddot{\vec{\omega}} = (\dot{A}_{xyz}^\beta \cdot \vec{\omega}_\Omega + \dot{A}_\psi^\beta \cdot \vec{\omega}_\xi + \dot{A}_\xi^\beta \cdot \vec{\omega}_\beta) + A_\psi^\beta \cdot \dot{\vec{\omega}}_\xi + A_\xi^\beta \cdot \dot{\vec{\omega}}_\beta + \dot{\vec{\omega}}_\theta \quad (83)$$

It can be seen here that the angular velocities and accelerations with subscripts ξ , β and θ belong to their respective letters in equation (80), as well as the transformations with each of them. The terms have been displayed so that the ones that are not second derivatives remain in a separate block. We will call this block $\ddot{\vec{\omega}}_0$. Then, this angular acceleration may be written inside the Extended Euler's Equation, which multiplies its 3 terms by A , B and C respectively. Given that, and remembering that the components y_g and z_g are 0, the result looks like this:

$$\begin{bmatrix} L \\ M \\ N \end{bmatrix} = \begin{bmatrix} A & 0 & 0 \\ 0 & B & 0 \\ 0 & 0 & C \end{bmatrix} (\dot{\vec{\omega}}_0 + A_\psi^\beta \cdot \dot{\vec{\omega}}_\xi + A_\xi^\beta \cdot \dot{\vec{\omega}}_\beta + \dot{\vec{\omega}}_\theta) - \begin{bmatrix} (B - C)\omega_2\omega_3 \\ (C - A)\omega_3\omega_1 + M_b x_g a_z \\ (A - B)\omega_1\omega_2 - M_b x_g a_y \end{bmatrix} \quad (84)$$

With this disposition it is much easier to solve for the second derivatives and obtain a final system of equations. In order to do so, the part of the angular acceleration that does not contain $\ddot{\vec{\omega}}_0$ can be rearranged as a matrix with three columns multiplying a vector with each acceleration ($\ddot{\xi}$, $\ddot{\beta}$ and $\ddot{\theta}$). This way, such product can be set as the left hand side of the formula while moving the remaining components to the right hand side, as can be seen in equation (85):

$$\begin{aligned} A_\psi^\beta \cdot \dot{\vec{\omega}}_\xi + A_\xi^\beta \cdot \dot{\vec{\omega}}_\beta + \dot{\vec{\omega}}_\theta &= \begin{bmatrix} A_1 & B_1 & 1 \\ A_2 & B_2 & 0 \\ A_3 & B_3 & 0 \end{bmatrix} \cdot \begin{bmatrix} \ddot{\xi} \\ \ddot{\beta} \\ \ddot{\theta} \end{bmatrix} \\ &= \begin{bmatrix} \frac{1}{A} & 0 & 0 \\ 0 & \frac{1}{B} & 0 \\ 0 & 0 & \frac{1}{C} \end{bmatrix} \begin{bmatrix} L + (B - C)\omega_2\omega_3 \\ M + (C - A)\omega_3\omega_1 + M_b x_g a_z \\ N + (A - B)\omega_1\omega_2 - M_b x_g a_y \end{bmatrix} - \dot{\vec{\omega}}_0 \end{aligned} \quad (85)$$

This equation is almost ready to find the second derivatives. The new terms

appearing here, A_i and B_i , belong respectively to the elements of the third and second column of the matrices A_ψ^β and A_ξ^β , which are the ones that remain after multiplying them with the vectors $\ddot{\omega}_\xi$ and $\ddot{\omega}_\beta$. Besides, let us call the right hand side of equation (85) as a matrix named K , whose rows will be K_1 , K_2 and K_3 . This way, equation (85) can be expressed as:

$$\begin{bmatrix} A_1 & B_1 & 1 \\ A_2 & B_2 & 0 \\ A_3 & B_3 & 0 \end{bmatrix} \cdot \begin{bmatrix} \ddot{\xi} \\ \ddot{\beta} \\ \ddot{\theta} \end{bmatrix} = \begin{bmatrix} K_1 \\ K_2 \\ K_3 \end{bmatrix} \quad (86)$$

With this form, all three movements of the blade are finally related between them and their derivatives. The last step is to solve for the required ξ and β , which leads to their respective formulas:

$$\ddot{\xi} = \frac{B_2 K_3 - B_3 K_2}{B_2 A_3 - B_3 A_2} \quad (87)$$

$$\ddot{\beta} = \frac{K_2 - A_2 \ddot{\xi}}{B_2} \quad (88)$$

These terms now can be finally added to the function Ode45 in matlab, so that the motion of the blades may be integrated.

While this procedure has been used in this project to integrate the movement of the blades, another different method is used later in further steps to find elements such as the trim position of the helicopter and its swash plate. It is based on the assumption that the flapping may be expressed as a series of sines and cosines, and by applying this formula to the second Euler equation -equation (70), it tries to obtain the respective coefficients a_0 , a_1 and a_1 . This method, which will be fully explained in that section, simplifies some terms, but is also accurate enough to obtain a fair approximation of the required trim positions.

3.2 Forces on the hinge

In the previous sections the aerodynamic forces on the blade were found, as well as the flapping and lagging which help to complete their equations. However, in order to find the forces in the helicopter to simulate the flight, those affecting the hinge between the blade and the main body must be obtained. In other words, the aerodynamic forces of the blade will cause a reaction on the helicopter's hinge, which will help it to move in flight. Remember that the helicopter and the blades are not just one rigid body, but the latter ones are considered to be rigid bodies separated from the main one.

Having said this, the procedure to obtain the forces at the hinge comes by the second Newton's law on the blade:

$$\sum \vec{F} \approx \vec{F}_{\text{aero}} + \vec{F}_{\text{blade's hinge}} = \frac{\partial}{\partial t}(m \cdot \vec{v}) = M_b \cdot \vec{a} \quad (89)$$

Here the force equations are being computed in the blade rigid body, so applying the third Newton's law the actual forces on the helicopter's hinge would have the opposite sign as those at calculated at the blade.

Since the result of this procedure will not be on the blades but on the helicopter, the reference frame used here will be the rotor disc. For that, the aerodynamic forces will be T , H_x and H_y from equations (59), (60) and (61) will need to be changed from their no feathering $-xyz$ frame to the disc one. This may be done by approximating the forces in the $-x$ and $-z$ directions in the following way^[22]:

$$T_{nf} \approx T_{disc} \quad (90)$$

$$H_{x,nf} - T_{x,nf} \cdot B_1 \approx H_{x,disc} \quad (91)$$

Where B_1 is the sine component of the feathering motion, which was expressed in equation (2). Given all that, the hinge forces on the helicopter are given by the following formula:

$$\vec{F}_{hinge} = - \begin{bmatrix} F_{blade's \ hinge,x} \\ F_{blade's \ hinge,y} \\ F_{blade's \ inge,z} \end{bmatrix} = - \begin{bmatrix} M_b a_x - H_x \\ M_b a_y - H_y \\ M_b a_z - T \end{bmatrix} \quad (92)$$

The remaining term now to complete this equation is the acceleration. However, this one is different from the one calculated earlier. To begin with, the previous one was the hinge acceleration, while now the acceleration at the blade's center of gravity is needed. Moreover, this time the desired reference frame is the $-xyz$ one, so the transformations will not go the same way as before.

Let us start by writing the coordinates of the blade's center of gravity from the shaft axis. This will include the distance from the axis to the hinge, plus the distance from the hinge to the actual center:

$$\vec{r}_{cg} = eR \cdot \vec{e}_{1,\psi} + \frac{R - eR}{2} \cdot \vec{e}_{1,\beta} = eR \cdot \vec{e}_{1,\psi} + r_g \cdot \vec{e}_{1,\beta} \quad (93)$$

Notice that these coordinates are written in two different reference frames. The first component is expressed in the $-\psi$ frame, while the second one is in the $-\beta$ one. This was done so because those were the planes for which each of the coordinates was easier to be expressed. And since we already have the transformation matrices between each frame, the coordinates can be easily written in the $-\psi$ reference frame by multiplying the second term times the inverse of the matrix A_ψ^β :

$$\begin{aligned}
(A_\psi^\beta)^{-1} &= (A_\psi^\xi)^T \cdot (A_\xi^\beta)^T = \begin{bmatrix} \cos\xi & -\sin\xi & 0 \\ \sin\xi & \cos\xi & 0 \\ 0 & 0 & 1 \end{bmatrix} \cdot \begin{bmatrix} \cos\beta & 0 & \sin\beta \\ 0 & 1 & 0 \\ -\sin\beta & 0 & \cos\beta \end{bmatrix} \\
&= \begin{bmatrix} \cos\xi\cos\beta & -\sin\xi & \cos\xi\sin\beta \\ \sin\xi\cos\beta & \cos\xi & \sin\xi\sin\beta \\ -\sin\beta & 0 & \cos\beta \end{bmatrix}
\end{aligned} \tag{94}$$

However, the values here for β are not exactly the same as the ones before. Since the ones previously calculated belong to a flapping located on the no feathering plane, now we must subtract them the effect of the feathering motion, like with the forces before. This time, the conversion is as follows:

$$\beta = \beta_{nf} + A_1 \sin\psi - B_1 \cos\psi \tag{95}$$

$$\dot{\beta} = \dot{\beta}_{nf} + \Omega A_1 \cos\psi + \Omega B_1 \sin\psi \tag{96}$$

$$\ddot{\beta} = \ddot{\beta}_{nf} - \Omega^2 A_1 \sin\psi + \Omega^2 B_1 \cos\psi \tag{97}$$

With this, the final vector for the position of the center of mass is:

$$\vec{r}_{cg} = (eR + r_g \cos\xi \cos\beta) \cdot \vec{e}_1 + r_g \sin\xi \cos\beta \cdot \vec{e}_2 - r_g \sin\beta \cdot \vec{e}_3 \tag{98}$$

Now the last step to obtain the components of the acceleration is to derive the position equation, taking into account that the coordinates $-e_i$ of the $-\psi$ frame are polar coordinates:

$$a_1 = r_g \left(\frac{\partial^2}{\partial t^2} (\cos\xi \cos\beta) - 2\Omega \frac{\partial}{\partial t} (\sin\xi \cos\beta) - \Omega^2 \cos\xi \cos\beta \right) - \Omega^2 eR \tag{99}$$

$$\begin{aligned}
&= -r_g (\ddot{\xi} \sin\xi \cos\beta + \ddot{\beta} \cos\xi \sin\beta + (\dot{\xi}^2 + \dot{\beta}^2 - 2\Omega \dot{\xi} - \Omega^2) \cos\xi \cos\beta \\
&\quad + (2\Omega - 2\dot{\xi}) \dot{\beta} \sin\xi \sin\beta) - \Omega^2 eR
\end{aligned}$$

$$a_2 = r_g \left(\frac{\partial^2}{\partial t^2} (\sin\xi \cos\beta) + 2\Omega \frac{\partial}{\partial t} (\cos\xi \cos\beta) - \Omega^2 \sin\xi \cos\beta \right) \tag{100}$$

$$\begin{aligned}
&= r_g (\ddot{\xi} \cos\xi \cos\beta - \ddot{\beta} \sin\xi \sin\beta - (\dot{\xi}^2 + \dot{\beta}^2 - 2\Omega \dot{\xi} - \Omega^2) \sin\xi \cos\beta \\
&\quad + (2\Omega + 2\dot{\xi}) \dot{\beta} \cos\xi \sin\beta)
\end{aligned}$$

$$a_3 = -r_g \frac{\partial^2}{\partial t^2} \sin\beta \tag{101}$$

$$= r_g (\dot{\beta}^2 \sin\beta - \ddot{\beta} \cos\beta)$$

The components of the acceleration are now in the $-\psi$ reference frame of the rotor disc; however, they must be displayed in certesian coordinates, so now their final form is:

$$a_x = a_1 \cos \psi - a_2 \sin \psi \quad (102)$$

$$a_y = a_1 \sin \psi + a_2 \cos \psi \quad (103)$$

$$a_z = a_3 \quad (104)$$

With the acceleration components just found in (102), (103) and (104), now equation (92) can finally be solved.

Notice an interesting and important fact about the hinge forces. Assume that the average forces have been computed, integrating the formulas along the whole revolution and dividing them by 2π . The inertial forces, since they form periodic movements, are eliminated in this process ^[23]. The consequence of this is that the magnitudes for the average hinge forces are actually the same as the average thrust and horizontal forces on the blade.

This is highly useful, because in order to find certain forces such as the trim ones, the average values will be needed -it makes no point in using a periodic formula for a behavior that should be maintained over time; it is actually better to find the mean value of such formula, as it was done with the thrust.

It will be seen in such trim that the average forces from the rotor needed there are the most representative; the horizontal H_x and vertical T ^[24]. Therefore, let us compute now such average in order to have the mean horizontal hinge force along a revolution.

Taking equation (60), its average value can be computed:

$$\begin{aligned} H_{x,\text{ave}} &\approx \frac{b}{2\pi} \int_0^1 \int_0^{2\pi} [dD(x, \psi) \sin \psi + dL(x, \psi)(\beta \cos \psi - \phi \sin \psi)] d\psi dx \quad (105) \\ &\approx \frac{b}{2\pi} \int_0^1 \int_0^{2\pi} \left[\frac{1}{2} \rho U_T^2 R \delta c \sin \psi \right. \\ &\quad \left. + \frac{1}{2} \rho a c R U_T^2 \left(\theta_0 + \theta_{\text{base}} + \frac{U_P}{U_T} \right) \left(\beta \cos \psi - \frac{U_P}{U_T} \sin \psi \right) \right] d\psi dx \end{aligned}$$

The first term involving equation (105) belongs to the aerodynamic drag, and its solution is:

$$H_{x,\text{drag}} = \frac{1}{4} \rho b c \delta \mu \Omega^2 R^3 \quad (106)$$

On the other hand, the second block of the equation is for the lift components, and can be expressed the following way:

$$H_{x,\text{lift}} = \frac{b}{2\pi} \int_0^1 \int_0^{2\pi} \frac{1}{2} \rho a c R \{ [(\theta_0 + \theta_{\text{base}}) U_T^2 + U_P U_T] \beta \cos \psi - [(\theta_0 + \theta_{\text{base}}) U_P U_T + U_P^2] \sin \psi \} d\psi dx \quad (107)$$

The integral of this equation would be done almost the same way as integrating equation (43). There is one difference here, though. Since now equation (107) is more complex than the lift one, the induced velocity will be assumed to have the average value v_{i0} instead of its Mangler and Squire formula^[25]. Besides that, the rest of the periodic terms like the flapping movement will be assumed to behave in their sine and cosine series, up to the first order coefficient, that is, $n = 1$:

$$\beta \approx a_0 - a_1 \cos \psi - b_1 \sin \psi \quad (108)$$

With all this into equation (107), and after computing the integrals, the final result is^[26]:

$$H_{x,\text{ave}} \approx \frac{1}{2} \rho a b c \Omega^2 R^3 \left[\frac{\mu \delta}{2a} - \theta_0 \left(\frac{1}{3} a_1 + \frac{1}{2} \mu \lambda \right) - \int_e^1 \left[\theta_{\text{base}} \left(a_1 x^2 + \frac{1}{2} \mu \lambda \right) \right] dx - \frac{3}{4} \lambda a_1 + \frac{1}{4} \mu a_1^2 - \frac{1}{6} a_0 b_1 + \frac{1}{4} \mu a_0^2 \right] \quad (109)$$

This equation right now is not very useful; however, it will come into scene when the trim condition is computed, so it will be important to remember it for then. Also, notice that this time the flapping coefficients a_0 , a_1 and b_1 do not disappear when integrating the formula, so later they will also need to be calculated. For that purpose it will be useful the analytical method for obtaining the flapping movement, which was mentioned in the previous section. Such method will solve for the different flapping components using a rather simplified form of the second Extended Euler Equation.

3.3 Main body forces and moments

Up until now the aerodynamic forces on the rotor have been obtained, and at the same time the blade movements too, so that the accelerations of the blades could be found and from that, by applying the second Newton's law, the reactions at the hinge. Those reactions, with the opposite sign, were the actual forces on the helicopter that truly help it move in flight.

These aerodynamic forces which were finally translated to the helicopter's main body are not the only ones affecting it, though. The helicopter, which in this project is considered as another rigid body besides the blades, has a mass, therefore there is weight affecting it. Furthermore, in the cases that cover this project,

which study overall the steady forward flight, there is another drag force besides the one computed on the blades. Such is the drag for the main body, in a similar way as the drag that would be drawn in the diagram of forces of a conventional aircraft.

Besides them, there is also the helicopter's tail, which most of the times has another smaller rotor which will produce more thrust in lateral directions, and sometimes there will be also a tailplane located there in order to enhance the stability. Such forces will also need to be calculated.

Not only that, but the moments must also be computed in order to obtain the full set of equations that will allow us to integrate the helicopter's movement. The location chosen to compute such moments will not be the center of gravity of the helicopter, but instead a point located at the intersection between the shaft axis and a plane normal to such axis which contains the center of gravity.

3.3.1 Tail rotor and tailplane

As it was just mentioned, most of the helicopters have a tail with a smaller rotor which helps balance forces and moments from the main one. The principal effect that must be counteracted from the main rotor is the torque produced by the rotation of the blades.

For this smaller rotor the average of the thrust will be taken this time, and for further simplicity it will be assumed that it only produces thrust, as the forces coming from here are usually much smaller than those of the main rotor (while the rotor must produce thrusts of the order of 10^4 N the tail rotor usually reaches a couple thousands)^[27]. Besides, the geometric pitch of the tail blades will be assumed to be constant, and the non-feathering angle to be parallel to the helicopter symmetry axis (that is, no cyclic feathering here).

Therefore, let us recall again the average thrust formula from equation (48). Here the subscript t indicates the helicopter's tail data:

$$\begin{aligned} T_t &= \frac{1}{4} \rho a b_t c_t \Omega_t^2 R_t^3 \left[\frac{2}{3} (\theta_{0,t} + \theta_{\text{base},t}) \left(1 + \frac{3}{2} \mu_t^2 \right) + \lambda_t \right] \\ &= \frac{1}{4} \rho a b_t c_t \Omega_t^2 R_t^3 \left[\frac{2}{3} (\theta_{0,t} + \theta_{\text{base},t}) \left(1 + \frac{3}{2} \mu_t^2 \right) + \frac{V}{\Omega_t R_t} \sin \alpha_{\text{nf},t} - \frac{v_{i,t}}{\Omega_t R_t} \right] \end{aligned} \quad (110)$$

In the same way that was done when calculating the aerodynamic rotor forces, now the induced velocity can be approximated with the help of the first part of equation (49), and by writing it in the tail thrust formula, the following expression is obtained:

$$\begin{aligned}
T_t &= \frac{\rho a b_t c_t \Omega_t^2 R_t^3}{4 + \frac{a b_t c_t \Omega_t}{2\pi V}} \left[\frac{2}{3} (\theta_{0,t} + \theta_{\text{base},t}) \left(1 + \frac{3}{2} \mu_t^2 \right) + \frac{V}{\Omega_t R_t} \sin \alpha_{\text{nf},t} \right] \\
&= \frac{2\pi V \rho a b_t c_t \Omega_t^2 R_t^3}{8\pi V + a b_t c_t \Omega_t} \left[\frac{2}{3} (\theta_{0,t} + \theta_{\text{base},t}) \left(1 + \frac{3}{2} \mu_t^2 \right) + \frac{V}{\Omega_t R_t} \sin \alpha_{\text{nf},t} \right]
\end{aligned} \tag{111}$$

As it was said before, apart from the tail rotor and its respective thrust, the helicopter may also have a tailplane around this area. This plate acts similarly to the HTP of conventional aircraft, increasing the stability of the body during flight. While there are no useful formulas here to obtain the angles of attack for this tailplane, statistical data may be used in order to get an estimation of its effect on the helicopter^[28].

To begin with, let us assume that there is a tailplane somewhere in the region of the helicopter's tail. Its most important effect will be the moment exerted due to the distance between itself and the center of gravity -or whichever center we are using to compute moments, like the one described previously. Another assumption is to ignore the fuselage where it is located^[29], although this was already assumed too when computing the main rotor and even the tail rotor forces.

As a reference for the angle of attack of the tailplane, there will be an angle α_{T0} , which will be the angle between the no-lift position of the tailplane and the datum line. This “datum line” consists of an imaginary line perpendicular to the rotor shaft. This way the position of the tailplane gets defined, and now only its actual angle of attack needs to be computed.

The following images a usual disposition of the helicopter and its tailplane in steady forward flight, as well as a diagram of the angles involved in finding the tailplane's angle of attack:

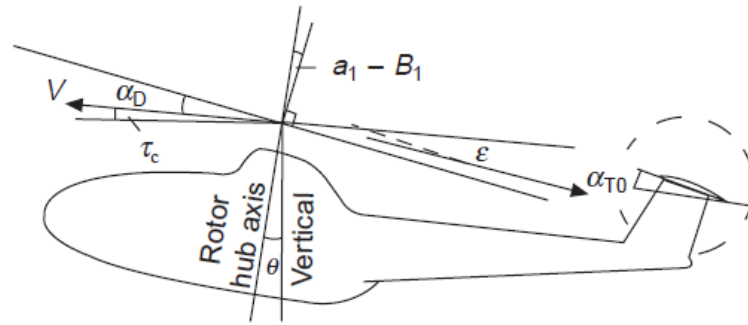


Figure 10: Helicopter with tailplane [30]

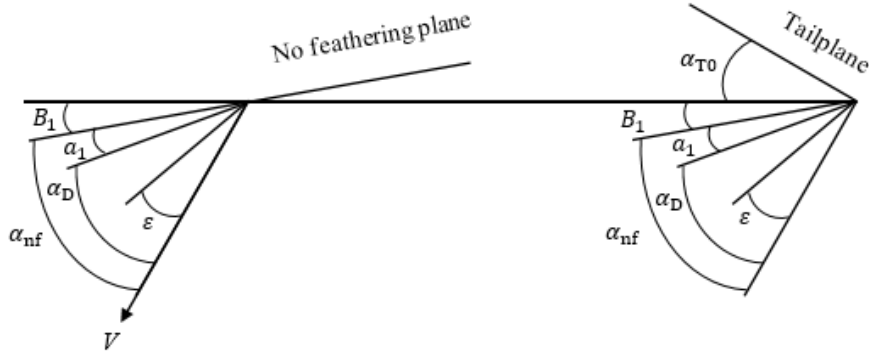


Figure 11: Exaggerated angles around the rotor and tailplane

Therefore, the angle of attack of the tailplane is given by the following expression:

$$\begin{aligned}
 \alpha_T &= \alpha_{T0} + B_1 + a_1 + \alpha_D - \varepsilon \\
 &= \alpha_{T0} + B_1 + \alpha_{nf} - \varepsilon \\
 &= \alpha_{T0} + \theta - \tau_c - \varepsilon
 \end{aligned} \tag{112}$$

Notice that the two first forms of expressing equation (112) are related to how the incidence angle may be interpreted. The third form, however, is somehow different. Instead of focusing on the different planes and positions of the rotor, the formula relies on the pitch angle of the whole helicopter and the climb angle of its flight.

However, all three forms of equation (112) have one term in common, and that is the downwash angle ε . As it was previously indicated, now there is not a straight-forward formula or set of equations that lead to knowing the value of ε . Nevertheless, the following two tables may be used, which were taken from the results of Heyson and Katzoff's experiments^{[31],[32]}.

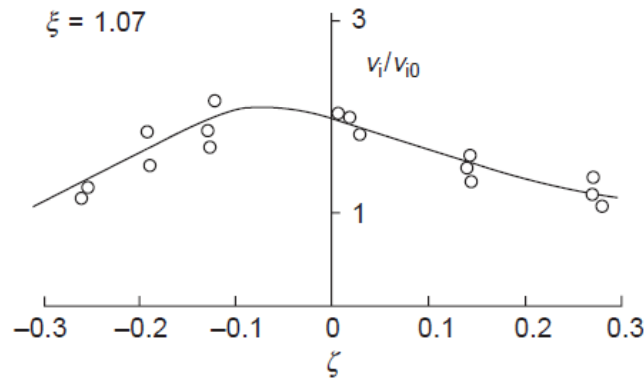


Figure 12: Relation of induced velocities and tailplane heights ($\xi = 1.07$) [33]

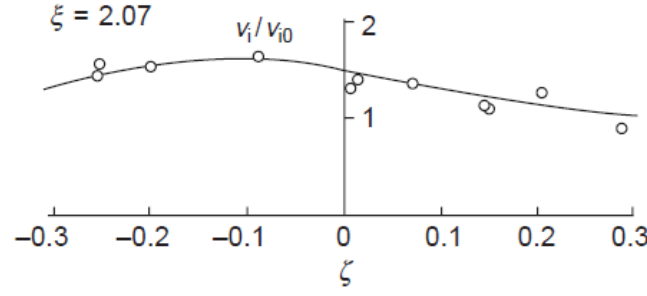


Figure 13: Relation of induced velocities and tailplane heights ($\xi = 2.07$) [34]

Now here ξ does not represent the lagging angle, but the distance between the shaft axis and the tailplane, in terms of the main rotor radius, $\xi = l_T$. Notice that such distance might be different from the two values displayed above, so the table with the closest number will need to be chosen. On the other hand, the term ζ represents another relation of distances between the rotor and the tailplane, just vertically this time.

To find ζ , let us assume that the tailplane is located at a certain vertical distance h_T above (positive) or below (negative) the rotor disc. Besides that, there will be a vertical distance between the rotor disc and the tip path plane, defined by $h_D = \xi R(B_1 + a_1)$ -the term a_1 comes from the sinusoidal form of the flapping movement when $\psi = 0$. Also, after the main rotor there are some downwash vortices with angle ε_0 , so the altitude of such vortices with respect to the tip path plane at the tailplane's location is $\varepsilon R(\varepsilon_0 - \alpha_D)$.

The angle ε_0 is given by the relation $\frac{v_{i0}}{V}$ on the tip path plane. It can be approximated the following way, in the TPP frame and the no feathering one:

$$\begin{aligned} \varepsilon_0 &= \frac{v_{i0}}{V} = \frac{\lambda_{i0}}{\hat{V}} \approx \frac{\lambda_{i0,D}}{\mu_D} \\ &\approx \frac{\lambda_{i0,nf} - \mu_{nf} a_1}{\mu_{nf}} \end{aligned} \quad (113)$$

This transformation between TPP and no feathering plane has been performed in a similar way as the forces from equations (90) and (91) were transformed from the no feathering to the rotor disc plane. Here the assumption was that the longitudinal angle between the no feathering plane and the TPP has the small value of $-a_1$ -from the flapping equation; so the relation between the advance ratio μ and the non dimensional, average induced velocity λ can be expressed the way it was written in equation (113).

Now that the three different relative heights have been defined, figure 14 shows how they are related in order to find the distance ζ :

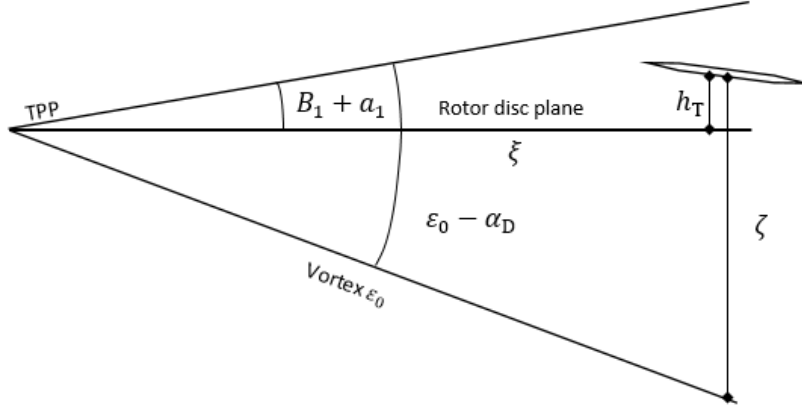


Figure 14: Tailplane with respect to TPP, rotor plane, and vortex ε_0

It can be seen above that the distance ζ is equal to the total height between the TPP and the vortex ε_0 , minus the difference between the heights over the rotor disc of the TPP and the actual tailplane. Said that so, the equation for ζ is:

$$\zeta = \xi R(\varepsilon_0 - \alpha_D) - (\xi R(B_1 + \alpha_1) - h_T) \quad (114)$$

The found value for ζ can be compared in the tables (12) and (13) -the one that suites best for the value of ξ - and from there an estimation for the downwash angle ε will be obtained.

The only remaining step is to compute the moment that the tailplane does on the helicopter, by solving the equation (112) for α_T and computing the moment, which is:

$$M_T = -\frac{1}{2}\rho V^2 S_T l_T R a_T \alpha_T \quad (115)$$

The term a_T , which represents the lift slope the same way as in the main rotor, has in this project a value of 3.5.

3.3.2 Total forces

In order to integrate the movement of the whole helicopter, there are now the forces at the hinge of the main rotor, the ones from the tail rotor and the moment of the tailplane, and also the forces affecting the main body of the helicopter itself, like the drag and the weight. Let us now change to a reference frame which involves the whole helicopter and not the rotor different points of view, as was done before.

Now the body axis of the helicopter will be used. However, other frames may be used if desired, each one with its respective advantages. The wind axes, for example, point their $-x$ direction always to the coming flow, which eliminates some $-z$ components from the equations. The body axes, on the other hand, make

sure that everything is computed with respect to the main helicopter, which may help when working with moments of inertia thanks to the symmetry of the vehicle.

Specifically, the direction of the body reference frame consist of an axis $-x$ pointing towards the cockpit, an axis $-y$ pointing towards the starboard of the helicopter and the axis $-z$ pointing downwards, as required by the right-hand rule.

In order to get a better study of the helicopter's behavior, the process will be divided into longitudinal motion (or how the pith of the vehicle varies during its flight), and lateral motion, focusing there on the yaw and roll movements. Said that so, the first case shall be the longitudinal one.

Let us observe figure 15, taken from the book Bramwell's Helicopter Dynamics. Before anything, note that the flapping angle a_1 is positive here in the clockwise direction. In this project, however, it would be negative in such direction, since the flapping is considered to be positive when tilting the blade downwards, as opposed to Bramwell. Besides that, there is no picture of the tailplane, either because at that part of the book it had yet to be introduced, or also because that might not be the case of a helicopter with a tailplane. Either way, these are just minor changes with respect to this project or just speculations, and do not prevent us from getting a good overview of how the forces work here.

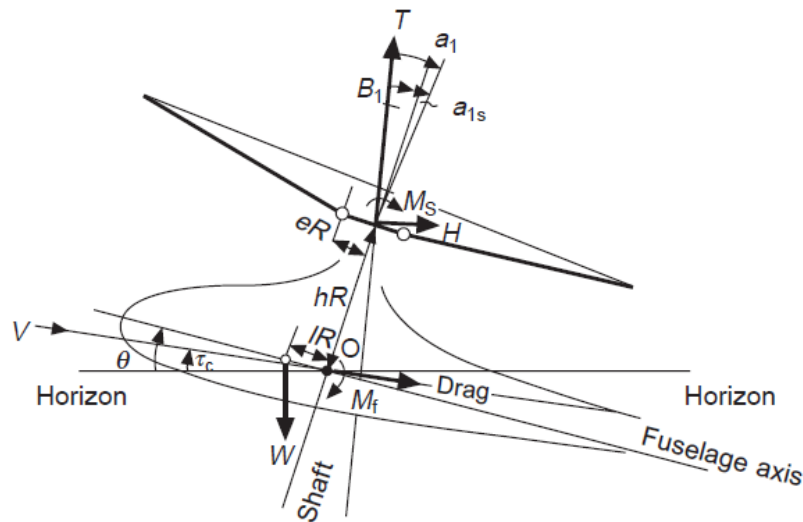


Figure 15: Forces on the rotor and main body [35]

In the picture also appear the forces from the rotor in their no feathering orientation. Right now that has already been solved, obtaining the hinge forces in the rotor frame from equation (92). The only further step necessary is to change such frame to the body reference frame, which is achieved by changing the sign of its $-x$ and $-z$ directions.

As for the rest of the forces, the weight W will have its $-x$ and $-z$ components depending on the value of the pitch angle θ , and the drag for each direction will

depend on the values of the angle $(\theta - \tau_c)$. Since we are dealing with the body reference frame, the tail rotor thrust, which is perpendicular to the helicopter's longitudinal plane, does not appear here. Hence, the longitudinal sums of forces are:

$$\sum F_x \approx -F_{x,\text{hinge}} - W \sin \theta - D \cos(\theta - \tau_c) \quad (116)$$

$$\sum F_z \approx -F_{z,\text{hinge}} + W \cos \theta - D \sin(\theta - \tau_c) \quad (117)$$

The fuselage drag D appearing here is defined in the following way:

$$D = \frac{1}{2} \rho V^2 S_{\text{PF}} \quad (118)$$

Where the term S_{PF} is the equivalent flat plate area^[36]. Besides, the angle τ_c is usually known, since it can be defined by the components of the helicopter's velocity V .

In order to get the equations for the forces, and assuming both constant mass on the helicopter and null lateral velocity v (for this case), the formulas are^[37]:

$$m[\dot{u} + q(W + w) - vr] \approx m[\dot{u} + q(W + w)] = \sum F_x \quad (119)$$

$$m[\dot{w} + pv - q(U + u)] \approx m[\dot{w} - q(U + u)] = \sum F_z \quad (120)$$

In the equations above, the terms u , v and w and their derivatives belong to the $-x$, $-y$ and $-z$ components of the helicopter's velocity and acceleration. On the other hand, the terms p , q and r represent the roll, pitch and yaw rates of the helicopter. Notice that by restraining the vehicle to just the $-xz$ plane, the rolling and yawing terms disappear, meaning that in a real, 6-degrees of freedom flight all these movements should be taken into account since they are all interrelated.

For the lateral case, things shall be different from this. Fortunately, by making the helicopter have a tailplane, the helicopter's pitching behavior has become more stable withing high speed forward flight^[38]. Thus, the full procedure explained over these sections -i.e. the forces being computed at each time step instead of just the average values per revolution- could be performed without finding too much trouble.

However, the helicopter's roll is more unstable than the pitching with a tailplane's aid^{[39],[40]}. Furthermore, now there are two coupled movements; the yaw and roll rotations. Since there are many variables involved in the calculations, and due to the results being now more unstable, this time the operations shall be made with the average values of the forces -the ones that were computed for T and H .

The following image may be considered as the equivalent of figure 15 for lateral flight:

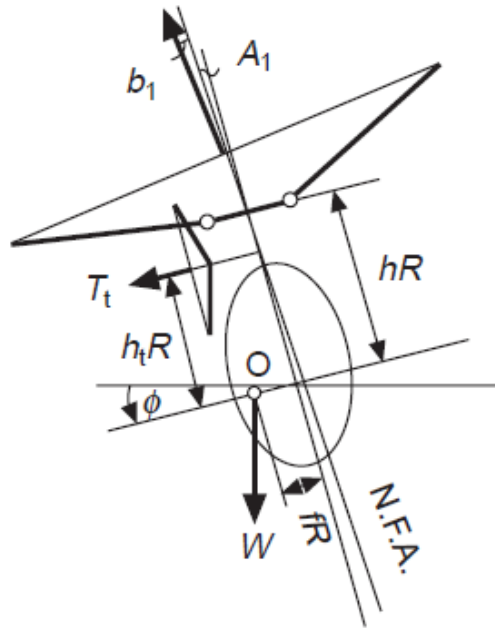


Figure 16: Forces on the rotor and main body [41]

From this figure it can be appreciated that when focusing on the lateral forces, the thrust is also slightly deviated due to the respective components of feathering and flapping. As with the previous case, this picture taken from Bramwell's Helicopter Dynamics uses flapping coefficients with the opposite sign as the ones in this project. The result is the same, though, since it is just an issue of sign criteria, and being coherent with one's chosen sign should lead to the same values.

Apart from that, and in order to compute the approximated lateral forces, the helicopter's orientation will be in the following order: yaw first, then pitch and finally roll. These angles will be named by ψ , θ and ϕ , respectively -not related to the ones involved in the blades position and incidence.

The transformation matrices for these angles are:

$$A_{\text{earth}}^{\psi} = \begin{bmatrix} \cos\psi & \sin\psi & 0 \\ -\sin\psi & \cos\psi & 0 \\ 0 & 0 & 1 \end{bmatrix} \approx \begin{bmatrix} 1 & \psi & 0 \\ -\psi & 1 & 0 \\ 0 & 0 & 1 \end{bmatrix} \quad (121)$$

$$A_\psi^\theta = \begin{bmatrix} \cos\theta & 0 & -\sin\theta \\ 0 & 1 & 0 \\ \sin\theta & 0 & \cos\theta \end{bmatrix} \approx \begin{bmatrix} 1 & 0 & -\theta \\ 0 & 1 & 0 \\ \theta & 0 & 1 \end{bmatrix} \quad (122)$$

$$A_{\theta}^{\phi} = \begin{bmatrix} 1 & 0 & 0 \\ 0 & \cos\phi & \sin\phi \\ 0 & -\sin\phi & \cos\phi \end{bmatrix} \approx \begin{bmatrix} 1 & 0 & 0 \\ 0 & 1 & \phi \\ 0 & -\phi & 1 \end{bmatrix} \quad (123)$$

With these matrices the components for weight and drag in the body frame are:

$$\vec{W}_{\text{body}} = A_{\text{earth}}^{\psi} A_{\psi}^{\theta} A_{\theta}^{\phi} \cdot \begin{bmatrix} 0 \\ 0 \\ W_{\text{earth}} \end{bmatrix} \quad (124)$$

$$\vec{D}_{\text{body}} = A_{\text{earth}}^{\psi} A_{\psi}^{\theta} A_{\theta}^{\phi} \cdot \begin{bmatrix} -D \cos \tau_c \\ 0 \\ D \sin \tau_c \end{bmatrix} \quad (125)$$

In lateral flight, and assuming small deviation angles for yaw, pitch and roll, the sum of forces may be expressed the following way:

$$\sum F_y \approx T_t + T(A_1 - b_1) + \vec{W}_{\text{body}}(2) + \vec{D}_{\text{body}}(2) \quad (126)$$

Now that the lateral force equation is written, and neglecting the disturbance $-x$ and $-y$ velocities, the formula for the forces in this direction is:

$$m[\dot{v} + r(U + u) - p(W + w)] \approx m[\dot{v} + rU - pW] = \sum F_y \quad (127)$$

3.3.3 Total moments

After seeing figures 15 and 16, it can be appreciated that the center of gravity of the helicopter is at a certain distance both longitudinally and laterally from the rotor's axis, and vertically from the rotor disc. Such distances, as a function of the main rotor radius R , shall be named lR , fR and hR . Therefore, the total distance from the point O -where we calculate the moment- to the center is:

$$O\vec{P}_{\text{cg}} = \begin{bmatrix} lR \\ fR \\ 0 \end{bmatrix} \quad (128)$$

On the other hand, from this point O there will be a distance $\xi R = l_T R$ to the tailplane (considered horizontal for simplicity), and another one $l_t R$ to the tail rotor. This tail rotor will be located also at a height $h_t R$ over the point O .

Given this, the sum of the moments concerning the main body plus the tailplane and tail rotor is:

$$\begin{bmatrix} M_{x,b} \\ M_{y,b} \\ M_{z,b} \end{bmatrix} = O\vec{P}_{\text{cg}} \wedge \vec{W}_{\text{body}} + \begin{bmatrix} 0 \\ -\frac{1}{2}\rho V^2 S_T \xi a_T \alpha_T \\ -l_t R T_t \end{bmatrix} \quad (129)$$

Besides these moments, there are the ones coming from the main rotor forces. Remember that, although the forces at the hinge have been computed, this hinge

is located at a distance eR from the rotor axis, and is rotating in time, so there will be a variable moment there. Recalling the hinge forces from equation (92), the moment at each time step around point O is:

$$\vec{M}_{\text{rotor}} = \begin{bmatrix} -eR\cos(\Omega t) \\ eR\sin(\Omega t) \\ -hR \end{bmatrix} \wedge \begin{bmatrix} -F_{x,\text{hinge}} \\ F_{y,\text{hinge}} \\ -F_{z,\text{hinge}} \end{bmatrix} + \begin{bmatrix} 0 \\ M_f \\ 0 \end{bmatrix} \quad (130)$$

Notice that an extra term M_f appears here. Such is the fuselage pitching moment, which is unknown, and depends on the helicopter's characteristics. For that reason, in this project it will be assumed to be 0; however do not forget that such term exists and should appear in the full sum of moments at the origin of moments O .

Given the previous formulas, the final expression for the sum of moments here is:

$$\vec{M} = \begin{bmatrix} L \\ M \\ N \end{bmatrix} = \vec{M}_{\text{rotor}} + \begin{bmatrix} M_{x,b} \\ M_{y,b} \\ M_{z,b} \end{bmatrix} \quad (131)$$

Do not get confused with the L , M and N terms when finding the flapping movements; those belonged to the moments due to the forces *on the blade*, not the whole sum of moments on all the helicopter.

Notice that this last expression has been made assuming to know the hinge forces at each time; however, if the case is the one where the average forces were found, the equation may be slightly changed.

To begin with, the average forces are found in the no feathering plane. Thus, the horizontal forces that will be multiplied by the height hR in order to obtain the $-x$ and $-y$ components of the rotor moments are -in their linearized form- TA_1 and $TB_1 - H$, respectively.

Besides them, the hinge forces are again located at a distance eR from the rotor axis, so there will be a set of moments due to the average of this distance times the vertical force, and a vertical torque Q given by the product of this distance and the horizontal hinge forces. It may be considered too as multiplying the distance times the resultant tangential force at the hinge, $H_{\text{hinge,rear}}$.

Focusing on the first of the two, the average components $-x$ and $-y$ of the moment resulting from the vertical force are^[42]:

$$\begin{aligned} M_x &= \frac{eR}{2\pi} \int_0^{2\pi} (M_b a_z - T) \sin\psi d\psi \\ &\approx -\frac{1}{2} b M_b e x_g \Omega^2 R^2 b_{1s} = -\frac{1}{2} b M_b e x_g \Omega^2 R^2 (A_1 - b_1) \end{aligned} \quad (132)$$

$$\begin{aligned}
M_y &= \frac{eR}{2\pi} \int_0^{2\pi} (M_b a_z - T) \cos\psi d\psi \\
&\approx -\frac{1}{2} b M_b e x_g \Omega^2 R^2 a_{1s} = -\frac{1}{2} b M_b e x_g \Omega^2 R^2 (B_1 + a_1)
\end{aligned} \tag{133}$$

The term x_g corresponds to the distance from the hinge to the blade's center of gravity, and the terms a_{1s} and b_{1s} belong to the flapping coefficients with respect to the rotor disc instead as to the non feathering plane, which may be expressed as:

$$a_{1s} = B_1 + a_1 \tag{134}$$

$$b_{1s} = A_1 - b_1 \tag{135}$$

Notice that both equations (132) and (133) are multiplied by the number of blades b so that their value is the *total* value taking into account all the blades.

The only remaining moment to be computed is Q in the $-z$ direction, which is obtained by multiplying the distance eR with the tangential horizontal force, or doing the cross product between the horizontal distance from the axis to the hinge and the horizontal forces. It is formulated as follows^[43]:

$$\begin{aligned}
Q &\approx \frac{b}{2\pi} \int_0^1 \int_0^{2\pi} x \frac{1}{2} \rho U_T^2 R^2 c \left[\delta - a \left(\theta \frac{U_P}{U_T} + \frac{U_P^2}{U_T^2} \right) \right] d\psi dx \\
&= \rho b c \delta \Omega^2 R^4 \frac{1 + \mu^2}{8} - \frac{\rho a b c R}{4\pi} \int_0^1 \int_0^{2\pi} x [(\theta_0 + \theta_{\text{base}}) U_T U_P + U_P^2] d\psi dx \\
&= \rho b c \delta \Omega^2 R^4 \frac{1 + 3\mu^2}{8} - (T\lambda + H\mu) R
\end{aligned} \tag{136}$$

Where:

$$\lambda = \frac{V \sin \alpha_{\text{nf}} - v_{i0}}{\Omega R} \tag{137}$$

With this torque, the extra average moments are completed to be written inside the rotor forces from equation (131).

Besides its calculation to complete the sum of forces, this torque Q is important both for computing the necessary trim conditions -which will be seen in the next section, and to have a value for the induced power, which is useful if the performance of the helicopter wants to be analyzed^[44].

Now that the moments are finally there, the last step is to write down the equations for the moment. In order to do so, the tensor of inertia for the helicopter comes into play, with the following expression^[45]:

$$I_{\text{helicopter}} = \begin{bmatrix} A & -F & -E \\ -F & B & -D \\ -E & -D & C \end{bmatrix} \quad (138)$$

Again, do not confuse these elements from the ones appearing in the calculation of the blade movements. Both belong to moments and products of inertia, but while the first ones belong to the blades, these ones right now represent those from the whole helicopter.

In order to give them some approximated value, Let us assume that the helicopter resembles the shape of an ellipsoid, without the tail. Being that the case, the values of A , B and C would be around $\frac{1}{5}m(a^2 + b^2)$, being a and b the radius in each of the principal directions from the point calculated. For example, let us say that the front view of the helicopter may be assumed as a circle of radius 1.5 m, and that the helicopter's length is around 5 m, which would mean a "radius" in that direction of 2.5 m. Furthermore, let us give the helicopter a mass of 3000 kg. Then, the values of A , B and C would be around $2700 \text{ kg} \cdot \text{m}^2$ for A and $5100 \text{ kg} \cdot \text{m}^2$ for B and C .

From the results just obtained, in this project the values for A , B and C were assumed to be 3000, 7000 and 7000 $\text{kg} \cdot \text{m}^2$, respectively. As for D , E and F , which represent the products of inertia of yz , xz and xy , the only problem was E . Assuming a symmetric helicopter in the xz plane, the terms F and D become 0. The last one E , then, was assumed to be 1000 $\text{kg} \cdot \text{m}^2$ for the sake of coherence between the orders of magnitude of all the components in the tensor of inertia.

Finally, with all these components estimated the second Newton's law for the moments may be applied^[46]. Note that for these equations the terms involving the product of two rotations in them have been neglected, leaving the formulas as follows:

$$A\dot{p} - E\dot{r} = L \quad (139)$$

$$B\dot{q} = M \quad (140)$$

$$C\dot{r} - E\dot{p} = N \quad (141)$$

4 Flight Trim

Up to now the forces on the rotor, tail and helicopter body have been calculated. Also, an approximation to their relative position in the helicopter's body reference frame has been done, in order to be able to integrate them and obtain the vehicle's movement.

However, before integrating two things need to be done first. The first one is to obtain the flapping analytical coefficients. Note that in previous sections some averages have been computed, for which the terms a_1 and b_1 from the flapping equations (44) and (45) have been used.

The other remaining task is to compute the trim conditions for the helicopter, so that there are some reference initial conditions from which one may deduce how the vehicle behaves. For that, the transformation of forces between the no feathering plane and the TPP will need to be done, so there will be a brief explanation on how those formulas change from one plane to another.

4.1 Analytical flapping

Let us first remember the approximated flapping equations:

$$\beta \approx a_0 - a_1 \cos\psi - b_1 \sin\psi \quad (142)$$

$$\frac{\partial\beta}{\partial\psi} \approx a_1 \sin\psi - b_1 \cos\psi \quad (143)$$

$$\frac{\partial^2\beta}{\partial\psi^2} \approx a_1 \cos\psi + b_1 \sin\psi \quad (144)$$

In order to obtain a value for the coefficients a_0 , a_1 and b_1 , the extended Euler's Equations of motions shall be applied; specifically equation (70). Let us write it down here too:

$$\begin{aligned} M &= B\dot{\omega}_2 - (C - A)\omega_3\omega_1 + M_b(z_g a_x - x_g a_z) \\ &= B\dot{\omega}_2 - (C - A)\omega_3\omega_1 - M_b x_g a_z \end{aligned} \quad (145)$$

Since z_g is assumed to be 0.

As it was said before when mentioning this procedure, takes up some assumptions in order to easily obtain the analytical coefficients. The first one, which has already been implemented in equation (145) was to neglect the $-z$ component of the distance from the hinge to the blade's center of gravity, in the blade's reference frame.

Another taken assumption is that the lagging motion is also neglected, so that the rotation of the blade $\vec{\omega}$ and its derivative in the blade's frame end up like this:

$$\vec{\omega} = \begin{bmatrix} \omega_1 \\ \omega_2 \\ \omega_3 \end{bmatrix} = \begin{bmatrix} -\Omega \sin \beta \\ \dot{\beta} \\ \Omega \cos \beta \end{bmatrix} \quad (146)$$

$$\dot{\vec{\omega}} = \begin{bmatrix} \dot{\omega}_1 \\ \dot{\omega}_2 \\ \dot{\omega}_3 \end{bmatrix} = \begin{bmatrix} -\Omega \dot{\beta} \cos \beta \\ \ddot{\beta} \\ -\Omega \dot{\beta} \sin \beta \end{bmatrix} \quad (147)$$

As for the hinge acceleration, since it is assumed to be driven only by the shaft rotation, it may be expressed like this in the blade's frame:

$$\vec{a} = \begin{bmatrix} -\Omega^2 e R \cos \beta \\ 0 \\ -\Omega^2 e R \sin \beta \end{bmatrix} \quad (148)$$

Now the cross product between the distance from the hinge to the blade's center of gravity and the acceleration may be done, obtaining the following result:

$$\vec{r}_g \wedge \vec{a} = \begin{bmatrix} y_g a_z - z_g a_y \\ z_g a_x - x_g a_z \\ x_g a_y - y_g a_x \end{bmatrix} = \begin{bmatrix} 0 \\ \frac{R-eR}{2} \Omega^2 e R \sin \beta \\ 0 \end{bmatrix} \quad (149)$$

The last thing to do here is change the terms $(C - A)$ by B , since remembering that $C = A + B$ due to the negligible thickness of the blade leads to that simplification. With all this done, and assuming that β is usually a small angle, equation (145) may be written as follows:

$$M = B(\ddot{\beta} + \Omega^2 \beta) + M_b \frac{R - eR}{2} \Omega^2 e R \beta \quad (150)$$

When trying to rearrange this equation to be able to separate the variables $\ddot{\beta}$ and β , there appears the term $\frac{M_b x_{cg} e R^2}{B}$, where the component $x_{cg} = \frac{1-e}{2}$ is the non dimensional distance from the hinge to the blade's center of gravity. Now assuming that the blade has uniform and constant mass, this term ends up being like this:

$$\frac{M_b x_{cg} e R^2}{B} = \frac{M_b \frac{1}{2} (1-e) e R^2}{\frac{1}{3} M_b (R - eR)^2} = \frac{3e}{2(1-e)} = \varepsilon \quad (151)$$

Again, this ε has nothing to do with the ones appearing earlier, and is exclusively used to compute the coefficients on this section.

With this previous formula, equation (150) may be finally represented like this:

$$\ddot{\beta} + \beta \Omega^2 (1 + \varepsilon) = \frac{M}{B} \quad (152)$$

In order to solve the equation for the coefficients of the flapping motion, the moment M must be obtained. For that, the lift force will be assumed to be most representative for this case^[47], neglecting both the drag force and the small deviation angle ϕ that orientates both forces in the vertical and horizontal position -like shown in figure 5 for vertical flight.

Thus, the moment M may be expressed as:

$$\begin{aligned} M &\approx \int_0^1 -RxdLdx = \int_0^1 -\frac{1}{2}\rho abcR^2(\theta U_T^2 + U_T U_P)x dx \\ &= -\frac{1}{2}\rho abc\Omega^2 R^4 \int_0^1 \left[(\theta_0 + \theta_{\text{base}})(x + \mu \sin\psi)^2 \right. \\ &\quad \left. + (x + \mu \sin\psi) \left(\lambda' + \mu \beta \cos\psi + x \frac{\partial \beta}{\partial \psi} \right) \right] x dx \end{aligned} \quad (153)$$

Developing the integrals from equation (153) leads to the following expression:

$$\begin{aligned} M &\approx -\frac{1}{2}\rho abc\Omega^2 R^4 \int_0^1 \left[\theta_0(x^3 + x\mu^2 \sin^2\psi + 2x^2\mu \sin\psi) \right. \\ &\quad + \theta_{\text{base}}(x^3 + x\mu^2 \sin^2\psi + 2x^2\mu \sin\psi) \\ &\quad + x^2\lambda' + x^2\mu\beta \cos\psi + x^3\frac{\partial \beta}{\partial \psi} \\ &\quad \left. + \mu \sin\psi \lambda' x + \mu^2 \beta \sin\psi \cos\psi x + \mu \sin\psi \frac{\partial \beta}{\partial \psi} x^2 \right] dx \\ &\approx -\frac{1}{8}\rho abc\Omega^2 R^4 \left[\theta_0 \left(1 + 2\mu^2 \sin^2\psi + \frac{8}{3}\mu \sin\psi \right) \right. \\ &\quad + 4 \int_e^1 \theta_{\text{base}}(x^3 + x\mu^2 \sin^2\psi + 2x^2\mu \sin\psi) dx \\ &\quad + \frac{4}{3}\hat{V} \sin\alpha_{\text{nf}} - 4 \int_0^1 x^2 \frac{v_i}{\Omega R} dx + \frac{4}{3}\mu\beta \cos\psi + \frac{\partial \beta}{\partial \psi} \\ &\quad \left. + 2\mu\hat{V} \sin\alpha_{\text{nf}} \sin\psi - 4\mu \sin\psi \int_0^1 x \frac{v_i}{\Omega R} dx + 2\mu^2 \beta \sin\psi \cos\psi + \frac{4}{3}\mu \sin\psi \frac{\partial \beta}{\partial \psi} \right] \end{aligned} \quad (154)$$

While the integral of the geometric pitch θ_{base} will depend on the data for each helicopter, the other two integrals with the induced velocity are these ones^[48]:

$$\begin{aligned} \int_0^1 x^2 \frac{v_i}{\Omega R} dx &= \frac{15\pi}{128} \frac{v_{i0}}{\Omega R} + \frac{15\pi}{128} \frac{v_{i0}}{\Omega R} \left(\frac{1 - \sin\alpha_D}{1 + \sin\alpha_D} \right)^{1/2} \cos\psi \\ &= \frac{15\pi}{128} \lambda_{i0} + \frac{15\pi}{128} \lambda_{i0} \nu^{1/2} \cos\psi \\ \int_0^1 x \frac{v_i}{\Omega R} dx &= \frac{1}{2} \lambda_{i0} + \frac{7\pi}{64} \lambda_{i0} \nu^{1/2} \cos\psi \end{aligned} \quad (155)$$

Furthermore, the terms with the product of several sines or cosines -without taking flapping's own sines and cosines into account for the moment- are:

$$\sin^2\psi = \frac{1}{2} - \frac{1}{2}\cos 2\psi \quad (156)$$

$$\sin\psi\cos\psi = \frac{1}{2}\sin 2\psi \quad (157)$$

By doing so, equation (154) may be separated in terms of sines and cosines the following way:

$$\begin{aligned} M = & -\frac{1}{8}\rho abc\Omega^2 R^4 \left[\left\{ \theta_0(1 + \mu^2) + 4 \int_e^1 \theta_{\text{base}} \left(x^3 + \frac{1}{2}\mu^2 x \right) dx \right. \right. \\ & \left. \left. - \frac{15\pi}{32}\lambda_{i0} + \frac{\partial\beta}{\partial\psi} \right\} \right. \\ & + \sin\psi \left\{ \frac{8}{3}\theta_0\mu + 8\mu \int_e^1 \theta_{\text{base}} x^2 dx + 2\mu\hat{V}\sin\alpha_{\text{nf}} - 2\mu\lambda_{i0} + \frac{4}{3}\mu\frac{\partial\beta}{\partial\psi} \right\} \\ & + \cos\psi \left\{ \frac{4}{3}\mu\beta - \frac{15\pi}{32}\lambda_{i0}\nu^{1/2} \right\} \\ & \left. + \sin 2\psi \left\{ \mu^2\beta - \frac{7\pi}{32}\mu\lambda_{i0}\nu^{1/2} \right\} - \cos 2\psi \left\{ \theta_0\mu^2 + 2\mu^2 \int_e^1 \theta_{\text{base}} x dx \right\} \right] \end{aligned} \quad (158)$$

If the terms belonging to β and $\dot{\beta}$ are moved to the left hand side of equation (152), and naming the components $\frac{\rho abc R^4}{B}$ as γ , the following expression for such side may be obtained:

$$\frac{\partial^2\beta}{\partial\psi^2} + \frac{\partial\beta}{\partial\psi} \left(\frac{\gamma}{8} + \frac{\gamma}{6}\mu\sin\psi \right) + \beta \left(1 + \varepsilon + \frac{\gamma}{6}\mu\cos\psi + \frac{\gamma}{8}\mu^2\sin 2\psi \right) = RHS \quad (159)$$

Where RHS refers to the rest of the right hand side calculated in equation (158). Now, developing the flapping motion as its sine and cosine series from equations (142), (143) and (144), the same as before can be done to the left hand side, with the following transformations in mind -besides the ones from (156) and (157):

$$\sin 2\psi \cos\psi = \frac{1}{2}(\sin\psi + \sin 3\psi) \quad (160)$$

$$\sin 2\psi \sin\psi = \frac{1}{2}(\cos\psi - \cos 3\psi) \quad (161)$$

$$\begin{aligned}
\frac{\partial^2 \beta}{\partial \psi^2} + \frac{\partial \beta}{\partial \psi} \left(\frac{\gamma}{8} + \frac{\gamma}{6} \mu \sin \psi \right) + \beta \left(1 + \varepsilon + \frac{\gamma}{6} \mu \cos \psi + \frac{\gamma}{8} \mu^2 \sin 2\psi \right) = \quad (162) \\
\left\{ (1 + \varepsilon) a_0 \right\} \\
+ \sin \psi \left\{ \frac{\gamma}{8} \left(1 - \frac{\mu^2}{2} \right) a_1 - \varepsilon b_1 \right\} \\
+ \cos \psi \left\{ \frac{\gamma}{6} \mu a_0 - \frac{\gamma}{8} \left(1 + \frac{\mu^2}{2} \right) b_1 - \varepsilon a_1 \right\} \\
+ \sin 2\psi \left\{ \frac{\gamma}{8} \mu^2 a_0 - \frac{\gamma}{6} \mu b_1 \right\} + \cos 2\psi \left\{ -\frac{\gamma}{6} \mu a_1 \right\} \\
+ \sin 3\psi \left\{ -\frac{\gamma}{16} \mu^2 a_1 \right\} + \cos 3\psi \left\{ \frac{\gamma}{16} \mu^2 b_1 \right\}
\end{aligned}$$

If the blocks belonging to sines and cosines with order $n \geq 2$ are neglected, then only 3 equations remain, belonging to the terms inside $\sin \psi$, $\cos \psi$, and neither sines or cosines. From this set of equations we finally get the 3 flapping coefficients:

$$a_0 = \frac{\gamma}{8(1 + \varepsilon)} \left[\frac{15\pi}{32} \lambda_{i0} - \frac{4}{3} \hat{V} \sin \alpha_{nf} - \theta_0 (1 + \mu^2) - 4 \int_e^1 \theta_{base} \left(x^3 + \frac{1}{2} \mu^2 x \right) dx \right] \quad (163)$$

$$\begin{aligned}
a_1 = \frac{1}{1 - \left(\frac{\mu^2}{2} \right)^2 + \left(\frac{8}{\gamma} \varepsilon \right)^2} \left[2\mu \left(1 + \frac{\mu^2}{2} \right) \left(\lambda_{i0} - \hat{V} \sin \alpha_{nf} - \frac{4}{3} \theta_0 - 4 \int_e^1 \theta_{base} x^2 dx \right) \right. \\
\left. + \frac{32}{3\gamma} \varepsilon \mu a_0 - \frac{15\pi}{4\gamma} \varepsilon \lambda_{i0} \nu^{1/2} \right] \quad (164)
\end{aligned}$$

$$b_1 = \frac{8\mu a_0}{6 + 3\mu^2} - \frac{16\varepsilon a_1}{2\gamma + \mu^2} - \frac{15\pi}{32 + 16\mu^2} \lambda_{i0} \nu^{1/2} \quad (165)$$

4.2 Forces at the tip path plane

There are some cases where the aerodynamic forces are taken from the TPP instead of the no feathering plane. The formulas that have appeared until now for such forces have been placed at the no feathering plane, so their expression in each of the planes might not be exactly the same.

In order to get a fair approximation for the forces between these planes, let us look to the following image.

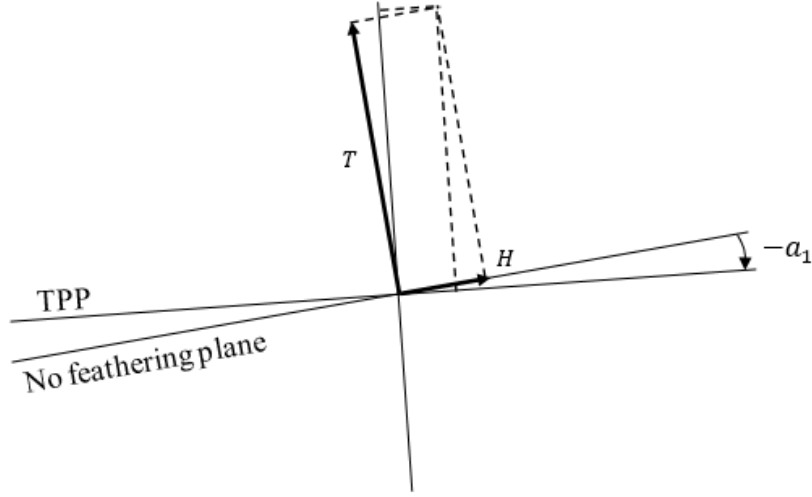


Figure 17: Force components in no feathering plane and TPP

Figure 17 shows the angle between the tip path plane and the non feathering plane, which is given by the longitudinal flapping angle. From the sine and cosine equations for flapping it can be seen that its effect is to cone the blades an angle a_0 , and to tilt their tip plane, the TPP, a longitudinal angle $-a_1$ backwards and a lateral angle $-b_1$ in the starboard direction. Thus, the angle from the no feathering plane to the TPP longitudinally is, as displayed in figure 17, $-a_1$.

Then, considering this angle to be generally small, the forces at the TPP may be approximated as follows:

$$T_D \approx T_{nf} \quad (166)$$

$$H_D \approx H_{nf} - T_{nf}(-a_1) \approx H_{nf} + Ta_1 \quad (167)$$

However, there are also the components related to the velocities which need to be changed from the no feathering plane to the TPP, λ and μ :

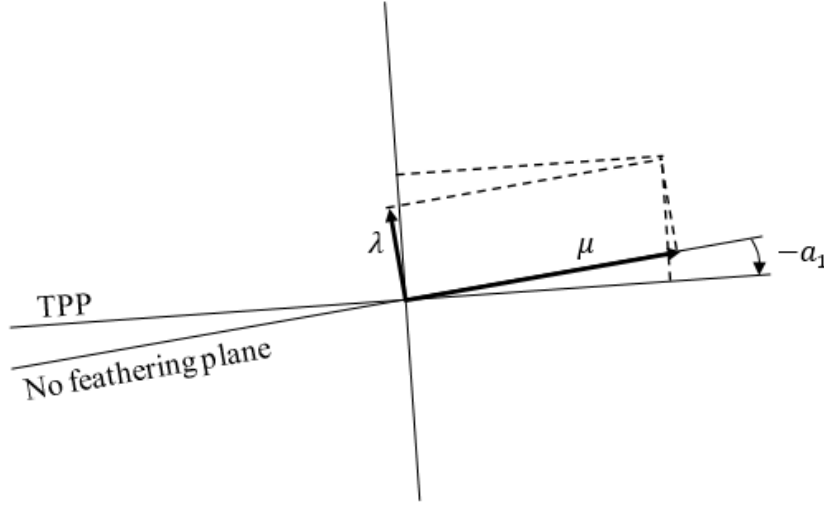


Figure 18: Velocity components in no feathering plane and TPP

$$\mu_D \approx \mu_{nf} \quad (168)$$

$$\lambda_D = \hat{V} \sin \alpha_D - \lambda_{i0} \approx \lambda_{nf} - \mu_{nf} a_1 \quad (169)$$

From these terms the flapping coefficients can be also adapted to express the flapping values from the TPP point of view. In order to do that, some simplifications shall need to be done to the coefficients' equations (163), (164) and (165) in order to make the changes more easily.

By neglecting the helicopter's hinge distance and approximating certain terms to match the average, vertical, non dimensional velocity $\lambda = \hat{V} \sin \alpha_{nf} - \lambda_{i0}$, the resultant equations are as follows (in the no feathering plane)^[49]:

$$a_0 \approx -\frac{\gamma}{8(1+\varepsilon)} \left[\theta_0(1+\mu^2) + 4 \int_e^1 \theta_{base} \left(x^3 + \frac{1}{2} \mu^2 x \right) dx + \frac{4}{3} \lambda \right] \quad (170)$$

$$a_1 \approx -\frac{2\mu(\frac{4}{3}\theta_0 + 4 \int_e^1 \theta_{base} x^2 dx + \lambda)}{1 - \frac{\mu^2}{2}} + \frac{8}{\gamma} \cdot \frac{\varepsilon}{1 - \frac{\mu^2}{2}} b_1 \quad (171)$$

$$b_1 \approx \frac{4(\mu a_0 - 1.1\nu^{1/2}\lambda_{i0})}{3(1 + \frac{\mu^2}{2})} - \frac{8}{\gamma} \cdot \frac{\varepsilon}{1 + \frac{\mu^2}{2}} a_1 \quad (172)$$

If the transformations from equations (168) and (169) are applied into these coefficients, and then the system formed by equations (170), (171) and (172) is solved, the resulting expressions are the following:

$$a_1 \approx - \frac{1 + (\frac{8}{\gamma}\varepsilon)^2 + 2\mu^2(1 + \frac{16}{9} \cdot \frac{1}{2+\mu^2} \cdot \frac{\varepsilon}{1+\varepsilon}) + \frac{3}{4}\mu^4}{1 - (\frac{\mu^2}{2})^2} \quad (173)$$

$$\times \left\{ \frac{2\mu(\frac{4}{3}\theta_0 + 4 \int_e^1 \theta_{\text{base}} x^2 dx + \lambda_D)}{1 - \frac{\mu^2}{2}} + \frac{8}{\gamma} \cdot \frac{\varepsilon}{1 - \frac{\mu^2}{2}} \cdot \frac{4.4\nu^{1/2}(\hat{V} \sin \alpha_D - \lambda_D)}{3(1 + \frac{\mu^2}{2})} \right. \\ \left. + \frac{4\mu\varepsilon}{3[1 - (\frac{\mu^2}{2})^2](1 + \varepsilon)} \left[\theta_0(1 + \mu^2) + 4 \int_e^1 \theta_{\text{base}} \left(x^3 + \frac{1}{2}\mu^2 x \right) dx + \frac{4}{3}\lambda_D \right] \right\}$$

$$a_0 \approx - \frac{\gamma}{8(1 + \varepsilon)} \left[\theta_0(1 + \mu^2) + 4 \int_e^1 \theta_{\text{base}} \left(x^3 + \frac{1}{2}\mu^2 x \right) dx + \frac{4}{3}(\lambda_D + \mu a_1) \right] \quad (174)$$

$$b_1 \approx \frac{4[\mu a_0 - 1.1\nu^{1/2}(\hat{V} \sin \alpha_D - \lambda_D)]}{3(1 + \frac{\mu^2}{2})} - \frac{8}{\gamma} \cdot \frac{\varepsilon}{1 + \frac{\mu^2}{2}} a_1 \quad (175)$$

Besides the flapping coefficients, the formulas for the average thrust T and horizontal force H , which were defined in equations (48) and (109), may also be expressed in terms of the TPP. This is important because such expressions will be used when computing the trim conditions, so everything should be as coherent as possible to find the desired values.

Having said this, let us recall the formulas for both forces, in the no feathering plane:

$$T = \frac{1}{4}\rho abc\Omega^2 R^3 \left[\frac{2}{3}\theta_0 \left(1 + \frac{3}{2}\mu^2 \right) + 2 \int_e^1 \theta_{\text{base}} \left(x^2 + \frac{1}{2}\mu^2 \right) dx + \lambda \right] \quad (176)$$

$$H_{x,\text{ave}} = \frac{1}{2}\rho abc\Omega^2 R^3 \left[\frac{\mu\delta}{2a} - \theta_0 \left(\frac{1}{3}a_1 + \frac{1}{2}\mu\lambda \right) - \int_e^1 \left[\theta_{\text{base}} \left(a_1 x^2 + \frac{1}{2}\mu\lambda \right) \right] dx \right. \\ \left. - \frac{3}{4}\lambda a_1 + \frac{1}{4}\mu a_1^2 - \frac{1}{6}a_0 b_1 + \frac{1}{4}\mu a_0^2 \right] \quad (177)$$

Now as it was deducted from figures 17 and 18, the thrust in the TPP may be approximated to the one at the no feathering plane. However, when writing its formula its components do need to be also expressed as the TPP ones, so some small changes must be made to its equation:

$$T_D = \frac{1}{4}\rho abc\Omega^2 R^3 \left[\frac{2}{3}\theta_0 \left(1 + \frac{3}{2}\mu^2 \right) + 2 \int_e^1 \theta_{\text{base}} \left(x^2 + \frac{1}{2}\mu^2 \right) dx + \lambda_D + \mu a_1 \right] \quad (178)$$

On the other hand, it has been seen how the horizontal force may be expressed as $H_D \approx H_{\text{nf}} + T a_1$. Besides that, the terms inside the equation also need to be

written in the new frame, so the final formula for the horizontal force in the TPP is:

$$\begin{aligned}
H_D &= \frac{1}{2} \rho abc \Omega^2 R^3 \left[\frac{\mu \delta}{2a} - \theta_0 \left(\frac{1}{3} a_1 + \frac{1}{2} \mu \lambda \right) - \int_e^1 \theta_{\text{base}} \left(a_1 x^2 + \frac{1}{2} \mu \lambda \right) dx \right. \\
&\quad \left. - \frac{3}{4} \lambda a_1 + \frac{1}{4} \mu a_1^2 - \frac{1}{6} a_0 b_1 + \frac{1}{4} \mu a_0^2 \right] + T_D a_1 \\
&= \frac{1}{2} \rho abc \Omega^2 R^3 \left[\frac{\mu \delta}{2a} - \theta_0 \left(\frac{1}{3} a_1 + \frac{1}{2} \mu (\lambda_D + \mu a_1) \right) - \int_e^1 \theta_{\text{base}} \left(a_1 x^2 + \frac{1}{2} \mu (\lambda_D + \mu a_1) \right) dx \right. \\
&\quad \left. - \frac{3}{4} (\lambda_D + \mu a_1) a_1 + \frac{1}{4} \mu a_1^2 - \frac{1}{6} a_0 b_1 + \frac{1}{4} \mu a_0^2 \right] \\
&\quad + \frac{1}{2} \rho abc \Omega^2 R^3 \left[\frac{1}{3} \theta_0 \left(a_1 + \frac{3}{2} \mu^2 a_1 \right) + \int_e^1 \theta_{\text{base}} \left(x^2 a_1 + \frac{1}{2} \mu^2 a_1 \right) dx + \frac{1}{2} \lambda_D a_1 + \frac{1}{2} \mu a_1^2 \right] \\
&= \frac{1}{2} \rho abc \Omega^2 R^3 \left[\frac{\mu \delta}{2a} - \frac{1}{2} \theta_0 \mu \lambda_D - \int_e^1 \theta_{\text{base}} \frac{1}{2} \mu \lambda_D dx - \frac{1}{4} \lambda_D a_1 - \frac{1}{6} a_0 b_1 + \frac{1}{4} \mu a_0^2 \right]
\end{aligned} \tag{179}$$

Remember that both here and in equation (178) the flapping coefficients shall be expressed in their TPP form, in order to keep all the variables in terms of such plane -mostly because now α_D would be used instead of α_{nf} .

4.3 Longitudinal trim

Now that both forces and flapping components are expressed as a function of the tip path plane, the equations for equilibrium of forces may be applied for the general body of the helicopter, including now the tailplane, tail rotor, weight and drag. The helicopter shall be put under certain flight conditions; that is, assuming steady forward flight, it shall have a velocity V and a climb angle τ_c , which will be given so as to perform the necessary calculations.

From this, the cyclic and collective pitch coefficients, θ_0 and B_1 , will be obtained, in order to fulfill the equilibrium equations at the given conditions.

Let us observe the following figure, which is a simplified version of figure 15:

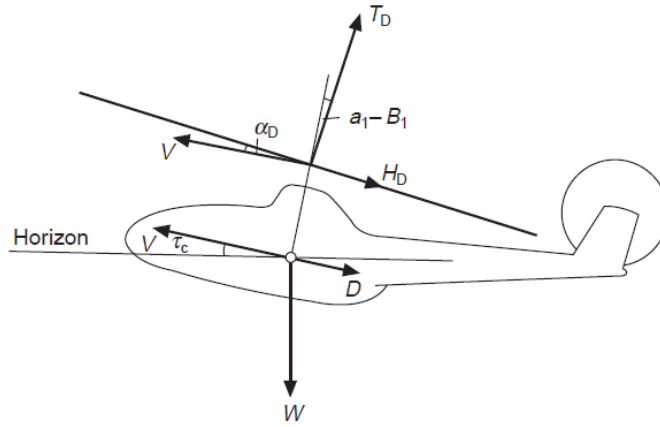


Figure 19: Longitudinal forces for trim [50]

As before, this figure has been obtained from the book Bramwell's Helicopter dynamics, and as such the signs of the flapping coefficients are inverted compared to this project. Furthermore, in figure 19 the angle $a_1 - B_1$ is displayed as going from the TPP to the rotor disc's frame, so the equivalent to figure 15 -from the rotor disc to the TPP, expressed using this project's flapping coefficients, would be $B_1 + a_1$. Finally, in this figure the tailplane does not appear, although for this project it is assumed to be there, so it will need to be taken into account in the momentum equation.

Given this figure, the first step to define the trim conditions is to write the equilibrium equations and then start solving for the unknown variables. A first unknown variable may be α_D , so it would be a good idea to write the equations in the earth reference frame, obtaining the following expressions:

$$T_D \cos(\alpha_D + \tau_c) - H_D \sin(\alpha_D + \tau_c) = W + D \sin \tau_c \quad (180)$$

$$T_D \sin(\alpha_D + \tau_c) + H_D \cos(\alpha_D + \tau_c) = -D \cos \tau_c \quad (181)$$

Where the angle τ_c is known and is one of the requisites for the trim conditions.

The angle $\alpha_D + \tau_c$ may be linearized, since in steady flight it is usually small^[51]. Besides, the $-z$ component of the horizontal force is also negligible compared to the same component of the thrust, so the previous equations may be rewritten like this:

$$T_D = W + D \sin \tau_c \approx W \quad (182)$$

$$T_D (\alpha_D + \tau_c) + H_D = -D \cos \tau_c \quad (183)$$

From these two equations, and remembering that τ_c is known, the incidence angle α_D can be solved for in equation (183). In order to do so, the whole equation may

be made non dimensional by dividing it by $\rho bc\Omega^2 R^3 = \rho\sigma S\Omega^2 R^2$ -where σ is the solidity and S the main rotor area. Thus, the expression has the following form:

$$\alpha_D \approx - \left[\frac{\frac{1}{2}\hat{V} \frac{S_{PF}}{\sigma S} \sin\tau_c + h_c}{w_c} + \tau_c \right] \quad (184)$$

Where h_c and w_c are the non dimensional expressions for the horizontal force and the weight -having divided them by $\rho bc\Omega^2 R^3$. Right now the incidence angle is unknown, so the flapping coefficients cannot be computed yet. Hence, the non dimensional horizontal force will need to be approximated to its first component from equation (179), $\frac{1}{2}\delta\mu$, which is its most important value in this formula^[52]. Such μ , expressed in terms of the TPP, is also a function of α_D . However, since that angle is inside a cosine, it can be approximated to \hat{V} .

The other choice is to not approximate μ , and the formula would need to be numerically solved, for example by estimating a value for α_D , and then solving continuously equation (184) with the last acquired value for α_D each time.

Once an acceptable value for α_D is obtained, the real μ may be obtained, an also the induced velocity λ :

$$\lambda = \hat{V} \sin\alpha_D - \lambda_{i0} = \mu \tan\alpha_D - \lambda_{i0} = \mu \tan\alpha_D - \frac{v_{i0}}{\Omega R} \quad (185)$$

Now the term v_{i0} can be estimated by applying the Momentum Theory for forward flight^[53]. First of all, the induced velocity for hover, which shall serve as reference to make v_{i0} non dimensional, may be expressed as:

$$v_{i,hover} = \sqrt{\frac{W}{2\rho S}} \quad (186)$$

Then, equation (29) may be applied, assuming that the non dimensional, vertical velocity $v_z/v_{i,hover}$ from the point of view of the TPP is negligible. This way, $V_x \approx V$. Assuming then that the thrust is approximated to the weight, and so $\bar{T} \approx 1$, and the non induced velocity may be finally solved:

$$v_{i0} = v_{i,hover} \sqrt{-\frac{V^2}{2} + \sqrt{\frac{V^4}{4} + 1}} \quad (187)$$

Now that both μ and λ are known, the collective pitch angle can be found to fulfill the equilibrium of forces. In order to do that, the non dimensional thrust equation t_c , whose value can be assumed to be the same as w_c , has the following formula:

$$t_c = \frac{T}{\rho bc\Omega^2 R^3} = \frac{a}{4} \left[\frac{2}{3}\theta_0 \left(1 + \frac{3}{2}\mu^2 \right) + 2 \int_e^1 \theta_{base} \left(x^2 + \frac{1}{2}\mu^2 \right) dx + \lambda_D + \mu a_1 \right] \quad (188)$$

Notice that here appears again a flapping coefficient, a_1 . However, as it could

be seen in equation (173), its expression in terms of the TPP is highly complex. For that reason, the hinge distance ε may be assumed to be negligible due to its usually small value^[54], in order to get a simpler expression for t_c :

$$\begin{aligned} t_c \approx w_c &= \frac{a}{4} \left[\frac{2}{3} \theta_0 \left(1 + \frac{3}{2} \mu^2 \right) + 2 \int_e^1 \theta_{\text{base}} \left(x^2 + \frac{1}{2} \mu^2 \right) dx + \lambda_D \right. \\ &\quad \left. - \mu \frac{2\mu(\frac{4}{3}\theta_0 + 4 \int_e^1 \theta_{\text{base}} x^2 dx + \lambda_D)}{1 + \frac{3}{2} \mu^2} \right] \\ &= \frac{a}{4} \left[\frac{2}{3} \theta_0 \frac{1 - \mu^2 + \frac{9}{4} \mu^4}{1 + \frac{3}{2} \mu^2} + 2 \int_e^1 \theta_{\text{base}} \left(x^2 + \frac{1}{2} \mu^2 \right) dx - \frac{8\mu^2}{1 + \frac{3}{2} \mu^2} \int_e^1 \theta_{\text{base}} x^2 dx \right. \\ &\quad \left. + \lambda_D \frac{1 - \frac{1}{2} \mu^2}{1 + \frac{3}{2} \mu^2} \right] \end{aligned} \quad (189)$$

From this expression, the collective pitch angle can be finally obtained:

$$\begin{aligned} \theta_0 &= \frac{3}{2} \cdot \frac{1 + \frac{2}{3} \mu^2}{1 - \mu^2 + \frac{9}{4} \mu^4} \left[\frac{4}{a} t_c - 2 \int_e^1 \theta_{\text{base}} \left(x^2 + \frac{1}{2} \mu^2 \right) dx \right. \\ &\quad \left. + \frac{8\mu^2}{1 + \frac{3}{2} \mu^2} \int_e^1 \theta_{\text{base}} x^2 dx - \lambda_D \frac{1 - \frac{1}{2} \mu^2}{1 + \frac{3}{2} \mu^2} \right] \end{aligned} \quad (190)$$

Now all the necessary components to calculate the flapping coefficients are known, so these may be finally obtained using equations (173), (174) and (175). With them, the horizontal force from equation (179) can be found, which will enable us to apply the equilibrium of moments in order to obtain the remaining unknown: B_1 , from the cyclic blade's pitch.

In the steps just explained, certain loops may be done in order to slightly refine some of the obtained variables. Despite the changes being low for some variables^[55], it could be useful to improve the results of values like the flapping coefficients.

In order to find the cyclic pitch coefficient B_1 , the equations for the moment shall be applied, assuming small feathering and flapping angles:

$$-WlR - T_D hR(B_1 + a_1) + H_D hR + M_f + M_T - M_s(B_1 + a_1) = 0 \quad (191)$$

Remember that in this project the term M_f is assumed to be 0. Besides, the term M_T is given by equation (115), where, in order to calculate ε , the angle ε_0 has been computed from the values of V and v_{i0} obtained here before. Lastly, the term $M_s(B_1 + a_1)$ comes from equation (133), where $M_s = \frac{1}{2} b M_b e x_g \Omega^2 R^2$.

Thus, the moment equation (191) may be rewritten in its non dimensional form as follows, dividing it by $\rho \sigma S \Omega^2 R^3$:

$$\begin{aligned}
& -w_c l - w_c h(B_1 + a_1) + h_c h + C_{m_f} \\
& -\frac{1}{2}\hat{V}^2 \frac{S_T l_T}{\sigma S} a_T (\alpha_{T0} + B_1 + a_1 + \alpha_D - \varepsilon) - C_{m_s}(B_1 + a_1) = 0
\end{aligned} \tag{192}$$

Where C_{m_f} and C_{m_s} are the non dimensional forms of M_f and M_s , respectively.

Given all this, now every component of the equation is known save for the cyclic pitch coefficient B_1 , so it can finally be solved for using the following expression:

$$B_1 = \frac{h_c h + C_{m_f} - \frac{1}{2}\hat{V}^2 \frac{S_T l_T}{\sigma S} a_T (\alpha_{T0} + \alpha_D - \varepsilon) - w_c l}{w_c h + C_{m_s} - \frac{1}{2}\hat{V}^2 \frac{S_T l_T}{\sigma S} a_T} - a_1 \tag{193}$$

Now the necessary components for the longitudinal trim at forward flight -the collective pitch, θ_0 , and the cyclic longitudinal feathering B_1 - have been obtained. Another useful value that can be found with this is that of the helicopter's trimmed pitch angle θ , since that could serve as a reference for the initial conditions when integrating the movement.

For that, the equation for the equilibrium of forces in $-x$ may be approximated in the no feathering reference frame^[56], assuming a small angle between this plane and the horizontal one:

$$D \cos \tau_c + H_D - T a_1 + W(\theta_{\text{trim}} - B_1) = 0 \tag{194}$$

Which, after solving for θ , gives finally the pitch angle at trim for the helicopter:

$$\begin{aligned}
\theta_{\text{trim}} &= B_1 + \frac{T a_1 - H_D - D \cos \tau_c}{W} \\
&\approx B_1 + a_1 - \frac{H_D}{W} - \frac{D \cos \tau_c}{W}
\end{aligned} \tag{195}$$

4.4 Lateral trim

The procedure to find the lateral trim is similar to the longitudinal one. Like before, the aim here is to find the remaining cyclic pitch coefficient, A_1 , which is related to the lateral tilting of the no feathering plane. Apart from this one, it will also be necessary to find the collective pitch of the tail rotor, so that the tail thrust adequately compensates those of the main rotor and the main body. It has been assumed that this is the only type of controlled pitch for the tailrotor, without including the cyclic pitch here.

Let us begin with the moment equilibrium equations. Approximating the moments in the $-z$ direction, the following formula may be written:

$$Q = l_t R T_t \quad (196)$$

The torque Q can be obtained directly from equation (136), since the terms $(T\lambda + H\mu)$ expressed in the TPP are still written in the same way, $(T_D\lambda_D + H_D\mu)$.

By doing that, the necessary thrust at the tail rotor for trim is:

$$T_t = \frac{Q}{l_t R} \quad (197)$$

With the tail rotor thrust now known, the cyclic feathering coefficient A_1 can be found. For that, the equation of moment equilibrium in the $-x$ direction must be applied, assuming a small banking angle^[57]:

$$WfR + ThR(A_1 - b_1) + T_t h_t R + M_s(A_1 - b_1) = 0 \quad (198)$$

Notice here that the center of gravity might be located with a lateral displacement fR from the actual origin of moments where the equation is computed, so it will need to be taken into account here. Since the rest of the variables are also known or have already been computed, the angle A_1 may be solved for:

$$A_1 = b_1 - \frac{WfR + T_t h_t R}{ThR + M_s} \approx b_1 - \frac{WfR + T_t h_t R}{WhR + M_s} \quad (199)$$

The trim bank angle ϕ can be obtained now by equating the equilibrium of forces in the $-y$ direction, neglecting the thrust's $-y$ component due to small angles^[58]:

$$T_t + W(\phi_{\text{trim}} + A_1 - b_1) = 0 \quad (200)$$

$$\phi_{\text{trim}} = b_1 - A_1 - \frac{T}{W} \quad (201)$$

Finally, the cyclic and feathering pitch of the blade are complete. The only remaining variable to obtain is the collective pitch for the tail rotor. For that, the average thrust equation (48) may be applied for the tail rotor. The thrust T is known, and the rotor data too. The advance ratio μ_t may be expressed as the main rotor's μ , and the term λ_t can be approximated to $\sigma_t t_{ct}/2\mu$ for high velocity forward flight, which is this case^[59]. Then, the term $\theta_{0,\text{tail}}$ may be solved for:

$$\theta_{0,\text{tail}} = \frac{3}{2(1 + \frac{3}{2}\mu_t^2)} \left[\frac{4}{a} t_{ct} - 2 \int_{e_t}^1 \theta_{\text{base}_t} \left(x^2 + \frac{1}{2}\mu_t^2 \right) dx - \lambda_t \right] \quad (202)$$

5 Results and Movement Integration

Now that all the process from obtaining the forces at the main rotor to establish the equations in order to integrate the movement have been described, let us do an example applying what has been explained over this project.

5.1 Helicopter and environment data

- Main rotor:

- $b = 4$
- $R = 8\text{m}$
- $e = 0.04$
- $c = 0.5\text{m}$
- $\theta_{\text{base}}(x > 0.4) = (\frac{4^\circ}{x}); \theta_{\text{base}}(x \leq 0.4) = 10^\circ;$
- $M_b = 40\text{kg}$
- $a = 5.7$
- $\delta = 0.013$
- $\Omega = 10\pi\text{rad/s}$

- Tail rotor:

- $b_t = 2$
- $R_t = 2.5\text{m}$
- $e_t = 0$
- $c_t = 0.35\text{m}$
- $\theta_{\text{base}_t} = 0^\circ;$
- $a_t = 5.7$
- $\Omega_t = 30\pi\text{rad/s}$
- $h_t = 1.2$
- $t_t = 2$

- Tailplane:

- $S_T = 1\text{m}^2$
- $l_T = 1.2$
- $a_T = 3.5$
- $\alpha_{T0} = 12^\circ$

- Fuselage:

- $W = 40000\text{N}$

- $S_{PF} = 2.5\text{m}^2$
- $A = 3000\text{kgm}^2$
- $B = 7000\text{kgm}^2$
- $C = 7000\text{kgm}^2$
- $D = 0\text{kgm}^2$
- $E = 1000\text{kgm}^2$
- $F = 0\text{kgm}^2$
- $h = 0.26$
- $l = 0.01$
- $f = 0$
- Flight conditions:
 - $\rho = 1.225\text{kg/m}^3$
 - $V_0 = 60\text{m/s}$
 - $\tau_{c0} = 0^\circ$

5.2 Trim conditions

With the data given in the previous section, the necessary computations to obtain the trim values may be performed. By following the steps described in sections (4.3) and (4.4), the components of the feathering and cyclic blade pitch are:

- $\theta_0 = 5.67^\circ$
- $B_1 = 2.73^\circ$
- $A_1 = -2.68^\circ$

For the tail rotor, the only component calculated was its collective pitch:

- $\theta_{0,\text{tail}} = 1.15^\circ$

As for the tailplane, the calculation was made for the angle ε . However, since this term could not be computed directly from formulas but from statistical data, its value was chosen both for trim and for the rest of the problem:

- $\varepsilon \approx 2.63^\circ$

Having defined all these components, the angles of trim could be approximated in order to have them as initial conditions when integrating the helicopter's movement. The pitch and bank angles were obtained from equations (195) and (201):

- $\theta_{\text{trim}} = -9.67^\circ$
- $\phi_{\text{trim}} = 1.15^\circ$

On the other hand, the initial velocity components U_0 and W_0 were computed first by finding the $-x$ and $-y$ components of the total velocity V_0 :

$$V_x = V \cos \tau_{c0} \quad (203)$$

$$V_z = V \sin \tau_{c0} \quad (204)$$

Finally, the body components were calculated taking into account the initial pitch:

$$U_0 = V_x \cos \theta_{\text{trim}} + V_z \sin \theta_{\text{trim}} \quad (205)$$

$$W_0 = V_x \sin \theta_{\text{trim}} - V_z \cos \theta_{\text{trim}} \quad (206)$$

Obtaining:

- $U_0 = 59.15\text{m/s}$
- $W_0 = -10.08\text{m/s}$

5.3 Rotor results

Before directly integrating the helicopter's motion, let us observe some variables along time to get a general view of their behavior.

The induced velocity distribution shall be good to begin with, because it is one of the first elements computed in the procedure of the rotor's forces. For simplicity, the results presented here for such velocity belong only to the calculations for one blade. The flight conditions are the ones presented at the beginning of this section, but the helicopter is assumed to be already stable in those conditions -i.e. the movement is not integrated here.

Figures 20, 21 and 22 show the different points of view for the induced velocity:

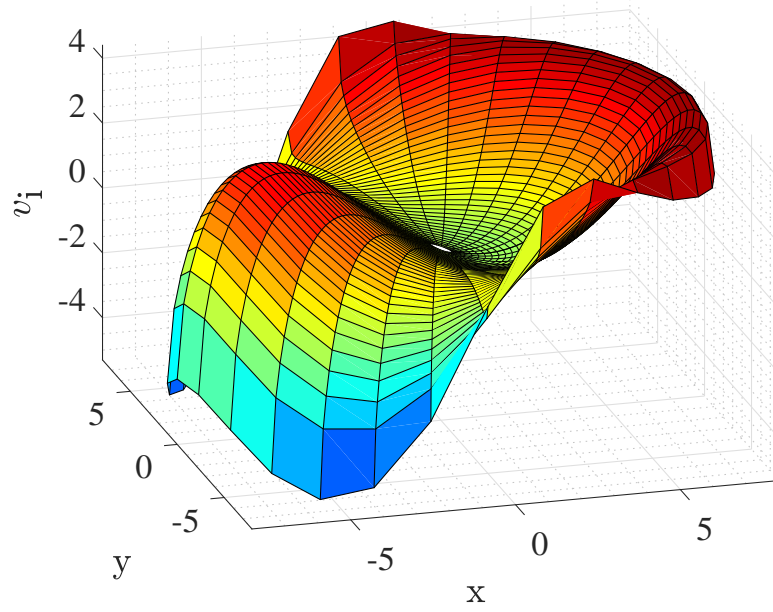
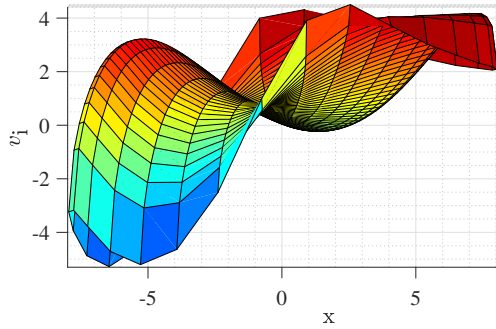
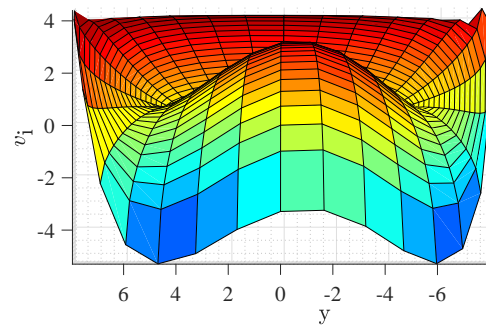


Figure 20: Induced velocity

Figure 21: Side view of v_i Figure 22: Front view of v_i

The first figure shows from an isometric view the general shape of the induced velocity distribution. It can be seen how there is an upwash at the front side of the rotor while at the rear parte the magnitude of the induced velocity is bigger. Moreover, both in figure (20) and (22) it can be appreciated that the velocity is practically symmetric with respect to the $-xz$ plane. There are minor differences, however, due to two reasons.

The first one is that the measurements have been taken at discrete times, and the accuracy of one point with respect to its equivalent at the other side of the symmetry plane might not be exact. On the other hand, the computations have also been made at each time step, so from one point to the next one certain variables such as the mean induced velocity might have very slightly changed, driven

by previous differences within the integration.

Besides from that, it can be seen from figure 21 that the lateral shape of the induced velocity coincides with that described previously in figure 8. The shape of the line at $y = 0$ follows the “S” pattern that has been referred in experiments.

Following the induced velocity, figure 23 shows the variation of the thrust distribution along the rotor disc. Same as before, the values between $\psi \rightarrow 360^\circ$ and $\psi \rightarrow 0^\circ$ are different due to those values being measured at different times, and the variables needed for them might have been slightly different.

In fact, the thrust distribution does not appear to be exactly “clean”; its values vary from more positive to more negative in certain external zones of the disc. However, this is mainly due to the effects of flapping, which alter the position and movement of the blades and hence the values of the thrust. Also, due to the effect that the flapping has in the TPP, it can be seen that the thrust distribution “looks” to be slightly rotated a small angle in the counter-clockwise direction -the small, light-blue change in the values near the axis should be more perpendicular to the $-x$ axis.

What is interesting about this contour are two things: first the dark blue, circular shape near the rotor’s axis. This shows how the low velocity of the blades inside that region strongly affects the production of thrust. Notice that in this project the stall has not been taken into account. It may happen either at the blade tips -here it was assumed that the thrust was produced over the whole blade span- or also in the closest area to the axis. This last effect occurs due to the relative velocity of the blade with the wind is such that the flow may come from the trailing edge instead of the leading edge, or simply because the relative velocity has a very steep incidence to the blade chord. In such case, a further study may as well be the evolution of the angle of attack until stall.

The other interesting thing is the sudden change of gradient of the thrust at $x = 0.4$. This is due to the change of the blade’s geometric pitch at this distance. It shows how the thrust distribution can vary depending on the type of twist that the blade might have.

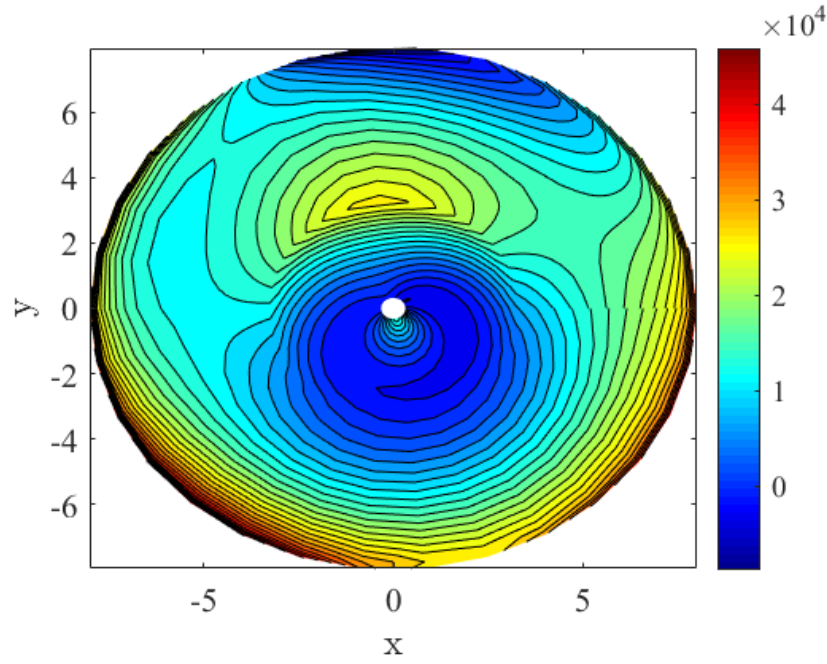


Figure 23: Thrust levels

The third set of figures belong to the blade's flapping, computed by the method presented in section (3.1).

As with the induced velocity, figures 24, 25 and 26 show the different points of view, this time of the blades' tip. Again, these are plots of just one of the blades so that the results are better seen. If all the blades were to be displayed, the results would have to be moved certain degrees to the corresponding position, but the overall behavior over the rotor would be still the same.

Here the most important figures are the two last ones, because they show how the resultant shape of the blades is tilted to the sides. This is indeed the orientation of the TPP, since such plane is given by the position of the blade's tips along the revolution.

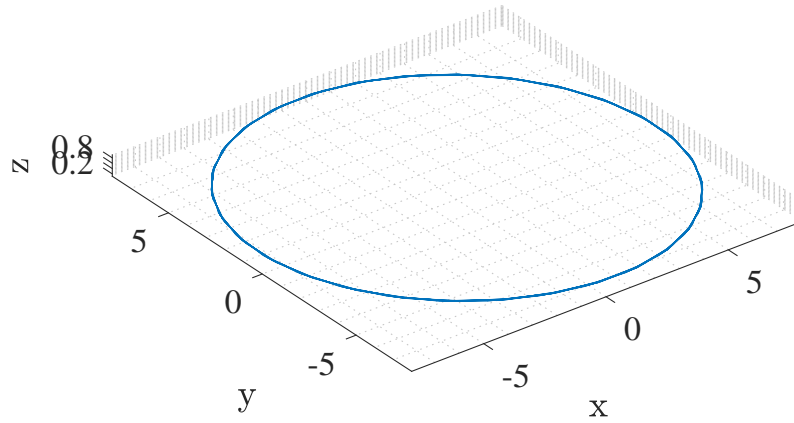


Figure 24: Bladde flapping

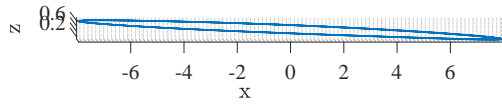


Figure 25: Side flapping view

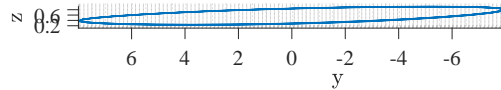


Figure 26: Front flapping view

In figure 25 it can be seen that the TPP is tilted backwards in forward flight. This is because the overall forces at the starboard side of the rotor are generally stronger, and due to the gyroscopic precession the blade's flapping ends up being higher at the front side of the rotor.

This leads to a second effect, which is seen in figure 26. The forces at the front part of the rotor disc are slightly stronger than the ones at the rear, so the TPP is also slightly tilted to the port side.

These two movements are compensated by means of the cyclic feathering, as it can be seen from the coefficients A_1 and B_1 , which turn the plane in opposite directions as the ones given by flapping -notice that the term B_1 is positive, thus

tilting forward the plane, and the term A_1 is negative, forcing the plane starboard.

5.4 Helicopter motion

After integrating the helicopter in the longitudinal motion, the results for the velocities and rotation in the $-xz$ plane are the following:

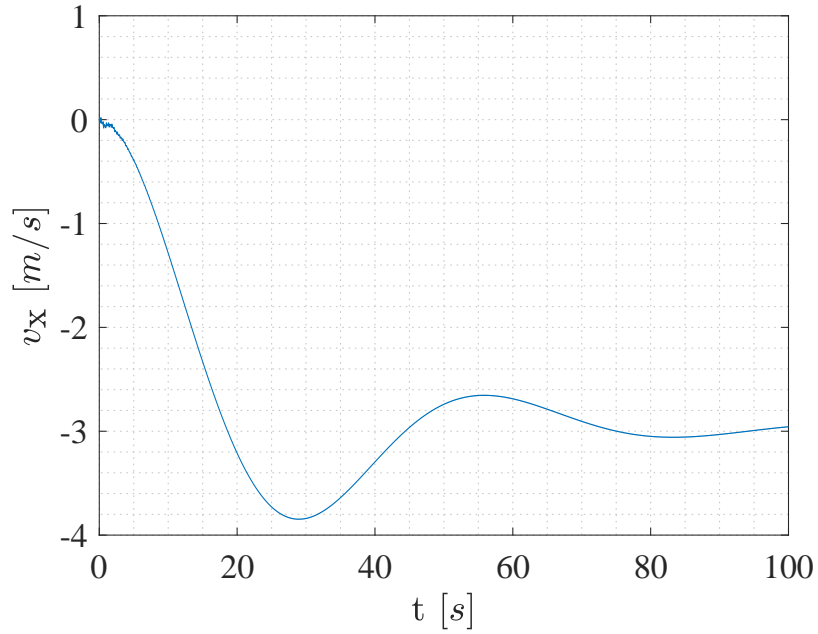


Figure 27: Horizontal velocity disturbance

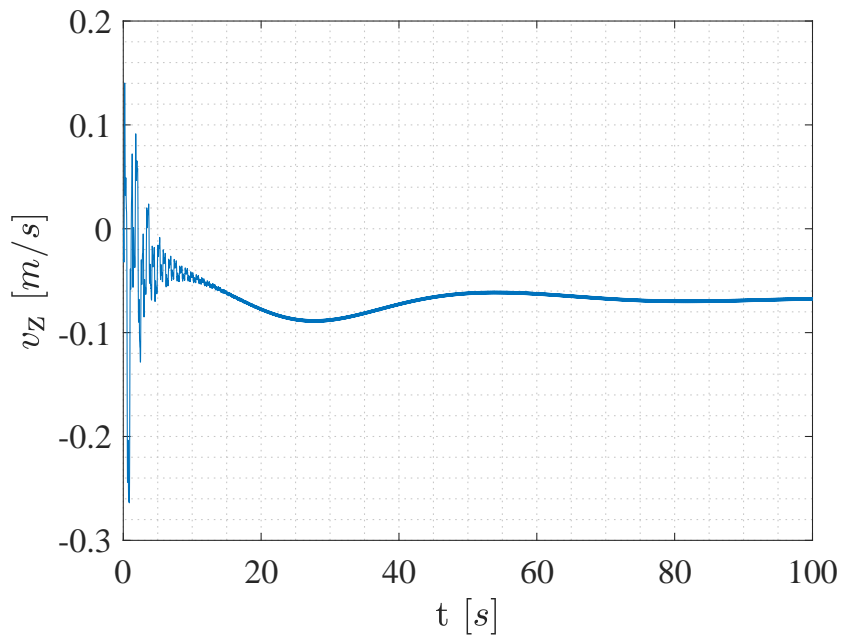


Figure 28: Vertical velocity disturbance

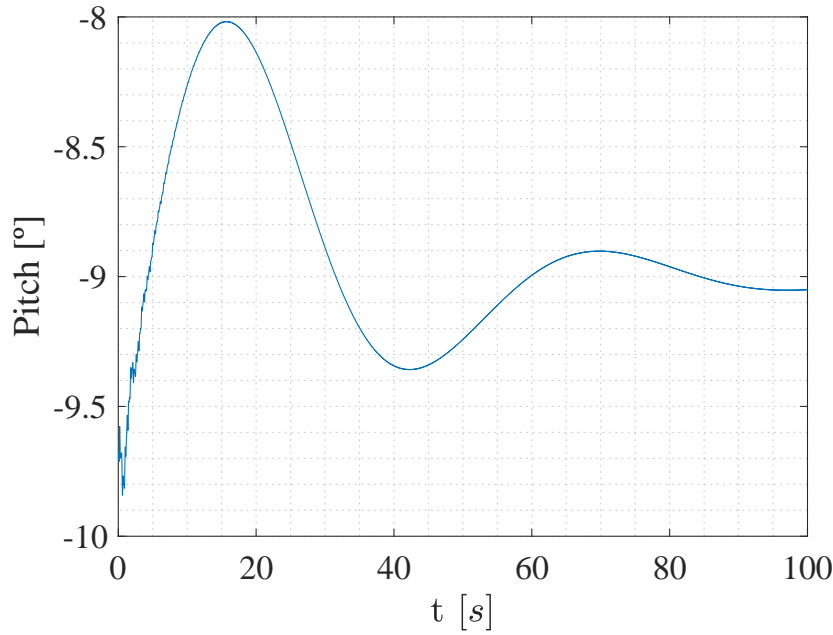


Figure 29: Pitch angle evolution

From figures 27, 28 and 29 it can be seen that the evolution in longitudinal flight is stable, at least with the aid of a tailplane. The results are not exact, as it can be seen that there is an offset between the initial disturbance values and the final ones in the velocities; and the pitch angle also varies a little. This, however, is within the expected results, since many assumptions have been taken over all these procedures, and the offset is rather small (the horizontal disturbance varies 2 or 3 m/s compared to the horizontal velocity U_0 , which is almost 60m/s).

Let us observe the evolution without a tailplane. The helicopter data is now the same, with the only change of setting the tailplane's area to 0, thus simulating that it simply does not exist. The procedure the would be exactly the same, and the results are presented in figures 30, 31 and 32.

Notice that this time the evolution is much worse and unstable. While last time the values kept slowly stabilizing, in this case after 10 seconds the divergence of the motion is notable, and after a few more seconds the simulation finally fails. This agrees with the stability studies for helicopters in forward flight^[60], that state that this case is generally unstable unless there is a tailplane, which will make the evolution more stable if the velocity is relatively high^[61].

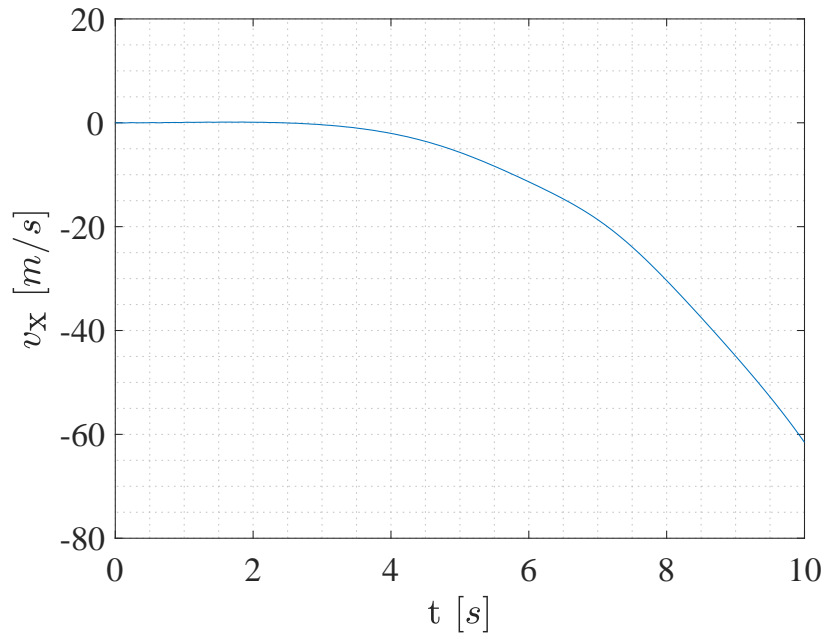


Figure 30: Horizontal velocity disturbance without tailplane

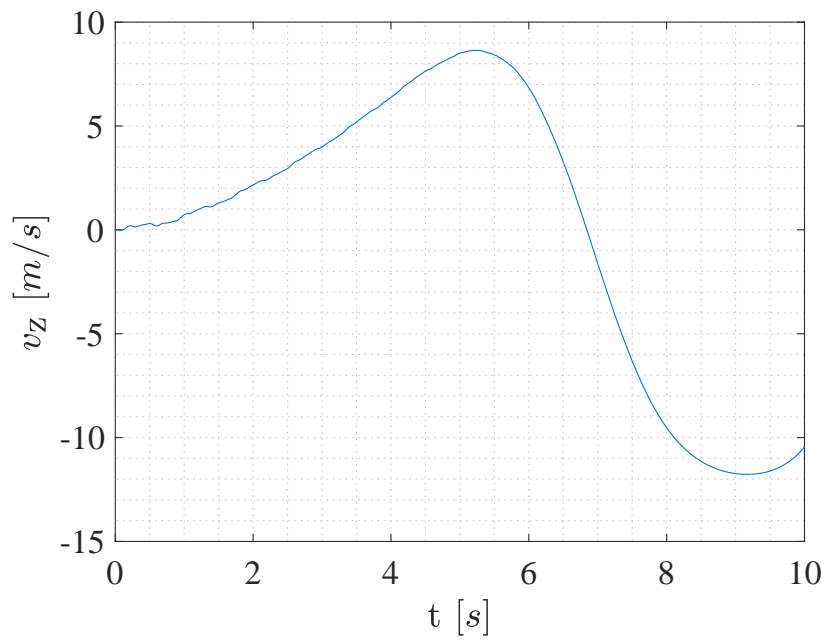


Figure 31: Vertical velocity disturbance without tailplane

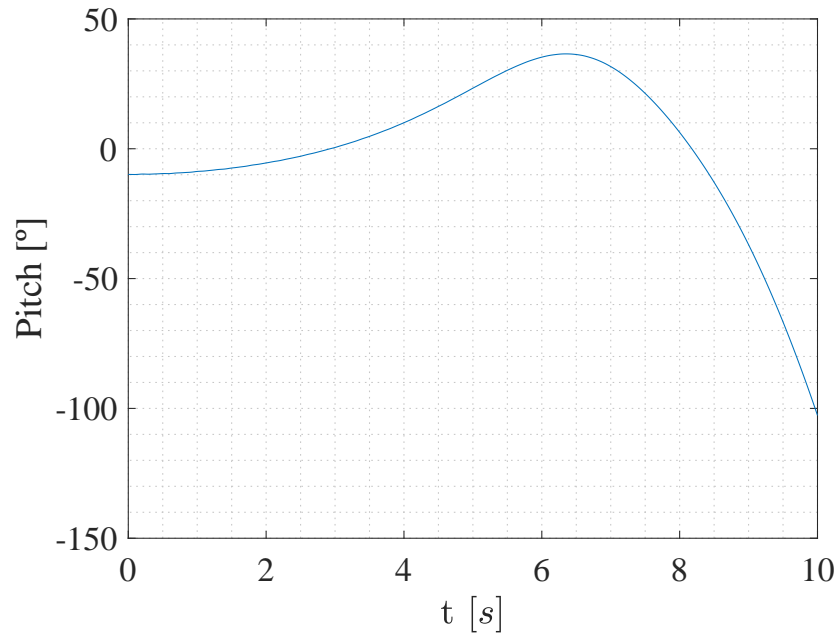


Figure 32: Pitch angle evolution without tailplane

Let us observe now the lateral case, involving yaw and roll:

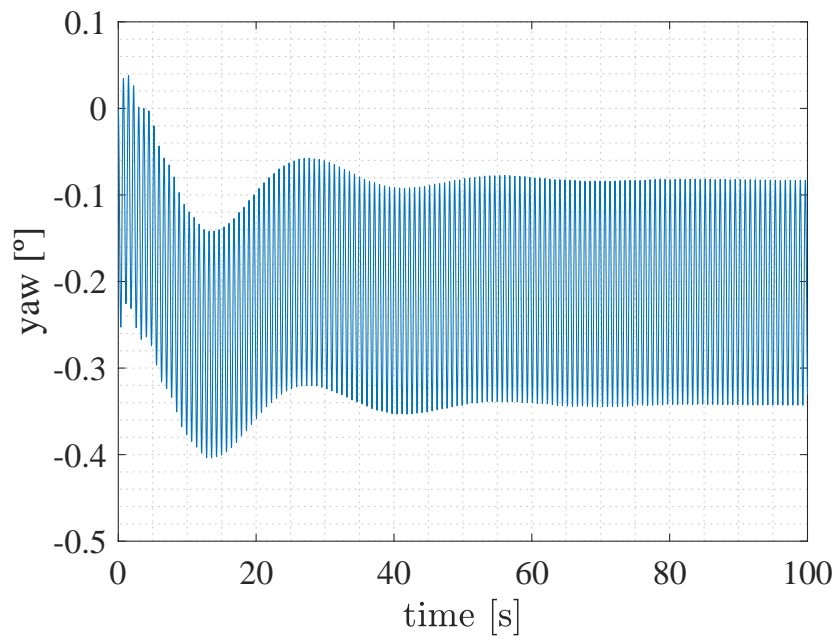


Figure 33: Yaw evolution

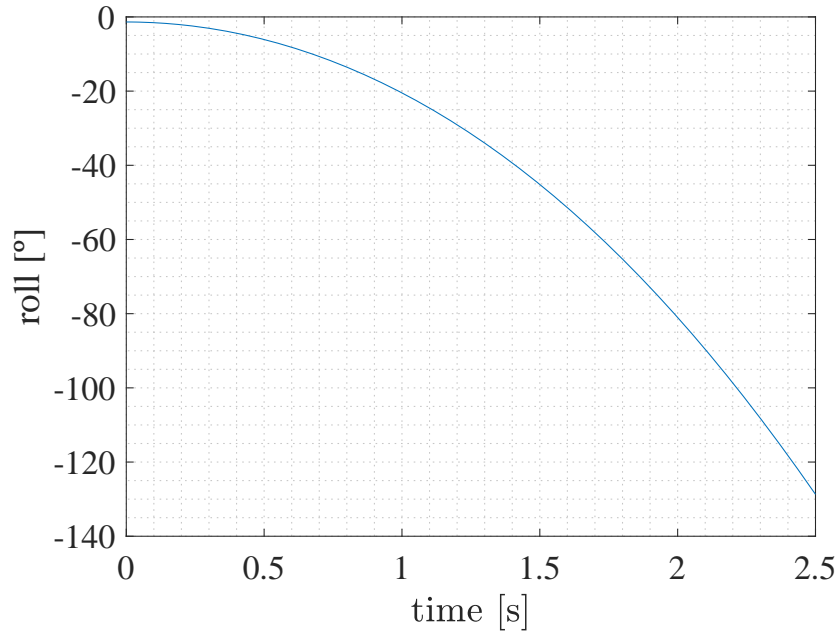


Figure 34: Roll evolution

Figures 33 and 34 present the yawing and rolling evolution -in a rather simple way, since they have been computed taking the averages of the forces, and neglecting each other's movements.

Figure 33 shows that the yaw has a convergent movement, despite the continuous oscillations due to inaccuracies in the computations. However, it can still be observed the general oscillation that the yaw makes before converging, which resembles to a “weathercock” movement somehow similar to the conventional aircraft’s “dutch roll”^[62].

On the other hand, there is the roll movement, which is much more unstable, as it was indicated previously in section (3.3.2). It diverges fast, and in order to correctly control it, it would be highly advisable to have a controller in the helicopter which reduces these effects. However, there are some effects that have been neglected in this project, such as the effect of the tail in roll, which may help to stabilize the helicopter. This will be subject of future studies.

Some studies have been made^[63] in order to evaluate controllers for helicopters, showing results such as the one displayed in figure 35, where the roll gets lower values after being controlled (the data of the problem may be different from this project and so were the results, but the relevant aspect here is the reduction in the roll magnitude):

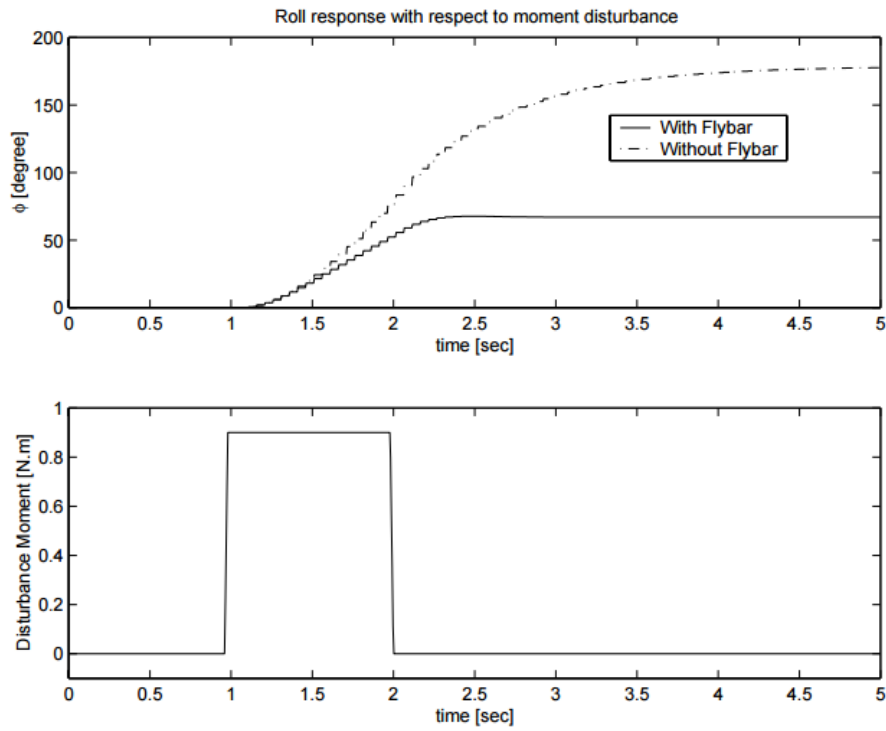


Figure 35: Roll with and without controller [64]

In this case the controller was a *flybar*, which consists of a gyro with an airfoil that helps increase the stability of the pitch and roll movements. It is an example of a mechanical controller; however, there are other, more sophisticated ones like the Automatic flight control systems that present a better control over the system and lack some of the disadvantages of the mechanical controllers, such as the drag increase^[65]

6 Conclusions and impact

The present thesis exposes the development of a numerical code that computes the different forces created on the rotor of a helicopter, including the flapping and lagging motion of the blades. afterwards it integrates the helicopter motion in a 6-dof model based on certain trim conditions for flight and the body forces of the helicopter itself.

In the following sections, some thoughts will be written about what could be improved in this project so that its usefulness and accuracy increased, as well as the possible applications that it might have. Also, an estimation of its cost will be performed, in order to get an idea of its value in a real-life case within the aerospace industry.

6.1 Future works

While the steps performed in this project cover many aspects of the forward flight, there are some elements that could be improved in order to have a more complete simulation tool in the future.

To begin with, both the lateral case and the longitudinal one without a tailplane were unstable, so a good first approach to improve the project could be to introduce some kind of controller in the model. Firstly, this would help to increase the stability when integrating the movement, but besides that, it could help design controlled flight cases.

For example, this time the integration was performed just by giving some initial conditions and seeing what happened afterwards. By using a controller, this flight would have been stable from the beginning. Then, some paths or disturbances could be programmed so that the helicopter model performed any desired flight.

This, of course, is speaking in terms of forward flight. Besides this, vertical flight may be also computed using methods described here, but the transition between vertical and forward flight -i.e. velocity relatively low- is not that easily calculated with BEMT. It would be interesting and useful to study methods that cover this transition case, so that the integration did not depend on whether the speed allows the computations to be made or not. For instance, in order to simulate a flight where the helicopter is initially hovering and afterwards accelerates up to $\mu = 0.15$ would require of this transition calculation. Thus, some method or model would be necessary here besides BEMT.

There are two more possible improvements facing future applications. Since this model evaluates the flight of the whole helicopter, it would be also interesting to add the concept of the induced power in future versions. This could help to study the general performance of the helicopter depending on the input characteristics, and would be useful to find an early approach of efficient rotor designs.

One final aspect to be looked into is the way the computations have been done. As it has been indicated, in the integration of this model two methods have been used: one that calculates the forces on the blades themselves at each time step, and another one that computed the average forces per revolution. This last method made much more use of already-made formulas, which were derived prior to the integration code. The consequence of this is that the simulation was much faster than using the first method. However, the first one offers a deeper insight of the rotor's mechanics -due to its more detailed procedure, so it may be more useful in order to introduce new concepts and observe how the behavior of the rotor changes.

Said this so, it would be a good idea to keep both procedures into account, and depending on the type and aim of any future application, use one or another.

6.2 Possible applications

Since the present project develops a procedure to integrate the flight of the helicopter, a direct application for it could be its implementation in a flight simulator. Since the intended reality of the model comes from real formulas and existing methods such as the Momentum Theory and the Blade Element Theory, such simulator could be used with academic or training purposes.

Assuming that a version is reached where all the flight envelope is covered, this method would function as a rather realistic one, without deepening into more elaborated concepts such as finite element aerodynamic models.

This application, as explained in the previous section, might require that the procedure to find the forces was the one that used the average formulas, since the intention in a flight simulator might as well be that the input is controlled in real time.

On the other hand, if the scope is to design controllers to enable a higher stability of the rotor, or even to improve the control response to a given input, maybe the first method is more appropriated. While the overall result of adding a controller could be observed with the average formulas, it would be interesting to see both how the controller itself works (more so if it is mechanical), and what the consequence is to the blades at each time. The aim of this application, hence, would be more devoted to investigation than to final products or training.

Either way, if a version is desired whose use for relevant purposes -such as pilot testing or training- is authorized, it might need to adapt to any requirements that organizations such as FAA or EASA could impose. For example, the FAA has a series of levels that evaluate the “readiness” or “completeness” of the product in order to use it with training purposes^[66].

6.3 Project Budget

The following list states the items that sum up the total budget of this project:

- Collaboration grant: Consisted of a period of 7 months, starting in November, working an average of 15 hours/week, granted by the Ministry of Education - 2000€.
- Hardware (computer), consisted of a Lenovo z70 laptop - 1230€.
- Matlab license, consisted of an education license provided by UC3M worth - 500€.

	Cost [€]
Collaboration grant	2000
Computer	1230
Matlab license	500
Total	3730

7 Appendix

- α Blade's angle of attack
- α_D Disc incidence with the coming flow
- α_{TP} TPP incidence with the coming flow
- α_{nf} Incidence angle of the no feathering plane
- α_T Tailplane angle of attack
- α_{T0} Angle between the tailplane and the rotor disc plane
- β Flapping angle
- $\dot{\beta}$ Flapping angular velocity
- $\ddot{\beta}$ Flapping acceleration
- χ Rotor wake angle
- δ Blade's drag coefficient
- η Component derived from the variable x in Mangler and Squire
- λ Non dimensional vertical velocity
- λ' Non dimensional vertical velocity in forward flight
- λ_c Non dimensional vertical velocity with respect to ΩR
- λ_i Non dimensional induced velocity with respect to ΩR
- λ_{i0} Non dimensional average induced velocity
- μ Advance ratio
- ν Component depending on the incidence (Mangler and Squire)
- Ω Rotor angular velocity
- ϕ Angle formed by U_T and U_P
- ϕ Roll angle
- ψ Azimuth position of the blade
- ψ Yaw angle
- ρ Air density
- σ Solidity
- τ_c Climb angle

- θ Blade pitch angle
- θ Helicopter pitch
- $\dot{\theta}$ Feathering velocity
- $\ddot{\theta}$ Feathering acceleration
- θ_0 Collective pitch angle
- $\theta_{0,\text{tail}}$ Collective tail pitch
- θ_{base} Geometric pitch angle
- θ_c Total cyclic pitch angle
- $\theta_{\text{feathering}}$ Pitch due to blade feathering
- θ_{tip} Geometric pitch at the end of the blade
- ε Downwash angle
- ε_0 Rotor vortex angle
- ξ Lagging angle
- ξ Distance to the tailplane
- $\dot{\xi}$ Lagging angular velocity
- $\ddot{\xi}$ Lagging acceleration
- ζ Distance between the tailplane and the rotor vortex
- A, B, C Blade moments of inertia
- A, B, C Helicopter moments of inertia
- a Blade's lift coefficient as a function of the angle of attack
- a_0 Analytic flapping component
- A_1 Cosine coefficient of the cyclic pitch
- a_1 Analytic flapping cosine coefficient
- a_{1s}, b_{1s} Flapping coefficients from the rotor disc
- A_a^b Transformation matrix
- \dot{A}_a^b Transformation matrix derivative
- A_{fb} Blade flapping transformation for the velocity
- $a_{x,y,z}$ Linear acceleration component

- b Total number of blades
- b_1 Analytic flapping sine coefficient
- B_1 Sine coefficient of the cyclic pitch
- BEMT Blade Element Momentum Theory
- c Blade's chord
- c_i Components from the Mangler and Squire formula
- C_L Lift coefficient
- C_{L_0} Lift coefficient when the angle of attack is 0
- C_{L_α} Lift coefficient when as a function of the angle of attack
- D Helicopter drag
- D TPP subscript
- dD Differential of drag per blade span
- D, E, F Helicopter products of inertia
- dH_i Differential of horizontal force along blade span
- dL Differential of lift per blade span
- dr Differential of blade's span
- dT Differential of thrust per blade span
- dx Non dimensional differential of blade span
- e Blade's hinge offset
- \vec{F}_i Force vector in the $-i$ reference frame
- h_c Non dimensional horizontal force
- h_D Distance between the TPP and the rotor plane
- H_i Horizontal force component
- h_t Vertical distance from the origin of moments to the tail rotor
- HTP Horizontal tail plane
- K Parameter used to estimate the induced velocity distribution
- l, f, h Non dimensional distances from the origin to the center of mass
- L, M, N Components of the moment vector

- l_T Non dimensional distance to the tailplane
- l_t Horizontal distance from the rotor axis to the tail rotor
- \vec{M}_i Moment vector in the $-i$ reference frame
- M_b Blade's mass
- M_f Helicopter pitching moment
- M_{Ti} Tailplane moment
- $_{nf}$ No feathering subscript
- p_c Pressure upstream from the rotor disc in vertical flight
- p_{lower} Pressure just below the rotor disc in vertical flight
- p, q, r Roll, pitch and yaw rates
- p_{upper} Pressure just above the rotor disc in vertical flight
- Q Rotor torque
- R Rotor radius
- r Position on the blade at r distance from the rotor axis
- \vec{r}_{cg} Distance from the axis to the blade's center of mass
- r_g Distance from the hinge to the blade's center of mass
- S Rotor area
- S_2 Control volume cross section downstream from the rotor disc
- S_c Control volume cross section upstream from the rotor disc
- S_{PF} Equivalent flat plate area
- S_{rotor} Control volume cross section in vertical flight at the rotor disc
- T Rotor thrust
- $_T$ Tailplane subscript
- $_t$ Tail rotor subscript
- \bar{T} Non dimensional thrust
- t Time
- t_c Non dimensional thrust
- TPP Tip path plane

- $_{\text{trim}}$ Trim conditions subscript
- T_t Tail rotor thrust
- U_P Vertical component of the velocity relative to the blade
- U_T Horizontal component of the velocity relative to the blade
- U, V, W Body's velocity initial components
- u, v, w Body's velocity disturbances
- $\dot{u}, \dot{v}, \dot{w}$ Body's acceleration components
- V Helicopter's velocity module
- \vec{V} Velocity vector
- \hat{V} Non dimensional velocity
- V' Forward flight velocity downstream from the rotor
- v_2 Wake's velocity downstream from the rotor disc
- \vec{V}_{blade} Blade velocity vector
- v_c Helicopter speed in vertical flight upstream from the rotor disc
- v_i Induced velocity
- \bar{v}_i Non dimensional induced velocity (with respect to hover values)
- v_{i0} Average induced velocity over the rotor
- V_z Vertical component of the velocity V
- W Velocity magnitude relative to the blade
- W Helicopter weight
- w_c Non dimensional weight
- w_i Angular velocity component
- \dot{w}_i Angular acceleration component
- x Non dimensional blade span
- x_g, y_g, z_g Distance from the hinge to the blade's center of mass

References

- [1] John M. Seddon, Simon Newman, “Rotor Mechanisms for Forward Flight”, in *Basic Helicopter Aerodynamics*, 3rd ed. 2011
- [2] John M. Seddon, Simon Newman, “Rotor in Vertical Flight: Momentum Theory and Wake Analysis”, in *Basic Helicopter Aerodynamics*, 3rd ed. 2011
- [3] John M. Seddon, Simon Newman, “Rotor Aerodynamics in Forward Flight”, in *Basic Helicopter Aerodynamics*, 3rd ed. 2011
- [4] Bramwell A. R. S., George Done & David Balmford, “Rotor Aerodynamics and dynamics in forward flight”, in *Bramwell’s Helicopter Dynamics*, 2nd ed. pp.78, 2001
- [5] Bramwell A. R. S., George Done & David Balmford, “Rotor Aerodynamics and dynamics in forward flight”, in *Bramwell’s Helicopter Dynamics*, 2nd ed.,pp.77-79, 2001
- [6] Glauert, H., in *A general theory of the autogiro*, Aeronautical Research Council R& M 1111, 1926
- [7] Bramwell A. R. S., George Done & David Balmford, “Rotor Aerodynamics and dynamics in forward flight”, in *Bramwell’s Helicopter Dynamics*, 2nd ed.,pp.47, 2001
- [8] Bramwell A. R. S., George Done & David Balmford, “Rotor Aerodynamics and dynamics in forward flight”, in *Bramwell’s Helicopter Dynamics*, 2nd ed.,pp.93-95, 2001
- [9] Bramwell A. R. S., George Done & David Balmford, “Rotor Aerodynamics and dynamics in forward flight”, in *Bramwell’s Helicopter Dynamics*, 2nd ed.,pp.93, 2001
- [10] Bramwell A. R. S., George Done & David Balmford, “Rotor Aerodynamics and dynamics in forward flight”, in *Bramwell’s Helicopter Dynamics*, 2nd ed.,pp.79, 2001
- [11] Bramwell A. R. S., George Done & David Balmford, “Rotor Aerodynamics and dynamics in forward flight”, in *Bramwell’s Helicopter Dynamics*, 2nd ed.,pp.80, 2001
- [12] Bramwell A. R. S., George Done & David Balmford, “Rotor Aerodynamics and dynamics in forward flight”, in *Bramwell’s Helicopter Dynamics*, 2nd ed.,pp.79-80, 2001
- [13] Mangler, K.W. and Squire, H. B., “The induced velocity field of a rotor”, *Aeronautical Research Council R&M 2642*, 1950, 2001
- [14] Bramwell A. R. S., George Done & David Balmford, “Rotor Aerodynamics and dynamics in forward flight”, in *Bramwell’s Helicopter Dynamics*, 2nd ed.,pp.81-83, 2001

- [15] Heyson, H. H. and Katzoff, S., "Induced velocities near a lifting rotor with non-uniform disc loading" *NACA Rep. 1319*, 1958.
- [16] Bramwell A. R. S., George Done & David Balmford, "Rotor Aerodynamics and dynamics in forward flight", in *Bramwell's Helicopter Dynamics*, 2nd ed.,pp.86, 2001
- [17] Bramwell A. R. S., George Done & David Balmford, "Basic mechanics of rotor systems and helicopter flight", in *Bramwell's Helicopter Dynamics*, 2nd ed.,pp.13, 2001
- [18] Stewart, W., in *Higher harmonics of flapping on the helicopter rotor*, Aeronautical Research Council CP 121, 1952.
- [19] John M. Seddon, Simon Newman, "Rotor Mechanisms for Forward Flight", in *Basic Helicopter Aerodynamics*, 3rd ed. 2011
- [20] Bramwell A. R. S., George Done & David Balmford, "Basic mechanics of rotor systems and helicopter flight", in *Bramwell's Helicopter Dynamics*, 2nd ed.,pp.22, 2001
- [21] Bramwell A. R. S., George Done & David Balmford, "Appendices", in *Bramwell's Helicopter Dynamics*, 2nd ed.,pp.359-363, 2001
- [22] Bramwell A. R. S., George Done & David Balmford, "Basic mechanics of rotor systems and helicopter flight", in *Bramwell's Helicopter Dynamics*, 2nd ed.,pp.27-28, 2001
- [23] Bramwell A. R. S., George Done & David Balmford, "Basic mechanics of rotor systems and helicopter flight", in *Bramwell's Helicopter Dynamics*, 2nd ed.,pp.23-25, 2001
- [24] Bramwell A. R. S., George Done & David Balmford, "Basic mechanics of rotor systems and helicopter flight", in *Bramwell's Helicopter Dynamics*, 2nd ed.,pp.30, 2001
- [25] Bramwell A. R. S., George Done & David Balmford, "Basic mechanics of rotor systems and helicopter flight", in *Bramwell's Helicopter Dynamics*, 2nd ed.,pp.99, 2001
- [26] Bramwell A. R. S., George Done & David Balmford, "Rotor aerodynamics and dynamics in forward flight", in *Bramwell's Helicopter Dynamics*, 2nd ed.,pp.100, 2001
- [27] Bramwell A. R. S., George Done & David Balmford, "Trim and performance in axial and forward flight", in *Bramwell's Helicopter Dynamics*, 2nd ed.,pp.126, 2001
- [28] Bramwell A. R. S., George Done & David Balmford, "Trim and performance in axial and forward flight", in *Bramwell's Helicopter Dynamics*, 2nd ed.,pp.123-125, 2001

- [29] Bramwell A. R. S., George Done & David Balmford, "Trim and performance in axial and forward flight", in *Bramwell's Helicopter Dynamics*, 2nd ed., pp.123, 2001
- [30] Bramwell A. R. S., George Done & David Balmford, "Trim and performance in axial and forward flight", in *Bramwell's Helicopter Dynamics*, 2nd ed., pp.123, 2001
- [31] Bramwell A. R. S., George Done & David Balmford, "Trim and performance in axial and forward flight", in *Bramwell's Helicopter Dynamics*, 2nd ed., pp.124, 2001
- [32] Heyson, H. H. & Katzoff, S., "Induced velocities near a lifting rotor with non-uniform disc loading", in *NACA Rep 1319*, 1958
- [33] Bramwell A. R. S., George Done & David Balmford, "Trim and performance in axial and forward flight", in *Bramwell's Helicopter Dynamics*, 2nd ed., pp.124, 2001
- [34] Bramwell A. R. S., George Done & David Balmford, "Trim and performance in axial and forward flight", in *Bramwell's Helicopter Dynamics*, 2nd ed., pp.125, 2001
- [35] Bramwell A. R. S., George Done & David Balmford, "Basic mechanics of rotor systems and helicopter flight", in *Bramwell's Helicopter Dynamics*, 2nd ed., pp.28, 2001
- [36] Bramwell A. R. S., George Done & David Balmford, "Trim and performance in axial and forward flight", in *Bramwell's Helicopter Dynamics*, 2nd ed., pp.117, 2001
- [37] Bramwell A. R. S., George Done & David Balmford, "Appendices", in *Bramwell's Helicopter Dynamics*, 2nd ed., pp.364, 2001
- [38] Bramwell A. R. S., George Done & David Balmford, "Flight dynamics and control", in *Bramwell's Helicopter Dynamics*, 2nd ed., pp.175, 2001
- [39] John Toal, "Helicopter Stability", *Helicopter training blog*, 18th August 2016, [Online], Available: <http://helicopterblog.com/?p=986> [Accessed May, 28th 2017]
- [40] Carl Banks, "Helicopter Dynamic Stability", The Pennsylvania State University, University Park, PA, Available: <http://www.aerjockey.com/papers/helicopter/report.html> [Accessed May, 28th 2017]
- [41] Bramwell A. R. S., George Done & David Balmford, "Basic mechanics of rotor systems and helicopter flight", in *Bramwell's Helicopter Dynamics*, 2nd ed., pp.31, 2001

- [42] Bramwell A. R. S., George Done & David Balmford, “Basic mechanics of rotor systems and helicopter flight”, in *Bramwell’s Helicopter Dynamics*, 2nd ed., pp.25, 2001
- [43] Bramwell A. R. S., George Done & David Balmford, “Rotor aerodynamics and dynamics in forward flight”, in *Bramwell’s Helicopter Dynamics*, 2nd ed., pp.100-103, 2001
- [44] Bramwell A. R. S., George Done & David Balmford, “Rotor aerodynamics and dynamics in forward flight”, in *Bramwell’s Helicopter Dynamics*, 2nd ed., pp.91, 2001
- [45] Bramwell A. R. S., George Done & David Balmford, “Appendices”, in *Bramwell’s Helicopter Dynamics*, 2nd ed., pp.362, 2001
- [46] Bramwell A. R. S., George Done & David Balmford, “Appendices”, in *Bramwell’s Helicopter Dynamics*, 2nd ed., pp.365, 2001
- [47] Bramwell A. R. S., George Done & David Balmford, “Rotor aerodynamics and dynamics in forward flight”, in *Bramwell’s Helicopter Dynamics*, 2nd ed., pp.103, 2001
- [48] Bramwell A. R. S., George Done & David Balmford, “Rotor aerodynamics and dynamics in forward flight”, in *Bramwell’s Helicopter Dynamics*, 2nd ed., pp.103-104, 2001
- [49] Bramwell A. R. S., George Done & David Balmford, “Rotor aerodynamics and dynamics in forward flight”, in *Bramwell’s Helicopter Dynamics*, 2nd ed., pp.107, 2001
- [50] Bramwell A. R. S., George Done & David Balmford, “Trim and performance in axial and forward flight”, in *Bramwell’s Helicopter Dynamics*, 2nd ed., pp.116, 2001
- [51] Bramwell A. R. S., George Done & David Balmford, “Trim and performance in axial and forward flight”, in *Bramwell’s Helicopter Dynamics*, 2nd ed., pp.116-117, 2001
- [52] Bramwell A. R. S., George Done & David Balmford, “Trim and performance in axial and forward flight”, in *Bramwell’s Helicopter Dynamics*, 2nd ed., pp.117, 2001
- [53] Bramwell A. R. S., George Done & David Balmford, “Rotor aerodynamics and dynamics in forward flight”, in *Bramwell’s Helicopter Dynamics*, 2nd ed., pp.78-79, 2001
- [54] Bramwell A. R. S., George Done & David Balmford, “Rotor aerodynamics and dynamics in forward flight”, in *Bramwell’s Helicopter Dynamics*, 2nd ed., pp.107, 2001

- [55] Bramwell A. R. S., George Done & David Balmford, “Trim and performance in axial and forward flight”, in *Bramwell’s Helicopter Dynamics*, 2nd ed., pp.118, 2001
- [56] Bramwell A. R. S., George Done & David Balmford, “Trim and performance in axial and forward flight”, in *Bramwell’s Helicopter Dynamics*, 2nd ed., pp.120, 2001
- [57] Bramwell A. R. S., George Done & David Balmford, “Basic mechanics of rotor systems and helicopter flight”, in *Bramwell’s Helicopter Dynamics*, 2nd ed., pp.30, 2001
- [58] Bramwell A. R. S., George Done & David Balmford, “Basic mechanics of rotor systems and helicopter flight”, in *Bramwell’s Helicopter Dynamics*, 2nd ed., pp.30, 2001
- [59] Bramwell A. R. S., George Done & David Balmford, “Trim and performance in axial and forward flight”, in *Bramwell’s Helicopter Dynamics*, 2nd ed., pp.126-127, 2001
- [60] Bramwell A. R. S., George Done & David Balmford, “Flight dynamics and control”, in *Bramwell’s Helicopter Dynamics*, 2nd ed., pp.163, 2001
- [61] Bramwell A. R. S., George Done & David Balmford, “Flight dynamics and control”, in *Bramwell’s Helicopter Dynamics*, 2nd ed., pp.164, 2001
- [62] Bramwell A. R. S., George Done & David Balmford, “Flight dynamics and control”, in *Bramwell’s Helicopter Dynamics*, 2nd ed., pp.173, 2001
- [63] S. K. Kim & D. M. Tilbury, “Mathematical Modeling and Experimental Identification of a Model Helicopter”, Department of Mechanical Engineering and Applied Mechanics, University of Michigan, MI 48109-2125, August 31, 2000, Available: <http://www-personal.umich.edu/~tilbury/papers/kt00jgcd.pdf> [Accesed June, 3rd 2017]
- [64] S. K. Kim & D. M. Tilbury, “Mathematical Modeling and Experimental Identification of a Model Helicopter”, Department of Mechanical Engineering and Applied Mechanics, University of Michigan, MI 48109-2125, August 31, 2000, Available: <http://www-personal.umich.edu/~tilbury/papers/kt00jgcd.pdf> [Accesed June, 3rd 2017]
- [65] Bramwell A. R. S., George Done & David Balmford, “Flight dynamics and control”, in *Bramwell’s Helicopter Dynamics*, 2nd ed., pp.178-179, 2001
- [66] S. Moore, “Training Device Types, Use and Credit”, Presented to DPE participants, Federal Aviation Administration, January 2015 [online], Available: https://www.faa.gov/about/office_org/field_offices/fsdo/orl/local_more/media/dpe/Training%20Devices.pdf, [Accesed June, 4th 2017]